Exploring Transcriptional Regulators that Control Emergent Behaviors in *Myxococcus xanthus*

By

Rion G. Taylor

DISSERTATION

Submitted in partial fulfillment of the requirements for the
degree of Doctor of Philosophy in Biology
in the Graduate School of Syracuse University

August 2008

Abstract

A swarm of the δ-proteobacterium *Myxococcus xanthus* is a distributed system; a population of superposable automata whose distribution is transparent so that it appears as one machine. These swarms contain millions of cells that act as a collective, exhibiting coordinated movement through a series of signals to create complex, dynamic patterns as a response to environmental cues. These self-organizing patterns are considered emergent, as they cannot be predicted by observing the behavior of the individual cells.

Self-organization in *M. xanthus* is ultimately controlled through gene expression via transcriptional regulators (TRs). We selected to examine the effect of TRs on development, an example of a distinct emergent pattern, and designed new assays to quantify this behavior. We measured the swarm's ability to develop using TR mutant strains and found that mutants previously characterized as producing no disparate phenotype actually did.

We identified, characterized, and quantified a second distinct emergent pattern in *M. xanthus* called chemotaxis. We define chemotaxis as the directed movement of a swarm up a nutrient gradient toward its source. This behavior can only be accomplished when the cells are in a cooperative, multicellular swarm. We have also demonstrated that chemotaxis is under transcriptional control by several members of the highly duplicated NtrC-like family of TRs. The combination of experimental and genetic evidence suggests that chemotaxis evolved after the establishment of the swarm by means of duplication and divergence of multiple signaling pathways.

Table of Contents

List of Tables

List of Figures

like element) box represents two 17-bp NtrC-binding sites that constitute the enhancer; they are centered at -108 and -140. (B) The σ^{54}-holoenzyme can bind to the promoter in a closed recognition complex, in which the DNA remains double-stranded. NtrC binds to the ELE, but only the phosphorylated form (NtrC-P) can activate transcription. Active oligomers of NtrC-P must contain not only the two dimers bound to the enhancer but also an additional dimer or dimers bound to these by protein-protein interactions. (C) NtrC-P contacts the σ^{54}-holoenzyme by means of a DNA loop. In a reaction that requires hydrolysis of ATP, NtrC-P catalyzes the isomerization of closed complexes between polymerase and the promoter to open complexes, in which the DNA around the transcriptional start site is locally denatured and the correct strand can be used as template. (D) As transcription is initiated, σ^{54} dissociates from the holoenzyme.

remove methyl groups at four specific glutamyl residues on each

receptor monomer. Receptor modification increases CheA activity

and decreases sensitivity to attractants. Feedback is provided by

CheB phosphorylation through CheA that increases CheB activity.

(B) A swarm of DK1253 (A+S-); T_n = 18 hours, TR = 1.23 ± 0.06.

(C) A swarm of DK1218 (A-S+); T_n = 23 hours, TR = 0.90 ± 0.15.

(D) and (E) Higher magnification view of DK1622 leading and lagging edges, respectively. Scale bars in (A) to (C), 1 mm; scale bar in (D) and (E), 0.5 mm.

Abbreviations

CTTYE   Nutrient-rich media

CTTSA   Nutrient-rich media in soft agar

EBP   Enhancer binding proteins

ECF   Extracytoplasmic function

EPS   Exopolysaccharide

gDNA   Genomic DNA

Kan   Kanamycin

MCP   Methyl-accepting chemotaxis protein

ORF   Open reading frame

RDM   Rapid development media

T_0 Tracking assay start point

T_n Tracking assay end point

TM   Time-lapse microcinematography

TPM   Starvation buffer

TR   Transcriptional regulators

Chapter 1: Introduction and Motivation

1.1 Introduction and Research Question

One of the important unanswered questions of modern biology is how cells self-organize to form complex multicellular patterns. The process requires intercellular communication to specify an organism's overall size and shape, define its segments, establish segment polarity, and set branching patterns for everything from multicellular development in bacteria to the nervous system in higher organisms. The life sciences are now in the post-genomic era, and, although we have access to the genetic makeup of many organisms, we are not close to understanding the intricate spatial and temporal signaling cascades needed for multicellular organization.

To gain insight into self-organization, we used the bacterium *Myxococcus xanthus* as a model. *M. xanthus* combines the genetic tractability of a prokaryote with the behavioral sophistication of a simple eukaryote. It exists as a self-organizing predatory swarm that has many of the characteristics of a multicellular organism. It produces complex, apparently intelligent, multicellular patterns without the need for any planning or control – a phenomenon called emergence. An *M. xanthus* swarm moves over a surface as it hunts cooperatively for prey. Under starvation conditions, thousands of *M. xanthus* cells move in a coordinated fashion to form aggregate structures called fruiting bodies, which contain dormant myxospores. These behaviors require the spatial and temporal control of cell movement, which is thought to be accomplished through cascades of transcriptional regulators (TR) that act as part of signal transduction networks. The *M. xanthus* genome is distinguished by an inordinate number of multi-site

DNA binding TRs. It has been proposed that all emergent *M. xanthus* behavior is controlled through these TRs. The work here will begin to address the following biological question: are the emergent patterns found in *M. xanthus* controlled through signals by way of a network of transcriptional regulators?

1.2 Contributions to the Field

In this dissertation, a number of novel approaches are presented that help further our understanding of how *M. xanthus* swarm behaviors manifest as emergent patterns. These approaches are described in short below:

- The application and testing of a phylogenomic map to predict gene function in *M. xanthus*. This approach is based on the hypothesis that pairs of sequence-dissimilar genes that are consistently co-inherited in the same sets of organisms are likely to be functionally linked.

- The analysis of transcriptional regulators (TR) in relation to how they affect emergent behaviors. This approach takes advantage of the newly developed protocols described in this work to examine the role that TRs such as the NtrC-like enhancer binding proteins (EBP) and the extracytoplasmic function (ECF) sigma factor play in pattern formation.

- The development of tools and methods for generating and characterizing large numbers of *M. xanthus* mutant strains. These include a high-throughput mutagenesis protocol that gives us the capability of generating

close to 100 mutant strains at a time and a custom microscope cluster, which gives us the ability to generate 8 time-lapse videos simultaneously.

It is well established that an *M. xanthus* swarm can sense and respond to its environment; it is capable of changing behavior in response to chemical signals. The techniques outlined in this work have given us the ability to measure the behavioral changes in TR mutant strains and compare them to wild type. This has permitted us to test the above hypothesis, and to at least partially, parse the TRs into different genetic networks.

1.3 Dissertation Overview

This dissertation is outlined as follows:

- **Chapter 2 – Background and Significance**
- **Chapter 3 – Methods for Studying Swarm-Level Motility**
- **Chapter 4 – *M. xanthus* Development as a Dynamic Process**
- **Chapter 5 – *M. xanthus* Chemotaxis as a Dynamic Process**
- **Chapter 6 – Conclusions**

Chapter 2: Background and Significance

2.1 Introduction

The origins of multicellularity – how single-celled organisms first began to cooperate and evolve as a coherent group and eventually as one single complex organism – is an important questions that remains to be answered (Pennisi, 2005). The fitness advantage that results from cooperation is the driving force behind the evolution of social behavior (Kreft & Bonhoeffer, 2005; Sachs *et al.*, 2004). Once a community is established, the functional autonomy of the individual is redefined: selection now acts on the contextual framework of the community as a whole (Buss, 1987; Szathmáry & Smith, 1995). Biofilms provide this framework for bacteria. Although any population embedded in a matrix attached to a surface technically qualifies as a biofilm (Crespi, 2001), biofilm communities are often quite complex. Many are swarm-intelligent systems that self-organize and can, in many respects, behave as a single entity. This type of group behavior is emergent (see below), and may not be observable in the behavior of an individual bacterium. Biofilms thus represent a fundamental paradigm of development for multicellular systems.

2.2 Self-Organization and Emergence

Self-organization is a process in which the internal organization of a system increases in complexity without being guided or managed by an outside source (Camazine *et al.*, 2001). It is considered emergent if the global behavior is unexpected and unpredictable based a lower level description of each individual's behavior. One visible indicator of emergence is the formation of

patterns (Ben-Jacob, 2003). These patterns are not created by a single event or rule and nothing commands the system to form a pattern. Instead, the interaction of each individual with its immediate surroundings causes a complex series of processes leading to self-organization (Corning, 2002). The high frequency of these patterns in biofilms is one indication that emergent self-organization might be common in microbes (Camazine *et al.*, 2001).

2.2.1 The Evolution of Self-Organization in Bacterial Populations

Bacteria have historically been characterized as planktonic cells grown in agitating nutrient-rich media, where each cell is metabolically and reproductively isolated (Kreft, 2004). These are *in situ* growth conditions. In nature, many bacteria are found almost exclusively within biofilms, where they exhibit a functional interdependence that cannot occur in agitating media (Westerhoff, 1985). The requisite extracellular matrix (composed of polysaccharides and proteins) is one obvious example of this interdependence. Construction of the matrix requires the combined capacity of the population; a single bacterium cannot produce sufficient polysaccharide. Cooperative biofilm behavior extends beyond the mere pooling of capacity; some biofilms sense and respond collectively to the environment (Bonner, 2000). This form of cooperation, known as "swarm intelligence," is accomplished through mechanisms similar to those found in social insect colonies. These colonies exchange complex and coordinated signals that unify the population's response to environmental stress,

thus allowing the population to avail itself of the advantages inherent in scale and specialization.

Once a biofilm is established, the iterative process of evolution becomes less obvious. Component cells interact with the environment only within the context of the biofilm, whereas the biofilm interacts directly with the environment. Selection occurs on both the biofilm and the individual cell, although the difference in environmental context results in different selective pressures and different outcomes. The evolution of component cells is the result of each individual cell competing with other cells within the biofilm. Simultaneously, the biofilm evolves as a unit to respond to changes in the external environment (Velicer *et al.*, 2000). As a result of this "disconnected" evolution, a biofilm may exhibit self-organizing behavior that appears to be uncoupled from the behavior of component cells – that is, it is unclear how observed changes in the behavior of individual cells results in the observed changes in the behavior of the biofilm as a whole. Again, self-organization is considered emergent if the global behavior is unexpected and unpredictable based a lower level description of each individual's behavior. Several examples of self-organization in biofilms are made manifest by the δ-proteobacterium *M. xanthus.*

2.2.2 *M. xanthus* as a Model Organism for the study of Self-Organizing Behavior

M. xanthus has a complex, multicellular lifecycle that includes vegetative growth, and multicellular chemotaxis and development (Figure 2.1) (Zusman *et al.*,

2007). Like other biofilm-forming microbes, myxobacteria exhibits social interactions that are usually associated with more complex eukaryotic cells (Kaiser, 2004). This has led to the use of *M. xanthus* as a model system for the study of self-organizing behaviors and their regulation. The cells lack flagella and are non-motile in liquid growth media, but can move via gliding motility (for details on gliding motility, see section 2.3) on solid growth substrates such as agar at speeds of 2 to 4 μm per minute (Spormann & Kaiser, 1995). *M. xanthus* cells exists as a swarm – a dynamic, predatory, saprophytic, single-species biofilm that exhibits self-organization in response to environmental cues. The swarm inhabits terrestrial environments such as soils and the surfaces of decaying plant matter. In these environments it must fulfill two major requirements for vegetative growth. First, it must be able to move over the underlying substratum in order to find sources of its primary nutrients: amino acids and small peptides (Reichenbach, 1999; Kaiser, 2006; Kaiser, 2003; Shimkets, 1999). These nutrients are found in the environment as free macromolecules and as macromolecules within living prey bacteria. Second, it must make available nutrients suitable for uptake by individual cells. The swarm accomplishes this through the lysis of prey bacteria and extracellular proteolysis of macromolecules. It has been recognized for several decades that high densities of *M. xanthus* cells are required for the efficient release of lytic and degradative enzymes (Rosenberg *et al.*, 1977). As a result, an individual *M. xanthus* cell must be able to modulate its motile behavior in response to varying nutrient levels, while remaining close to other cells. For *M. xanthus* cells to

coordinate their movement, they must communicate with each other and

synchronize their behavior (Shimkets, 1999; Kaiser, 2004).
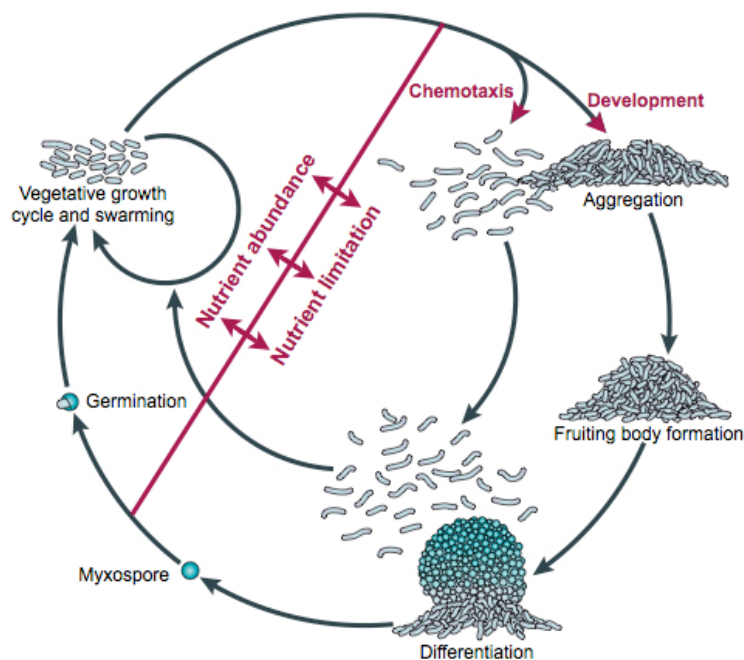
Figure 2.1: Life cycle of *Myxococcus xanthus*. *M. xanthus* cells are usually found on solid substrates. When nutrients are abundant, the swarm grows vegetatively. Upon starvation, cells either move outward in search of additional macromolecules or prey (chemotaxis), or aggregate at discrete foci to form mounds and then macroscopic fruiting bodies (development). The rod-shaped cells in the fruiting bodies differentiate and form spherical myxospores that are metabolically quiescent and environmentally resistant. When nutrients become available, the spores in the fruiting body germinate to form an 'instant' swarm and complete the life cycle. (Adapted from Zusman *et al.*, 2007)

2.2.3 *M. xanthus* Self-Organization as Emergent Behavior

Although there is some degree of ambiguity regarding the threshold at which

collective behavior becomes emergent, populations that are universally accepted

as examples of emergent behavior do share some common characteristics.

Social insect colonies (such as ants) demonstrate these well. First, the

population is robust with respect to assault on individuals: large numbers of

individual ants can be destroyed without significantly altering the fitness of the

colony. Second, the success of the colony is extremely sensitive to small

changes in the behavior of individuals, even those that do not measurably affect the fitness of the individual ant. For example, if the behavior of an ant population were altered so that foragers no longer brought food back to the nest, but merely consumed enough for their own sustenance, the fitness of the altered foragers would not be impaired. However, the colony would be devastated.

Likewise, in *M. xanthus*, disrupting certain genes has also been shown to affect swarm behavior without significantly altering the survivability, or even the observable behavior, of individual cells. One well-studied example is the *FrzS* gene, which, when disrupted, has almost no visible effect on individuals, but impairs swarm expansion (Ward *et al.*, 2000). One explanation is that FrzS is responsible for some uncharacterized cellular function related to coordinated group movement (Mignot *et al.*, 2005). Given the complexity of the genetic networks that control emergent behavior in biofilms (Kroos, 2007), identifying hypothetical genes that disrupt them is difficult, and the effect of these genes may only become apparent within the context of the behavior of the biofilm as a whole.

2.3 *M. xanthus* Motility

M. xanthus cells move over surfaces via gliding motility, which is movement in the direction of the long axis of the cell at a solid–liquid interface without the aid of flagella (Figure 2.2, A^+S^+) (McBride, 2001). They accomplish this using two genetically separate motility systems (Hodgkin *et al.*, 1979; Hodgkin & Kaiser, 1979). The first powers the movement of individual cells away from large

swarms in an <u>a</u>dventurous manner, and is therefore called A-motility (Figure 2.2, A^+S^-). The molecular mechanics of A-motility remain disputed; both directed slime secretion (Wolgemuth *et al.*, 2002) and the contraction and twisting of the cell (Mignot *et al.*, 2007) have been proposed. The second motility system, called <u>s</u>ocial or S-motility (Figure 2.2, A^-S^+), requires cell-cell contact and involves the movement of groups of cells. S-motility functions through type IV pili (long, flexible appendages found at the poles of cells) and cell surface macromolecules known as fibrils (made up of polysaccharides and proteins). The pili of individual cells can attach to either the underlying surface or the fibrils produced by other cells and then retract, pulling the cell and providing the motive force for groups of cells to move together (Sun *et al.*, 2000).

A^+S^+ A^-S^+ A^+S^-
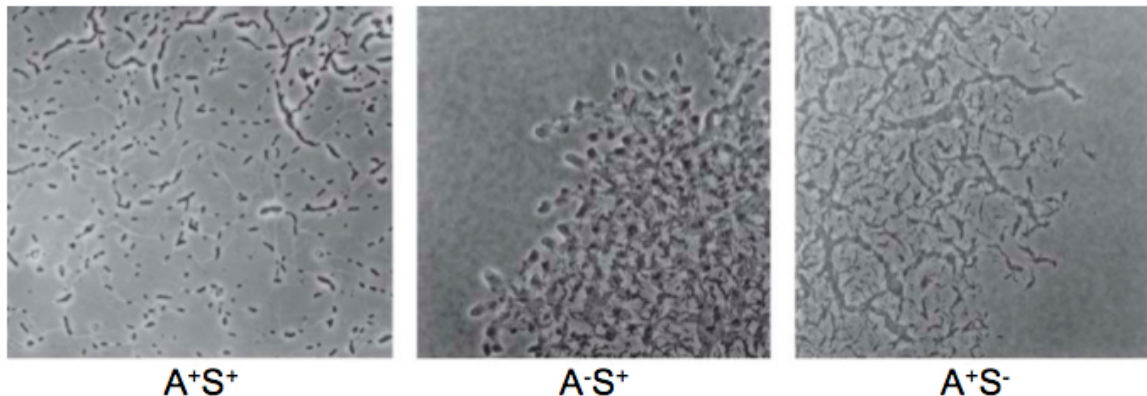
Figure 2.2: Distribution of cells at the swarm edges of a wild-type swarm (A^+S^+), an s-motility swarm (A^-S^+), and an a-motility swarm (A^+S^-). (Reprinted from Kaiser, 2006)

Under nutrient rich conditions, an *M. xanthus* swarm undergoes expansion, moving and growing symmetrically outward from the point of inoculation. Swarm expansion is a motility driven process that utilizes both the A- and S- systems synergistically; disruption of either motility system significantly diminishes the swarm expansion rate, and mutant strains lacking both A- and S-

motility do not expand (with the exception of expansion due to growth). Wild-type

swarm expansion requires the coordination of A- and S- motility systems, which

is evident by the fact that the expansion rate of wild-type (A^+S^+) swarms is

greater than the sum of the expansion rates of A^+S^- and A^-S^+ cells. The dynamic

patterns that form during swarm expansion are most obvious at the swarm edge,

where the formation of flares can be observed. Flare morphology includes

peninsulas, islands, and isolated cells that move outward from the edge of the

swarm, forming the patterns that lead to swarm expansion (Fontes & Kaiser,

1999). It is believed that through a system of signals (Shimkets, 1999; Kaiser,

2004), all of the cells in a swarm communicate and coordinate their behavior, so

that the entire swarm can function as one machine, changing their behavior in

response to environmental cues. The swarm will break symmetry in response to

stress such as nutrient limitation. The most thoroughly studied example of *M.*

xanthus symmetry breaking is the self-organizing behavior called development.

A second example of *M. xanthus* self-organization occurs when a swarm breaks

symmetry and moves up a gradient of nutrients toward its source. We refer to

this behavior as chemotaxis.

2.3.1 Development

Under nutrient-limiting conditions, *M. xanthus* cells will synchronize a change in

behavior and initiate a complex program of self-organization that transitions the

swarm from an evenly distributed population of cells to densely packed

aggregates called fruiting bodies (Figure 2.3). A fruiting body is a spherical

structure of approximately 1×10^5 cells; the vast majority of which differentiate into metabolically quiescent stress-resistant spores (Kaiser, 2006). The whole process is called development, and it is the most thoroughly studied example of *M. xanthus* self-organization. The potential purpose of fruiting prior to sporulation can be inferred from a fruiting body's physical properties: it is small (1/10 mm), tightly packed, and sticky. If a moving object, such as the leg of an insect, comes in contact with a fruiting body, all of the *M. xanthus* spores contained within will likely be transported as a unit. This way, if carried to a new food source, thousands of *M. xanthus* spores can rapidly emerge together as a swarm, rather than having to re-establish a swarm from a single cell (Reichenbach, 1999). Development, however, is not the only example of self-organizing behavior.
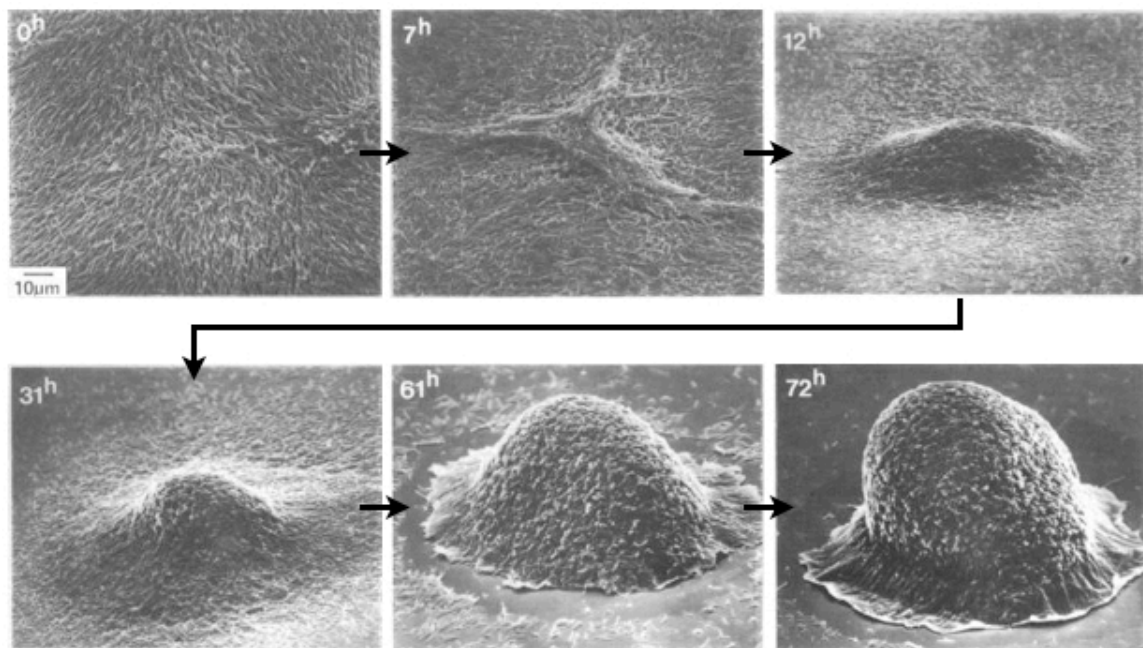
Figure 2.3: Images of *M. xanthus* fruiting body formation acquired by scanning electron microscopy. Numbers in the upper left corner indicate hours after the onset of starvation. At t=0 hours, the swarm appears as an approximately evenly distributed population. During the next 72 hours, the millions of cells in the swarm coordinate their movement, pick fixed points, an then aggregate at those points. By t = 72 hours, fruiting bodies have formed. The final fruiting body contains approximately 100,000 bacteria organized so that the cells at the interior of the fruiting body differentiate to form resistant spores. The final structure measures approximately 1/10mm in diameter. (Reprinted from Kuner & Kaiser, 1982)

2.3.2 Chemotaxis

If an *M. xanthus* swarm is placed on an agar substrate containing limited

nutrients in the form of a gradient, the swarm can break symmetry and move up

the gradient toward the nutrient source (Shi *et al.*, 1993; Kearns & Shimkets,

1998; Ward *et al.*, 1998). Although this result has been reported multiple times,

there is disagreement regarding its exact nature. Initially, movement toward an

attractant was considered evidence that *M. xanthus* was capable of chemotaxis

(Ho & McCurdy, 1979). Others hypothesize that *M. xanthus* cells are inherently

incapable of chemotaxis, and propose that a swarm moves toward a nutrient

source via elasticotaxis; the directed movement of cells in response to physical

stress on a substrate (Dworkin, 1983; Fontes & Kaiser, 1999). Subsequent

research has alternately claimed to show evidence either for or against

chemotaxis toward nutrients (Tieman *et al.*, 1996; Shi *et al.*, 1994; Shi & Zusman,

1994a; Dworkin & Eide, 1983) (for a detailed explanation of this controversy, see

Chapter 5). Interestingly, there is consistent evidence that *M. xanthus* responds

to gradients of repellents (Shi & Zusman, 1994a; Shi & Zusman, 1994b). The

first molecule identified as a chemoattractant for single cells of *M. xanthus* was

the lipid phosphatidylethanolamine (PE) (Kearns & Shimkets, 1998). As a major

component of bacterial cell walls, PE is a logical candidate to mediate taxis

toward prey bacteria.

Although there are unanswered questions regarding the mechanism *M.*

xanthus uses to identify and locate prey, there is consensus that a swarm can

respond to prey bacteria. For the past 30 years peer-reviewed articles have described *M. xanthus* as a "wolf-pack" (Dworkin, 1973; Rosenberg *et al.*, 1977; Kaiser *et al.*, 1979; Burchard, 1982; Dworkin, 1999; Spormann, 1999; Kaiser, 2001; Velicer, 2003; Black & Yang, 2004). This descriptive implies that a swarm 'hunts' through a coordinated system of recognizing, tracking, and devouring prey. We have independently confirmed that an *M. xanthus* swarm can move up a nutrient gradient in agar (Taylor & Welch, 2008). This material is presented in detail in Chapter 5.

2.4 Transcriptional Regulation of Emergent Behavior in *M. xanthus*

 From a genomics perspective, the complexity of *M. xanthus* emergent behaviors is reflected in its 9 Mb chromosome, one of the largest known prokaryotic genomes (Goldman *et al.*, 2006). A survey of the *M. xanthus* genome reveals striking peculiarities, specifically in signaling pathways. It encodes for 99 serine/threonine kinases (STPK), 137 sensor and hybrid histidine protein kinases (HPK), 48 sigma-factors, and over 53 NtrC-like activators. An analysis of both one- and two-component regulators in *M. xanthus* reveals regulatory networks atypical among prokaryotes. *M. xanthus'* signaling networks branch, often having at least two components, with sites for sensory input upstream of the regulators of transcription (Kroos, 2007). This is attributed to the large number of multi-site DNA binding transcriptional regulators (TRs) found in *M. xanthus*. In contrast, the number of single-site DNA-binding TRs, such as the TetR family of

regulators, is unusually low. *M. xanthus* has only 310 DNA-binding TRs, compared to other soil bacteria: *Streptomyces coelicolor* and *S. avermitilis* have 584 and 530, respectively. This deficit in single-site DNA-binding TRs, and the relative abundance of multi-site TRs, may point to a regulatory system capable of receiving multiple signals and regulating multiple genes. The relative number and type of TRs has profound ramifications for the possible structure of transcription networks and, by extension, the relationship between TR function and multicellular phenotype.

One important class of TRs is the NtrC-like activators, also known as σ^{54} enhancer binding proteins (EBP). *M. xanthus* contains 53 NtrC-like EBPs (Jelsbak *et al.*, 2005), which bind to sigma-54 promoters found upstream of target ORFs (Open Reading Frames) and help σ^{54} bound RNA Polymerases make the transition from a closed to an open complex thus activating transcription (Figure 2.4). They are known to participate in two-component signal transduction pathways, often partnering with STPKs and HPKs (Yang & Kaplan, 1997; Wu & Kaiser, 1995; Lu *et al.*, 2005; Sun & Shi, 2001). Expression studies suggest that NtrC-like EBPs are functioning during all stages of normal development (Jelsbak *et al.*, 2005; Sun & Shi, 2001; Caberoy *et al.*, 2003; Gorski & Kaiser, 1998). In addition, mutational analysis shows that NtrC-like EBPs are important for the expression of over half of the genes required for normal development (N. Caberoy, personal communication). For example, disruption of the NtrC-like EBP *actB* causes changes in the expression level of genes during aggregation, leading to defects in sporulation (Gorski *et al.*, 2000). Frequently,

these mutants display aberrant phenotypes when observed at either the

individual cell or swarm levels.
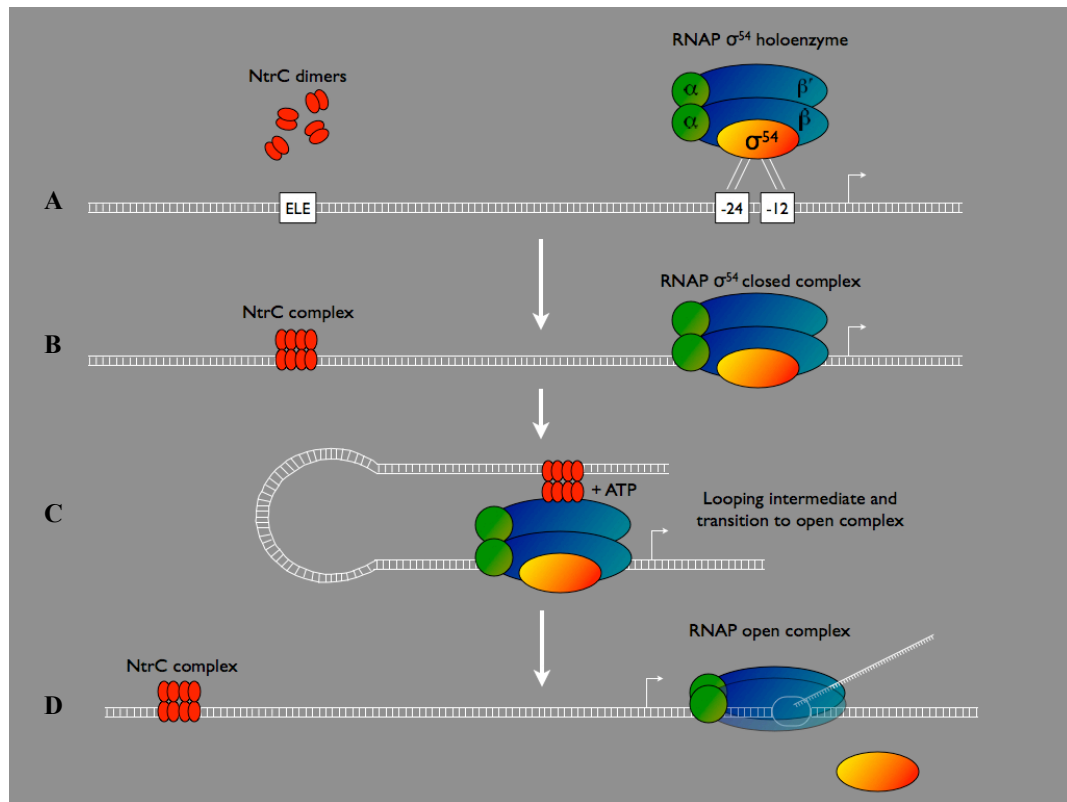
Figure 2.4: Transcriptional activation by NtrC. (A) Conserved promoter sequences recognized by σ^{54}-holoenzyme lie at sites -12 and -24 with respect to the start site of transcription. The ELE (enhancer-like element) box represents two 17-bp NtrC-binding sites that constitute the enhancer; they are centered at -108 and -140. (B) The σ^{54}-holoenzyme can bind to the promoter in a closed recognition complex, in which the DNA remains double-stranded. NtrC binds to the ELE, but only the phosphorylated form (NtrC-P) can activate transcription. Active oligomers of NtrC-P must contain not only the two dimers bound to the enhancer but also an additional dimer or dimers bound to these by protein-protein interactions. (C) NtrC-P contacts the σ^{54}-holoenzyme by means of a DNA loop. In a reaction that requires hydrolysis of ATP, NtrC-P catalyzes the isomerization of closed complexes between polymerase and the promoter to open complexes, in which the DNA around the transcriptional start site is locally denatured and the correct strand can be used as template. (D) As transcription is initiated, σ^{54} dissociates from the holoenzyme. (Adapted from Wyman *et al.*, 1997)

Another important class of TRs is the extracytoplasmic function (ECF)

sigma factor, also known as σ^E. The ECF sigma factors belong to a subfamily of

the σ^{70} class of 'house-keeping' activators and, in most cases, seem to function

in response to stress events occurring in the extracytoplasm (Lonetto *et al.*,

1994). It is thought that the ECF factors are sequestered in the inner membrane

by specific anti-sigma factors. In the presence of a stimulus, these anti-sigma

factors are degraded thus releasing the ECF factor (Missiakas & Raina, 1998).

M. xanthus contains 38 ECF sigma factors (Lee Kroos, personal communication),

only one of which has been characterized – CarQ. *M. xanthus* produces

carotenoids; light-protective agents that prevent cell lysis in the presence of high

intensity light. Their synthesis is light inducible and regulated by the ECF factor

CarQ. CarQ is sequestered to the inner membrane by the anti-sigma factor

CarR. In the presence of high intensity light, specifically blue light, CarR is

degraded by a periplasmic light-induced signal. This leads to the release of

CarQ from the membrane and the subsequent expression of genes involved in

carotenoid synthesis (Figure 2.5) (Gorham *et al.*, 1996; Whitworth & Hodgson,

2001).
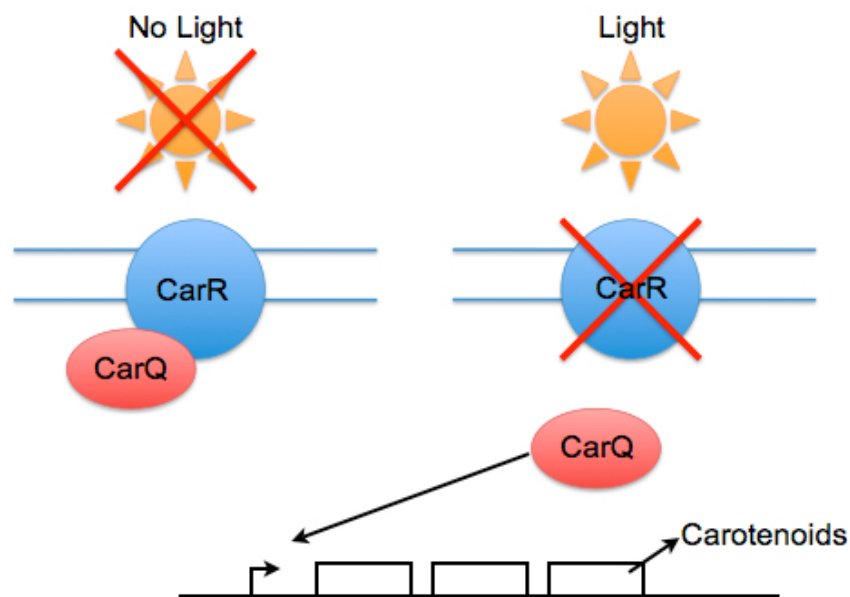
Figure 2.5: Model of regulation of light-induced carotenogenesis in *M. xanthus*. In the presence of high intensity light, CarR is degraded, releasing CarQ to mediate the transcription of genes that produce photoprotective carotenoids. (Adapted from Whitworth & Hodgson, 2001)

It has been proposed that TRs, such as the NtrC-like EBPs and the ECF sigma factors, control most processes that occur during the lifecycle of *M. xanthus* (Jelsbak *et al.*, 2005). Perhaps this is due to their ability to respond to environmental cues. Because of their ability to respond to specific extracytoplasmic stress stimuli, it is believed the ECF sigma factors play an important role in the regulation of *M. xanthus* development. We have explored this possibility by examining mutant strains under development conditions. Interestingly, when using the standard development assay, only two of the 33 ECF mutant strains examined showed an abnormal phenotype. In Chapter 4, data will be presented that shows, when assayed under different conditions, the ECF sigma factors do, in fact, play an important role in *M. xanthus* development.

Prior to the work presented in Chapter 5, no TRs had been identified to directly regulate chemotaxis. There have been limited efforts to make such identifications, largely due to the lack of a specific assay and the controversy that exists over the mechanism *M. xanthus* uses to detect prey. It has been shown, however, that groups of *M. xanthus* cells are capable of directed movement toward prey (Pham *et al.*, 2005), and it is thought that this process occurs through chemotaxis (Shi *et al.*, 1993), elasticotaxis – responses to surface irregularities (Dworkin, 1983), or a combination of both. At least eight operons containing chemotaxis homologs are known to exist in the *M. xanthus* genome (Goldman *et al.*, 2006). Three of these, *frz*, *dif*, and *che4*, have been shown to play a role in the directed motility of *M. xanthus* in its environment (Bustamante *et al.*, 2004; Yang *et al.*, 1998; Vlamakis *et al.*, 2004). Interestingly, the NtrC-like

EBP CrdA is thought to regulate the transcription of the *che3* operon which plays a role in regulating development (Kirby & Zusman, 2003).

2.5 Summary

In nature, many biofilms represent self-organized systems. This is evident by the high frequency of pattern formation. These patterns are emergent if they cannot be predicted by observing the behavior of the component cells. Two of these patterns, development and chemotaxis, can be easily observed in *M. xanthus* swarms.

Viewed from the group perspective of a swarm, development and chemotaxis toward prey are clearly different behaviors. However, viewed at the individual perspective of a cell, this difference is less obvious. An individual *M. xanthus* cell observed during development will look much the same as one observed during chemotaxis; it moves, sends and receives signals, and coordinates its behavior with surrounding cells. The differences between development and chemotaxis only become obvious at swarm-level, over time; they cannot be predicted based on the observation of individual cells. Hence development and chemotaxis are emergent.

These behaviors are manifest based on the environmental conditions – usually nutrient stress. In order for the swarm to efficiently respond to these stresses, it relies on a robust signal transduction network. NtrC-like EBPs are known to play an important role in all aspects of the *M. xanthus* lifecycle including the control of pattern formation. They are also known to act as response

regulators in two-component networks. The ECF Sigma factors are involved in stress responses and presumed to be important in the regulation of development. Because of their importance, we believe that fully understanding the mechanisms behind *M. xanthus*' robust and redundant signal transduction networks will give insight to the evolution of multicellularity (self-organization).

2.6 References

Ben-Jacob, E. (2003). Bacterial self-organization: co-enhancement of complexification and adaptability in a dynamic environment. *Philos Transact A Math Phys Eng Sci, 361*, 1283-312.

Black, W. P., & Yang, Z. (2004). *Myxococcus xanthus* chemotaxis homologs DifD and DifG negatively regulate fibril polysaccharide production. *J Bacteriol, 186*, 1001-8.

Bonner, J. T. (2000). *First signals: the evolution of multicellular development*. Princeton: Princeton University Press.

Burchard, R. P. (1982). Trail following by gliding bacteria. *J Bacteriol, 152*, 495-501.

Buss (1987). *The Evolution of Individuality*. Princeton, NJ: Princeton University Press.

Bustamante, V. H., Martínez-Flores, I., Vlamakis, H. C., & Zusman, D. R. (2004). Analysis of the Frz signal transduction system of *Myxococcus xanthus* shows the importance of the conserved C-terminal region of the cytoplasmic chemoreceptor FrzCD in sensing signals. *Mol Microbiol, 53*, 1501-13.

Caberoy, N. B., Welch, R. D., Jakobsen, J. S., Slater, S. C., & Garza, A. G. (2003). Global mutational analysis of NtrC-like activators in *Myxococcus xanthus*: identifying activator mutants defective for motility and fruiting body development. *J Bacteriol, 185*, 6083-94.

Camazine, S., Deneubourg, J. L., Franks, N. R., Sneyd, J., Theraylaz, G., & Bonabeau, E. (2001). *Self-organization in biological systems*. Princeton University Press.

Corning, P. A. (2002). The Re-Emergence of "Emergence": A Venerable Concept in Search of a Theory. *Complexity, 7*, 18-30.

Crespi (2001). The evolution of social behavior in microorganisms. *Trends Ecol Evol, 16*, 178-83.

Dworkin (1973). Cell-cell interactions in the myxobacteria. In *Symp Soc Gen Microbiol* (pp. 125-42).

Dworkin, M. (1983). Tactic behavior of *Myxococcus xanthus*. *J Bacteriol, 154*, 452-9.

Dworkin, M. (1999). Fibrils as extracellular appendages of bacteria: their role in contact-mediated cell-cell interactions in *Myxococcus xanthus*. *Bioessays, 21*, 590-5.

Dworkin, M., & Eide, D. (1983). *Myxococcus xanthus* does not respond chemotactically to moderate concentration gradients. *J Bacteriol, 154*, 437-42.

Fontes, M., & Kaiser, D. (1999). Myxococcus cells respond to elastic forces in their substrate. *Proc Natl Acad Sci U S A, 96*, 8052-7.

Goldman, B. S., Nierman, W. C., Kaiser, D., Slater, S. C., Durkin, A. S., Eisen, J., *et al.* (2006). Evolution of sensory complexity recorded in a myxobacterial genome. *Proc Natl Acad Sci U S A, 103*, 15200-5.

Gorham, H. C., McGowan, S. J., Robson, P. R., & Hodgson, D. A. (1996). Light-induced carotenogenesis in *Myxococcus xanthus*: light-dependent membrane sequestration of ECF sigma factor CarQ by anti-sigma factor CarR. *Mol Microbiol, 19*, 171-86.

Gorski, L., & Kaiser, D. (1998). Targeted mutagenesis of sigma54 activator proteins in *Myxococcus xanthus*. *J Bacteriol, 180*, 5896-905.

Gorski, L., Gronewold, T., & Kaiser, D. (2000). A sigma(54) activator protein necessary for spore differentiation within the fruiting body of *Myxococcus xanthus*. *J Bacteriol, 182*, 2438-44.

Ho, J., & McCurdy, H. D. (1979). Demonstration of positive chemotaxis to cyclic GMP and 5'-AMP in *Myxococcus xanthus* by means of a simple apparatus for generating practically stable concentration gradients. *Can J Microbiol, 25*, 1214-8.

Hodgkin, J., & Kaiser, D. (1979). Genetics of gliding motility in *Myxococcus xanthus* (Myxobacterales): genes controlling movement of single cells. . *Mol Gen Genet, 171*, 167-76.

Hodgkin, J., & Kaiser, D. (1979). Genetics of gliding motility in *Myxococcus xanthus* (Myxobacterales): two gene systems control movement. *Mol Gen Genet, 171*, 177-91.

Jelsbak, L., Givskov, M., & Kaiser, D. (2005). Enhancer-binding proteins with a forkhead-associated domain and the sigma54 regulon in *Myxococcus xanthus* fruiting body development. *Proc Natl Acad Sci U S A, 102*, 3010-5.

Kaiser, D. (2001). Building a multicellular organism. *Annu Rev Genet, 35*, 103-23.

Kaiser, D. (2003). Coupling cell movement to multicellular development in myxobacteria. *Nat Rev Microbiol, 1*, 45-54.

Kaiser, D. (2004). Signaling in myxobacteria. *Annu Rev Microbiol, 58*, 75-98.

Kaiser, D. (2006). A Microbial Genetic Journey. *Annu Rev Microbiol, 60*, 1-25.

Kaiser, D., Manoil, C., & Dworkin, M. (1979). Myxobacteria: cell interactions, genetics, and development. *Annu Rev Microbiol, 33*, 595-639.

Kearns, & Shimkets (1998). Chemotaxis in a gliding bacterium. *Proc Natl Acad Sci U S A, 95*, 11957-62.

Kirby, J. R., & Zusman, D. R. (2003). Chemosensory regulation of developmental gene expression in *Myxococcus xanthus*. *Proc Natl Acad Sci U S A, 100*, 2008-13.

Kreft, J. U. (2004). Biofilms promote altruism. *Microbiology, 150*, 2751-60.

Kreft, J. U., & Bonhoeffer, S. (2005). The evolution of groups of cooperating bacteria and the growth rate versus yield trade-off. *Microbiology, 151*, 637-41.

Kroos, L. (2007). The Bacillus and Myxococcus developmental networks and their transcriptional regulators. *Annu Rev Genet, 41*, 13-39.

Kuner, J. M., & Kaiser, D. (1982). Fruiting body morphogenesis in submerged cultures of *Myxococcus xanthus*. *J Bacteriol, 151*, 458-61.

Lonetto, M. A., Brown, K. L., Rudd, K. E., & Buttner, M. J. (1994). Analysis of the Streptomyces coelicolor sigE gene reveals the existence of a subfamily of eubacterial RNA polymerase sigma factors involved in the regulation of extracytoplasmic functions. *Proc Natl Acad Sci U S A, 91*, 7573-7.

Lu, A., Cho, K., Black, W. P., Duan, X. Y., Lux, R., Yang, Z., *et al.* (2005). Exopolysaccharide biosynthesis genes required for social motility in *Myxococcus xanthus*. *Mol Microbiol, 55*, 206-20.

McBride, M. J. (2001). Bacterial gliding motility: multiple mechanisms for cell movement over surfaces. *Annu Rev Microbiol, 55*, 49-75.

Mignot, T., Merlie, J. P., & Zusman, D. R. (2005). Regulated pole-to-pole oscillations of a bacterial gliding motility protein. *Science, 310*, 855-7.

Mignot, T., Shaevitz, J. W., Hartzell, P. L., & Zusman, D. R. (2007). Evidence that focal adhesion complexes power bacterial gliding motility. *Science, 315*, 853-6.

Missiakas, D., & Raina, S. (1998). The extracytoplasmic function sigma factors: role and regulation. *Mol Microbiol, 28*, 1059-66.

Pennisi, E. (2005). How did cooperative behavior evolve? *Science, 309*, 93.

Pham, V. D., Shebelut, C. W., Diodati, M. E., Bull, C. T., & Singer, M. (2005). Mutations affecting predation ability of the soil bacterium *Myxococcus xanthus*. *Microbiology, 151*, 1865-74.

Reichenbach, H. (1999). The ecology of the myxobacteria. *Environ Microbiol, 1*, 15-21.

Rosenberg, E., Keller, K. H., & Dworkin, M. (1977). Cell density-dependent growth of *Myxococcus xanthus* on casein. *J Bacteriol, 129*, 770-7.

Sachs, J. L., Mueller, U. G., Wilcox, T. P., & Bull, J. J. (2004). The evolution of cooperation. *Q Rev Biol, 79*, 135-60.

Shi, W., & Zusman, D. R. (1994). Sensor/response in *Myxococcus xanthus* to attractants and repellents requires the frz signal transduction system. *Res Microbiol, 145*, 431-5.

Shi, W., & Zusman, D. R. (1994). Sensory adaptation during negative chemotaxis in *Myxococcus xanthus*. *J Bacteriol, 176*, 1517-20.

Shi, W., Köhler, T., & Zusman, D. R. (1993). Chemotaxis plays a role in the social behaviour of *Myxococcus xanthus*. *Mol Microbiol, 9*, 601-11.

Shi, W., Köhler, T., & Zusman, D. R. (1994). Isolation and phenotypic characterization of *Myxococcus xanthus* mutants which are defective in sensing negative stimuli. *J Bacteriol, 176*, 696-701.

Shimkets, L. J. (1999). Intercellular signaling during fruiting-body development of *Myxococcus xanthus*. *Annu Rev Microbiol, 53*, 525-49.

Shimkets, L. J., Dworkin, M., & Keller, K. H. (1979). A method for establishing stable concentration gradients in agar suitable for studying chemotaxis on a solid surface. *Can J Microbiol, 25*, 1460-7.

Spormann, A. M. (1999). Gliding motility in bacteria: insights from studies of *Myxococcus xanthus*. *Microbiol Mol Biol Rev, 63*, 621-41.

Spormann, A. M., & Kaiser, A. D. (1995). Gliding movements in *Myxococcus xanthus*. *J Bacteriol, 177*, 5846-52.

Sun, H., & Shi, W. (2001). Genetic studies of mrp, a locus essential for cellular aggregation and sporulation of *Myxococcus xanthus*. *J Bacteriol, 183*, 4786-95.

Sun, H., Zusman, D. R., & Shi, W. (2000). Type IV pilus of *Myxococcus xanthus* is a motility apparatus controlled by the frz chemosensory system. *Curr Biol, 10*, 1143-6.

Szathmáry, E., & Smith, J. M. (1995). The major evolutionary transitions. *Nature, 374*, 227-32.

Taylor, R. G., & Welch, R. D. (2008). Chemotaxis as an emergent property of a swarm. *Submitted,*

Tieman, S., Koch, A., & White, D. (1996). Gliding motility in slide cultures of *Myxococcus xanthus* in stable and steep chemical gradients. *J Bacteriol, 178*, 3480-5.

Velicer, G. J. (2003). Social strife in the microbial world. *Trends Microbiol, 11*, 330-7.

Velicer, G. J., Kroos, L., & Lenski, R. E. (2000). Developmental cheating in the social bacterium *Myxococcus xanthus*. *Nature, 404*, 598-601.

Vlamakis, H. C., Kirby, J. R., & Zusman, D. R. (2004). The Che4 pathway of *Myxococcus xanthus* regulates type IV pilus-mediated motility. *Mol Microbiol, 52*, 1799-811.

Ward, M. J., Lew, H., & Zusman, D. R. (2000). Social motility in *Myxococcus xanthus* requires FrzS, a protein with an extensive coiled-coil domain. *Mol Microbiol, 37*, 1357-71.

Ward, M. J., Lew, H., Treuner-Lange, A., & Zusman, D. R. (1998). Regulation of motility behavior in *Myxococcus xanthus* may require an extracytoplasmic-function sigma factor. *J Bacteriol, 180*, 5668-75.

Westerhoff, H. V. (1985). Thermodynamics and control of proton motive free-energy transduction. *Biomed Biochim Acta, 44*, 929-41.

Whitworth, D. E., & Hodgson, D. A. (2001). Light-induced carotenogenesis in *Myxococcus xanthus*: evidence that CarS acts as an anti-repressor of CarA. *Mol Microbiol, 42*, 809-19.

Wolgemuth, C., Hoiczyk, E., Kaiser, D., & Oster, G. (2002). How myxobacteria glide. *Curr Biol, 12*, 369-77.

Wu, S. S., & Kaiser, D. (1995). Genetic and functional evidence that Type IV pili are required for social gliding motility in *Myxococcus xanthus*. *Mol Microbiol, 18*, 547-58.

Wyman, C., Rombel, I., North, A. K., Bustamante, C., & Kustu, S. (1997). Unusual oligomerization required for activity of NtrC, a bacterial enhancer-binding protein. *Science, 275*, 1658-61.

Yang, C., & Kaplan, H. B. (1997). *Myxococcus xanthus* sasS encodes a sensor histidine kinase required for early developmental gene expression. *J Bacteriol, 179*, 7759-67.

Yang, Z., Geng, Y., Xu, D., Kaplan, H. B., & Shi, W. (1998). A new set of chemotaxis homologues is essential for *Myxococcus xanthus* social motility. *Mol Microbiol, 30*, 1123-30.

Zusman, D. R., Scott, A. E., Yang, Z., & Kirby, J. R. (2007). Chemosensory pathways, motility and development in *Myxococcus xanthus*. *Nat Rev Microbiol, 5*, 862-72.

Chapter 3: Methods for Studying Swarm-level Emergent Behaviors

3.1 Introduction

M. xanthus development and chemotaxis have significant similarities that make them suitable for comparison. They both involve coordinated changes in motility that result in large clusters of cells directing their movements to fixed points on a surface. This coordinated motility is likely the result of cell-cell communication, evidenced by the fact that neither behavior is possible by individual cells (Kaiser, 2004; Taylor & Welch, 2008). Both development and chemotaxis satisfy all of the conditions necessary to be considered emergent; differences in individual cell behavior between development and chemotaxis are likely to be small and non-obvious. Both development and chemotaxis are behaviors that can be quantified, such that it is possible to characterize and correlate relatively subtle differences in the success of mutants. Although these behaviors are sufficiently similar to permit comparison, they are also different enough that they can be separated. Development and chemotaxis take place under very different experimental conditions (nutrient deprivation versus a gradient of nutrient), and they have completely different fates (spore-containing fruiting bodies versus movement towards a nutrient source). To aid in the study of these two behaviors, we developed a set of tools, which allow us to quickly, and efficiently predict/identify, generate, and characterize large numbers of mutant strains. In this chapter, these tools will be introduced and the materials and methods used to conduct the research described in this dissertation will be presented.

3.2 Development of Genomic Tools for *M. xanthus*

Historically, random transposon mutagenesis – disruption of an ORF through DNA recombination – was utilized. Although some important research is based on this, random mutagenesis methods have a low success rate for targeting genes of interest; only 1% of 12,000 *magellan-4* insertions (a transposon mutagenesis process) inactivated A-motility in an S– background (Youderian *et al.*, 2003). In 2001, the *M. xanthus* pseudo-genome (a 4 – 4.5X average coverage sequenced by the Monsanto Company) was released (Jakobsen *et al.*, 2004). In 2004, the sequence was completed and released to the public by the Institute for Genomic Research (TIGR). This reveled that the genome incodes an estimated 7,457 genes and made it possible to make a targeted selection of each based on paralogy to known motility-linked proteins (Caberoy *et al.*, 2003). This, however, yielded only a 10% success rate of targeting genes with actual motility defects.

The TIGR annotation of the *M. xanthus* genome relies primarily on BLAST to assign a function to each open reading frame (ORF). These functions are based on pairwise sequence homology. While BLAST is invaluable in the first stage of genome annotation, it is still fundamentally a genetic method rather than a genomic method. A solitary BLAST result only describes pairwise relationships between a query gene and a database of external genes, and does not directly provide information on the possible interaction partners of a gene within a genome. An annotation that provides data on the possible interactions within a

genome is referred to as a mesoscale annotation because it parses a genome into subsets of genes that work together.

The genome sequence of any organism contains far more information than is gained from pairwise BLAST. The computational detection of these interacting sets, or modules (Hartwell et al., 1999) is a topic of considerable interest, and several mesoscale annotations have recently been developed. These methods include the use of gene fusions as "Rosetta Stones" (Marcotte *et al.*, 1999), the tracking of correlated mutations to infer interactions (Gertz *et al.*, 2003; Pazos & Valencia, 2002), the enumeration of conserved operons (Overbeek *et al.*, 1999), and the calculation of phylogenetic profiles (Pellegrini *et al.*, 1999). A host of novel approaches for visualizing high-dimensional biological data sets have been described, including hierarchical clustering (Eisen *et al.*, 1998), planar graph drawing (Barabási & Oltvai, 2004), singular value decomposition (Alter *et al.*, 2000), and variants of multidimensional scaling (Werner-Washburne *et al.*, 2002; Kim *et al.*, 2001). The development of these algorithms coincided with a rapid rise in the number of sequenced genomes, a data set that presents particularly attractive opportunities for computational module detection.

3.2.1 Phylogenomics

We have developed and tested an *M. xanthus* phylogenomic map (Srinivasan *et al.*, 2005). Phylogenomics is a mesoscale annotation based on the premise that pairs of sequence-dissimilar ORFs that are consistently co-inherited in the same

sets of organisms are likely to be functionally linked (Marcotte *et al.*, 1999). By comparing each ORF within the genome of *M. xanthus* against the complete set of ORFs within the genomes of over 350 sequenced prokaryotes, we predicted the characterization each *M. xanthus* ORF according to its evolutionary history. These predictions are then visualized through a combination of multidimensional scaling and force-directed placement using the computer program VxInsight (Sandia National Laboratories). The resulting visualization is a topographical map that clusters genes with similar evolutionary histories into mountains, which can then be annotated to reflect likely functional groups. To experimentally validate the map, we hypothesized that the disruption of different genes within the same predicted functional module (mountain) would produce similar phenotypes, since each disruption might cause the same network to fail. We should therefore be able to predict the phenotype of mutants of uncharacterized genes based on their phylogenomic proximity to genes of known function. To this end, we used known motility genes as phylogenomic map 'landmarks' around which more ORFs were selected for disruption. A total of 15 uncharacterized ORFs in five mountains were chosen in this manner as shown in Figure 3.1. Each ORF was then disrupted using targeted mutagenesis and experimentally validated. Here, the experimental methodology used to verify the predictions is described.
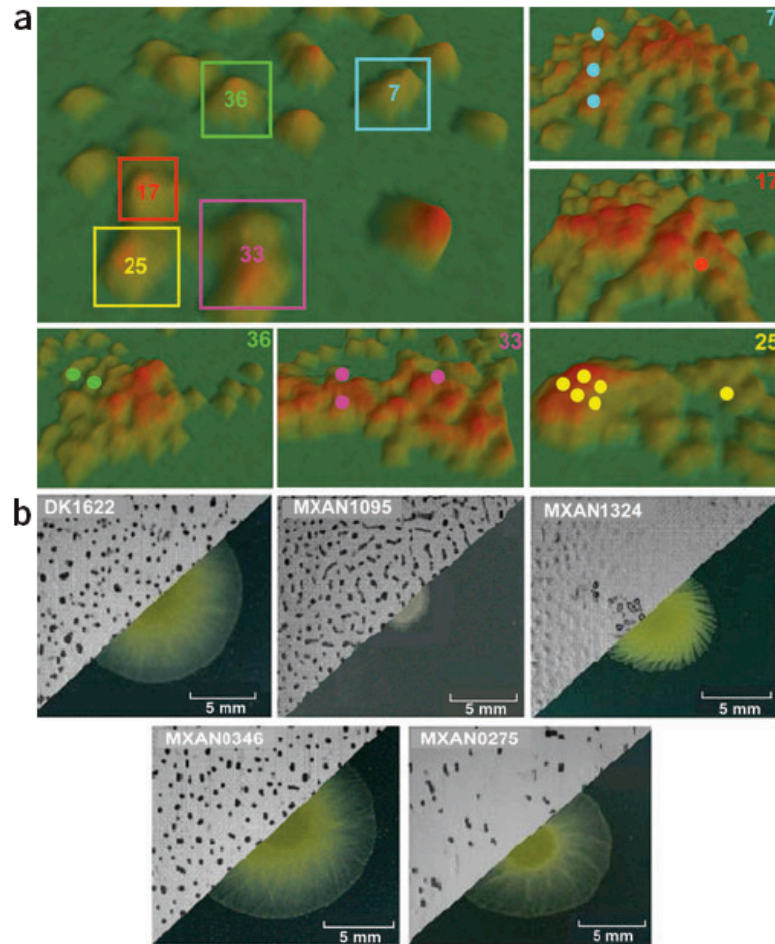
Figure 3.1: Experimental validation of phylogenomic map predictions in *M. xanthus*. (a) Colored boxes denote mountains selected for experimental validation. The specific proteins that were selected for disruption are colored in each medium resolution view. (b) Assay images of representative mutant strains displaying aggregation (top) and growth (bottom) phenotypes. From left to right: DK1622 wild type (+/+), MXAN1095 (+/–), MXAN1324 (–/–), MXAN0346 (+/+), and MXAN0275 (–/+).

Verification of functional interactions predictions proposed via

phylogenomic mapping was accomplished through the generation of mutant *M.*

xanthus strains. Strain creation was accomplished through homologous

recombination, a target mutagenesis method that is widely used in the field of *M.*

xanthus research (Plamann *et al.*, 1994). In general, a plasmid containing

internal fragments of the target gene along with a marker gene that confers

kanamycin resistance is engineered, transformed into *Escherichia coli*, multiplied,

extracted, and allowed to undergo homologous recombination with the genome of wild-type *M. xanthus* cells (Figure 3.2). Colonies of successful transformants are selected using the marker gene and tested for phenotype deficiencies. Plasmid insertion it confirmed via Southern blot analysis.
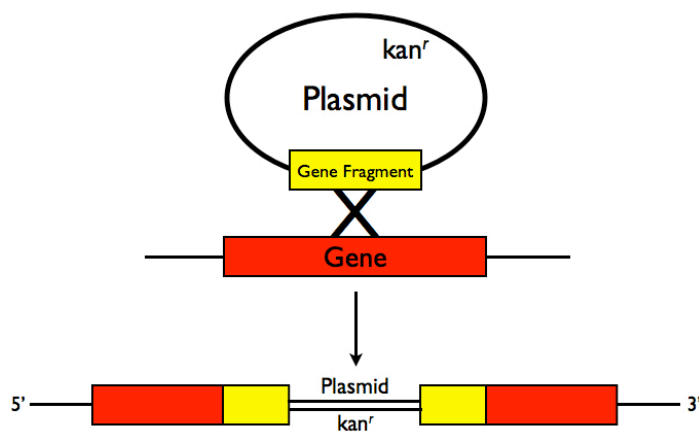
Figure 3.2: Disruption of target genes by homologous recombination. Internal fragments of the target gene are cloned into a plasmid vector that confers resistance to kanamycin. After electroporation of the plasmid clones into wild-type *M. xanthus* cells, a single homologous crossover produces a tandem duplication of the internal fragment and incorporation of the vector into the chromosomal copy of the gene. The likely result of the crossover is a disrupted copy of the target gene. (Adapted from Caberoy *et al.*, 2003).

Confirmation of phylogenomic mapping functional interaction predictions for *M. xanthus* was done through aggregation and swarm expansion assays. Both of these assays are standard phenotype assays that are widely used and accepted by the community of researchers that study *M. xanthus* (Whitworth, 2008).

Results. When assayed for defects in swarm expansion and aggregation, 12 of the 15 ORFs targeted (for disruption on the basis of phylogenomic proximity to known motility proteins) displayed defects in either individual motility or development (Table 3.1). This success rate of 80% significantly exceeds

other methods of finding new genes involved in *M. xanthus* motility. The

outcome of the plasmid insertion protocol is similar to the effect of random

transposon mutagenesis – disruption of an ORF through DNA recombination.

Again, other mutagenesis methods have a much lower success rate; only 1% in

the case of *magellan-4* insertions and only 10% in mutations based on paralogy.

Given the conservative estimate that 5% of *M. xanthus* proteins are essential for

motility (Kroos *et al.*, 1990; Youderian *et al.*, 2003) and that 2% of all mutants are

defective for development (Kroos *et al.*, 1990), it is highly unlikely that 12 of the

15 ORFs chosen using phylogenomic mapping would have defects in these

motility pathways if chosen at random (based on Youderian *et al.* and Caberoy *et*

al. results). Thus, we believe the phylogenomic map will be a crucial tool to help

elucidate the mechanics of both development and chemotaxis.

Table 3.1: Mutant phenotypes of proteins selected for disruption using the *M. xanthus* phylogenomic map. We chose proteins that were likely to give phenotypes of interest, particularly with respect to motility and cellular development. Each protein was assayed for normal (+) or defective (–) growth (cell motility) or development (coordinated swarm motility) as compared to *M. xanthus* wild type. These results show that 12 out of 15 (80%) proteins are deficient for swarm expansion or aggregation.

Mount	MXAN	Swarm Expansion	Development
7	MXAN6450	–	–
7	MXAN2136	+	+
7	MXAN7171	–	+
17	MXAN3003	+	–
25	MXAN1448	+	–
25	MXAN0346	+	+
25	MXAN1995	–	–
25	MXAN4718	–	+
25	MXAN1095	–	+
25	MXAN0275	–	–
33	MXAN5605	–	–
33	MXAN5610	–	–
33	MXAN2648	–	–
36	MXAN2464	+	+
36	MXAN1324	–	–

3.2.2 Coexpression

The completion of whole genome sequences allowed for the development of new tools to characterize the interactions among genes. Microarray expression experiments have become indispensable for researchers who study gene function. Genes can now be monitored for expression during development, and new mesoscale annotation methods have been developed to further enhance our understanding of gene function. Recent microarray expression data for *M. xanthus* has been used to create a coexpression map (Suen *et al.*, 2006). The authors obtained a total of 212 *M. xanthus* microarray experiments spanning multiple experimental conditions from the laboratories of Professor Anthony Garza (Syracuse University) and Professor Mitchell Singer (University of California, Davis).

This form of annotation clusters groups of genes that are co-expressed within microarray experiments and is visualized in the same manner as the phylogenomic map. The basic hypothesis behind this type of clustering analysis is that genes that are coexpressed are likely to be functionally linked (Eisen *et al.*, 1998; Ge *et al.*, 2001; Hughes *et al.*, 2000). This technique was successfully applied to over 500 microarray experiments for *Caenorhabditis elegans* (Kim *et al.*, 2001), demonstrating that functionally related ORFs could be grouped according to their gene expression patterns across different experimental conditions. The use of the coexpression map is discussed in detail in Chapter 6.

3.3 Efficient Phenotype Characterization

In order to efficiently generate and characterize the large number of predictions

generated by the phylogenomic and coexpression maps, several new assay

methods have been developed. Mutant strains of the predicted ORFs can now

be generated 96 at a time in a high-throughput manner. These mutant strains

can be characterized by employing a custom microscope cluster and a novel

assay capable of processing 8 mutant strains in a 24-hour period. When these

methods are used in concert, the characterization of mutant strains is no longer a

rate limiting process.

3.3.1 High-Throughput Mutagenesis

In order to characterize the large number of predictions generated by the

phylogenomic and coexpression maps, we needed an efficient way to generate

multiple targeted mutants at one time. To accomplish this, we developed a high-

throughput mutagenesis protocol based on the standard homologous

recombination protocol mentioned above. This work is currently being prepared

for publication.

Extract chromosomal DNA. Wild-type *M. xanthus* culture were

inoculated into a flask containing 10 ml of nutrient-rich CTTYE media (1.0%

Casitone (Difco Laboratories), 0.5% yeast extract (Difco Laboratories), 10.0 mM

Tris-HCl (pH 8.0), 1.0 mM KH_2PO_4, 8.0 mM $MgSO_4$) and incubated at 32°C with

vigorous swirling until the cells reached mid-exponential growth phase (5×10^8

cells/ml). The cells (3 mL) were collected and pelleted by centrifugation (16,300

$\times$ g). The supernatant was discarded and the remaining cell pellet was used for

genomic DNA (gDNA) isolation using a Wizard Genomic DNA Extraction Kit

(Promega). The following changes were made to the genomic DNA isolation

instructions: during the last step, the pellet was re-hydrated by re-suspending in

50 μl of DNase/RNase free water (Gibco) and storing at 4°C overnight.

Electrophoresis was carried out and documented to confirm the gDNA isolation

succeeded.

Polymerase Chain Reaction. Primers corresponding to 400-600 base

pair (bp) gene fragments for each ORF were selected using the program Primer3

(http://frodo.wi.mit.edu/primer3/input.htm). The forward and reversed primers

were ordered (Invitrogen) and shipped pooled and lyophilized in 96-well plates.

The primers were re-hydrated to 50 pmole in DNase/RNase free water. The

PCR reaction was prepared with a master mix outlined in Table 3.2.

Table 3.2: PCR master mix components. The following were mixed together in the amounts shown to
generate a PCR master mix. Note: More mix was generated than necessary to account for discrepancies in
aliquoting.

Amount	Content
1.5 ml x 110	gDNA template
0.5 ml x 110	10mM dNTP (New England Biolabs)
2.5 ml x 110	10 X Buffer (New England Biolabs)
0.5 ml x 110	50mM MgCl2 (Invitrogen)
1.25 ml x 96	Dimethyl sulfoxide (Sigma)
0.25 ml x 96	Recombinant Taq DNA Polymerase at 5 units per 1 ml (Invitrogen)

Next, 4 μl of the re-hydrated pooled primers and 6.5 μl of the master mix were

added to each well of a 96-well PCR plate using a 12-channel multichannel

pipette (Eppendorf). The PCR plate was sealed with foil and the reaction carried

out in a PTC-225 DNA Engine Tetrad Thermal Cycler (MJ Research)

programmed using the following settings.

> Cycle Settings:
> 1. 1 cycle: 4 minutes at 95°C
> 2. 30 cycles:
>   a. 30 seconds at 95°C
>   b. 1 minute at 5°C below the primer's annealing temperature (2-3°C below lowest primer's annealing temperature if the primers have different annealing temperatures)
>   c. 1 to 3 minutes at 72°C (time depends on length of product – approximately 1 minute per Kbase)
> 3. 1 cycle: 10 minutes at 72°C
> 4. Hold at 2-10°C

To confirm the PCR reaction, 3 µl loading dye was added to 7 µl of the PCR

product. Each sample was loaded into its corresponding well of a 96-well E-Gel

pre-cast electrophoresis gel (Invitrogen) also loaded with 5 µl of E-Gel Low

Range Quantitative DNA Ladder (Invitrogen) as a marker in the marker lanes.

The results were documented using a Multi-Image Light Cabinet (Alpha Innotech

Corporation). Each unsuccessful reaction was repeated individually using the

conditions listed above. If the second attempt was unsuccessful, new primers for

that ORF were ordered.

Cloning and Electroporation into *E. coli.* Before starting the procedure,

96 Luria broth (LB) plates with Kanamycin (Kan) (1.0% tryptone (Difco), 0.5%

yeast extract (Difco), 0.5% NaCl, 1.5% Bacto Agar (Difco), and 0.1% Kan (Sigma,

40 mg/ml stock)) were prepared by spreading 80 µl of 20 mg/mL X-gal in

dimethylformamide (Research Products International) onto each. Next, the PCR

2.1-TOPO TA cloning kit (Invitrogen) was used according to the instructions

provided. The procedure was modified in the following ways: 1) the salt solution was diluted 1:4 with DNase/RNase free water, and 2) the electrocompetent *E. coli* strain Top10F cells were diluted by adding 20 μl of cold DNase/RNase free water to each vial. The TOPO reaction (Table 3.3) was performed in 96-well plates and incubated at room temperature for 30 minutes.

Table 3.3: TOPO reaction mixture per well. The following components were added to each well of a 96-well plate in the amounts listed.

Amount	Content
2 ml	PCR product (diluted 1:9 with DNase/RNase free water)
0.5 ml	salt solution (diluted 1:4 with DNase/RNase free water)
0.5 ml	TOPO vector

While the TOPO reaction was incubating, 20 μl of the diluted electrocompetent cells were pipetted into each well of a cold 96-well BTX Electroporation plate (BTX Harvard Apparatus). Keeping this plate on ice helps prevent arcing during electroporation (arcing reduces the electroporation success rate). After the incubation, the entire 3 μl of each TOPO reaction was added to its corresponding well of the electroporation plate. The cells were then electroporated by columns using a BTX HT-100 96 Well Plate Handler (Harvard Apparatus) attached to a BTX ECM630 electroporation unit (Harvard Apparatus) at 2500 V, 200 Ω, and 25 μF. (Figure 3.3, A)

Once all columns were electroporated, the cells were recovered by pipetting the contents of each well into 900 μl of LB that had been aliquoted into each well of a 96-deep well plate (Promega). The plates were covered with foil, and incubated at 37°C for one hour with gentle swirling. After this incubation,

500 μl of cells from each well were spread onto the LB+Kan+X-gal plate prepared earlier and incubated at 37°C overnight. If the plasmid was successfully incorporated into the *E. coli* cells, the colonies appeared white.

The following day, four white colonies from each plate were patched onto a new LB+Kan plate (to be more cost effective, each LB+Kan plate was divided into two sections so that two strains can be patched on each plate). In addition, 50 ml Erlenmeyer flasks containing 5 mL LB+Kan media (5mL of LB, 2.5 μl of 40 mg/ml Kanamycin) were inoculated with one culture from each of the 96 patched colonies. Both the liquid cultures and patch plates were incubated overnight at 37°C (liquid cultures were incubated with vigorous swirling). The original LB+Kan+X-gal culture plates were stored at 4°C as backup in case the patches failed to grow.

The next day, the patched plates that successfully grew colonies were moved to 4°C for short-term storage. Then, 7 ml of the 10 ml liquid culture was pelleted and resuspended in 2 ml of LB broth and 2 ml of 50% glycerol. This was split between two cryovials and placed at -80°C for long-term storage. The remaining 3 ml of liquid culture was pelleted and stored at -20°C in preparation for plasmid isolation.

96-well Plasmid Isolation (miniprep). The plasmids were isolated from the *E. coli* by using a Wizard SV Plasmid 96-well Purification Kit (Promega) while following the protocol provided with the following changes: at the last step the plasmids were eluted with 100 μl DNase/RNase free water. Plasmids were

stored in the provided 96-well elution plate at -20°C in preparation for insert

confirmation.

Gene Fragment Insert Confirmation. Each isolated plasmid was

checked for the correct insert by performing an EcoRI digest. The reaction (Table

3.4) was performed in 96-well plates and incubated overnight at 37°C.

Table 3.4: EcoRI digest mixture per well. The following components were added to each well of a 96-well plate in the amounts listed.

Amount	Content
8 µl	Plasmid
1 µl	EcoRI (Promega)
1 µl	BSA (provided with EcoRI) diluted 1:10 with DNase/RNase free water
2 µl	10× buffer (provided with EcoRI)
8 µl	DNase/RNase free water

After the overnight incubation, the digested plasmids were confirmed via

electrophoresis on a 96-well E-Gel with Low Range Quantitative DNA Ladder in

the marker lanes. If the PCR products were correctly inserted into the TOPO

vector, two bands were visible: the first band at 4 Kb corresponding to the TOPO

vector and the second band at the correct position based on the size of the PCR

product for that gene (approximately 400-600 bp). The results were

documented.

Plasmid Dialysis. All confirmed plasmid preps from the EcoRI digests

were dialyzed to reduce the chances of arcing during electroporation into *M.*

xanthus. Dialysis was performed in 8 × 12-well plates containing cold

DNase/RNase free water on which nitrocellulose dialyzing membranes (Miliipore)

with a pore size of 0.025 µm were floating. The plasmids were dialyzed by

carefully pipetting 20 µl of each onto the dialyzing membranes (Figure 3.3, B).

Plasmids were dialyzed for one hour at 4°C, which was experimentally found to

be a sufficient amount of time. After dialysis, the plasmids were carefully

pipetted off of membranes and into a new 96-well plate.

Electroporation of *M. xanthus*. In order to make wild-type *M. xanthus*

cells electrocompetent, 150 ml of mid-exponential growth phase cells (enough for

one 96-well plate dialyzed plasmids) were pelleted and washed three times in

100 ml of DNase/RNase free water. The cells were then re-suspended in 500 ml

of DNase/RNase free water and 50 µl aliquots were added to each well of 96-well

BTX Harvard electroporation plate at room temperature. To each well of cells, 6

µl of dialyzed plasmid was added. The plate containing the cells/plasmids was

electroporated by columns using a BTX HT-100 96 Well Plate Handler (Harvard

Apparatus) attached to a BTX ECM630 electroporation unit (Harvard Apparatus)

at 2400 V, 475 Ω, and 25 µF.   After electroporation, the cells were moved into a

96-deep well plate containing 2.5 ml CTTYE in each well and allowed to recover

overnight with vigorous swirling.

The next day, 500 µl of the recovered *M. xanthus* cells were added to a

tube containing of 3 mL CTTSA (1.0% Casitone (Difco Laboratories), 10.0 mM

Tris-HCl (pH 8.0), 1.0 mM KH_2PO_4, 8.0 mM $MgSO_4$, 0.7% Difco Bacto Agar) and

poured over the top of a CTTYE+Kan plates. The remaining recovered cells

were added to a second tube of CTTSA and poured over the top of a second

CTTYE+Kan plate. The plates were incubated at 32°C until individual colonies

appeared (5 to 10 days). Once colonies appeared, they were patched on fresh

CTTYE+Kan plate and incubated at 32°C. Once grown (approximately 3 days), the cells were added to Erlenmeyer flasks containing 10 ml CTTYE+Kan media and incubated overnight at 32°C with vigorous swirling.

Once the liquid culture reached mid-exponential growth phase, 3 ml was pelleted in preparation for correct insertion confirmation using the PCR protocol described below. The remainder of the culture was pelleted and resuspended in 2 ml CTTYE and 2 ml of 50% glycerol. This was split between two cryovials and placed at -80°C for long-term storage.

PCR confirmation. PCR was performed on chromosomal DNA isolated from each mutant strain as described above. The insert was verified by using the vector primers M13F and M13R (Invitrogen) in addition to a chromosomal DNA primer located 500 bp upstream from the start of the ORF (Viswanathan *et al.*, 2007). The use of both the forward and reverse M13 primers in addition the external chromosomal DNA primer gives the ability to not only detect if the insert was correctly incorporated into the genome, but to detect if there were multiple copies inserted.

Results. To test this high-throughput mutagenesis method, primers for previously uncharacterized ORF hypothesized to be one-component regulators were generated. By using the protocol outlined above, we have been able to disrupt 96 of these ORFs at a time with an overall success rate of 76%. The protocol has been streamlined (Figure 3.3, C) so that generating this number of mutant strains at one time takes approximately the same amount of time as generating one mutant strain. In addition, by using this protocol, we have been

able to reduce the cost associated with the standard one-at-a-time mutagenesis protocol from approximately $150.00 per mutation to $35.00 per mutation. With the success rate and the cost effectiveness of this high-throughput protocol, it is now feasible to generate an entire 'knock-out' library for *M. xanthus*. To this end, this protocol is currently being utilized in two laboratories: Dr. Kim Murphy (Waldorf College) is using it to generate mutant strains for all 2,924 hypothetical proteins found in *M. xanthus*, and Jinyuan Yang (Welch Lab, Syracuse University) is using it to generate mutant strains for the ATP-binding cassette (ABC) transporters in *M. xanthus*.

Step 1	Step 2	Step 3	Step 4	Step 5	Step 6
Primer Selection	Amplicons Generation (PCR)	Ligation into Plasmid	Electroporation into *E. coli*	*E. coli* Colony Selection	Plasmid Isolation
Whole Genome	High-Throughput	High-Throughput	High-Throughput	Serial	High-Throughput

Step 7	Step 8	Step 9	Step 10	Step 11	Step 12
Plasmid Dialysis	Electroporation into *M. xanthus*	*M. xanthus* Colony Selection	Genomic DNA Isolation	Confirmation (PCR)	Long-Term Storage
Serial	High-Throughput	Serial	High-Throughput	High-Throughput	Serial

Figure 3.3: High-throughput mutagenesis. (A) An image of the BTX HT-100 96-well plate handler (top) attached to a BTX ECM630 electroporation unit (bottom). A 96-well electroporation plate can be seen on top of the plate handler. (B) An image of the dialysis process being carried out 12-well plates. The plates

are on ice with nitrocellulose membranes visible in each well. (C) A flowchart of the high-throughput mutagenesis protocol.

3.3.2 Construction of Microscope Cluster and Analysis Tools

In order to efficiently characterize the swarm level, emergent behavior of the mutant strains generated by the protocol described above, we constructed a cluster of 8 microscopes, each capable of capturing time-lapse videos. Once captured, the videos are transferred to an analysis/storage computer with enough memory to process and store thousands of videos. In order to keep costs to a minimum, the microscope cluster was built in-house with off-the-shelf and refurbished parts. This setup has proven useful to several members of the *M. xanthus* community, including the laboratories of Professor David Zusman (University of California, Berkeley), Professor Lee Kroos (Michigan State University), and Professor Anthony Garza (Syracuse University). In addition, Professor Lawrence Shimkets (University of Georgia) has modified this setup to suit the needs of his laboratory.

Eight Nikon E400 microscopes were purchased and outfitted with 2X, 4X, and 10X objectives each. To cut costs, the microscopes were purchased as refurbished units. In addition, eight Insight2 cameras (Diagnostic Instruments, Inc.) and eight heated stages (20/20 Technologies) were purchased. The cameras were packaged with highly modifiable image acquisition software (SPOT), which eliminated the need to purchase expensive third party software. The SPOT application was installed on eight iBook G3 notebook computers (Apple, Inc.) that were purchased, at the time, as previous generation

technology. This made the computers extremely economical. To extend the

usefulness of the cluster, two microscopes were outfitted with fluorescence

capabilities by the addition of Uniblitz shutter controls (Vincent Associates) and a

quartz crystal light source (EXFO Life Science). To keep costs to a minimum, a

custom liquid light guide was manufactured in order to split the light source. This

allowed one light source to be used simultaneously by two microscopes. All the

various components were assembled in-house into nodes, each consisting of a

microscope, three objectives, an Insight camera, a heated stage, and a

controlling computer. Each of the eight nodes were networked together into a

cluster and linked to an Apple G4 tower computer which is used to compile,

analyze, and store the time-lapse videos generated by the cluster (Figure 3.4).

The G4 tower has been upgraded with a 1 terabyte RAID system. This large

amount of memory is needed to store the vast amount of data generated by the

cluster. Each 24-hour time-lapse image sequence (video) consists of up to 1,440

individual images each of which has a maximum resolution of 1600 x 1200

pixels. In other words, each video takes approximately 4.6 gigabytes of storage.
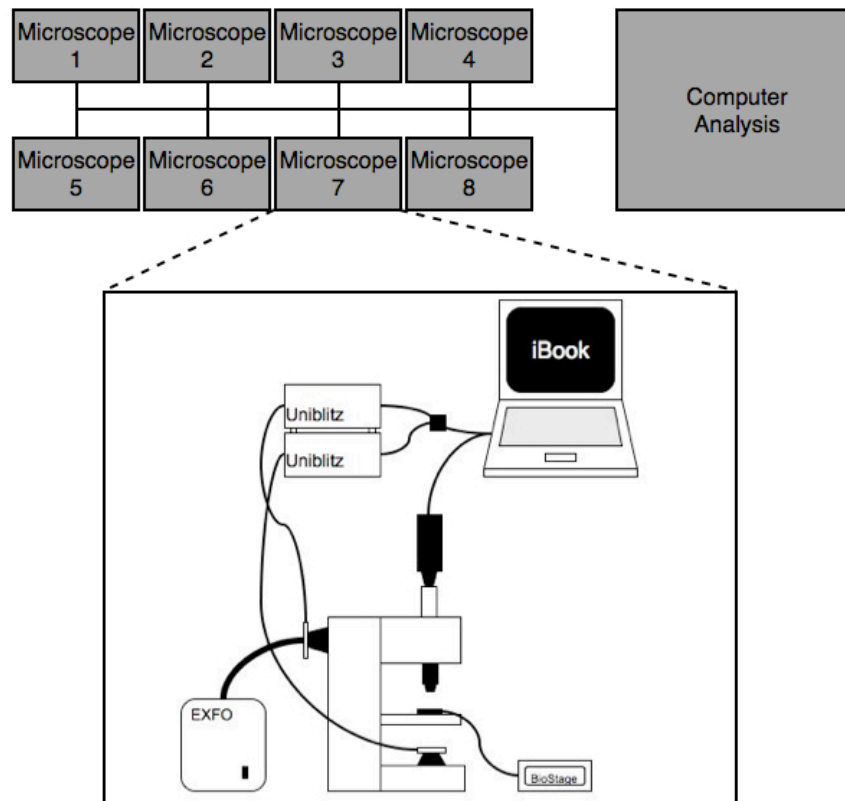
Figure 3.4: Welch laboratory microscope cluster. Each microscope node (inset) consists of a Nikon E400 microscope, objectives, a heated stage, an Insight camera, and a notebook computer. Each node is networked together and linked to a master controller computer. Two of the nodes are set up with fluorescence capabilities that consist of the EXFO light source and two Uniblitz shutters.

Building the cluster in house with off-the-shelf parts took a considerable amount of time and effort; however, the resulting setup represented a significant savings when compared to an out-of-the-box microscope cluster (a savings of 40% or approximately $80,000). In addition, the cluster is highly modifiable and easy to upgrade so that the usefulness of this system will not become obsolete.

3.3.3 Phenotypic Analysis

We developed an assay that allows us to efficiently and quickly capture multiple time-lapse videos of swarm-level emergent behavior. The assay is rigorous enough to allow consistent replication of quantifiable data and the resulting videos allow us to track subtle changes in swarm behavior. In addition to being rigorous, the assay is highly modifiable and can be used to collect data on both development and chemotaxis (discussed in detail in Chapters 4 and 5, respectively). The video capture is carried out on the cluster of custom microscopes discussed above. This work is currently being prepared for publication.

Time-lapse microcinematography (TM) has become a standard way to study prokaryotic motility (Curtis *et al.*, 2007; Mignot *et al.*, 2005; Stoodley *et al.*, 2001; O'Toole *et al.*, 2000; O'Toole & Kolter, 1998; Dalton *et al.*, 1994). Traditionally, TM is performed by using filter paper wicks, thin agar pads, or agar slabs as substrates (Dworkin, 1983; Dworkin & Eide, 1983; Wu & Kaiser, 1997; Bustamante *et al.*, 2004). When used to generate image sequences for general illustrations of bacterial movement, these methods are adequate and cheap. However, if image sequences are needed to generate reproducible and quantitatively rigorous data, these methods are time consuming, prone to desiccation, and unreliable. Variations due to human error could cause a wide array of problems, including irregularities in the agar surface that could dramatically affect the behavior of the bacteria being studied and differences in the focal plane from one side of the assay substrate to the other. To solve these problems, we have designed a TM chamber that is sufficiently rigorous to yield

reproducible results by employing the use of silicone gaskets that are both inexpensive and reusable. In addition, the chamber has proven to stay wet and aerobic for more than a week over a wide array of media types and agar concentrations. A brief summary of the chamber construction is provided here. In addition, the adaptability of the TM chamber is explained in detail. (For a detailed description of the chamber construction, see Appendix I)

The initial steps follow standard strain growth protocols such as the one discussed above. Once the cells have reached mid-exponential growth phase, they are harvested, washed, and concentrated. A sterile 2 x 2 cm, 0.5-mm-thick silicone rubber gasket (Grace Bio-Lab Inc.) is placed on top of a flame-sterilized glass cover slip to create a small well in the center. Media in 1% molten agar is cooled to 65°C and poured into the well and subsequently covered by a flame-sterilized glass microscope slide to flatten the agar. A second glass slide is placed underneath the cover slip for structural support and the complex is clamped together with binder clips until the agar has cooled and hardened. Once hardened, the binder clips and both slides are removed exposing the agar surface. Any visible water droplets are allowed to evaporate. A 0.5 µl aliquot of the concentrated *M. xanthus* cell culture is placed in the center of the agar and allowed to dry (< 1 minute). A second sterile gasket is placed on top of the first gasket to create an air space and the TM chamber is completed by placing a flame-sterilized microscope slide on top of this second gasket (Figure 3.5, A).
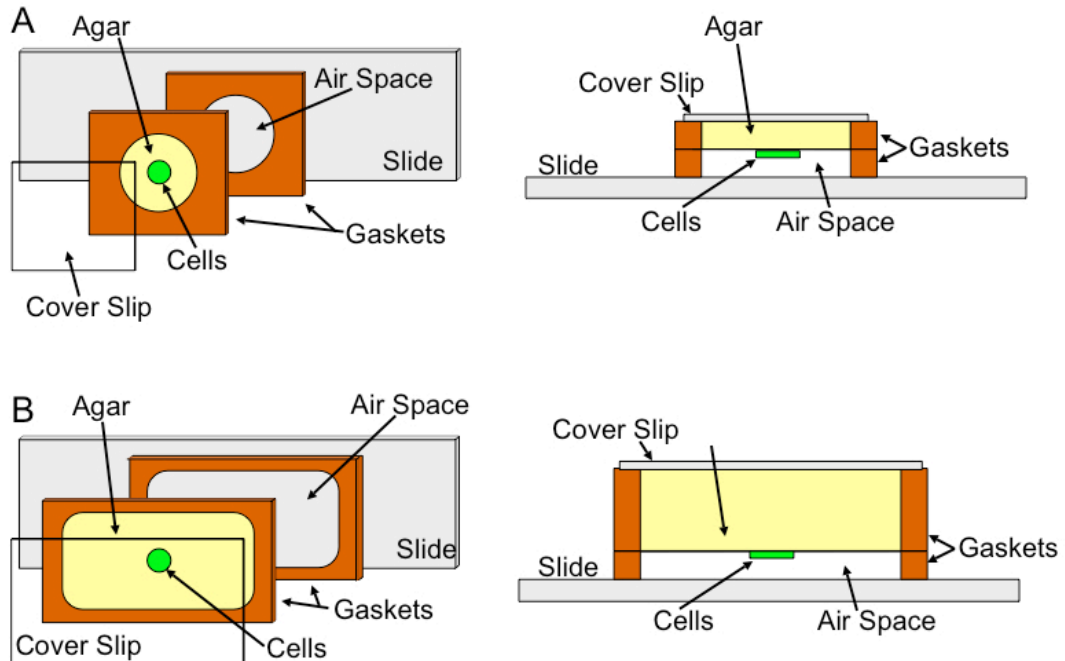
Figure 3.5: Cartoon illustration of the TM chamber. (A) shows the standard TM chamber in exploded view and cross section. (B) shows the use of larger gaskets.

The completed chamber is now placed on a heated stage of the microscope and images are acquired at preset intervals that are determined based on the motility rate of the cells. For example, individual *M. xanthus* cells move at a rate of approximately one cell length per minute. If images are acquired of an *M. xanthus* swarm at that same rate (one image per minute), the resulting time-lapse video will appear smooth during playback. Once the image acquisition is complete, the images are compiled into a sequential matrix and played back at a high enough rate that they appear to be moving (Figure 3.6). This time-lapse video can now be analyzed using a variety software packages.
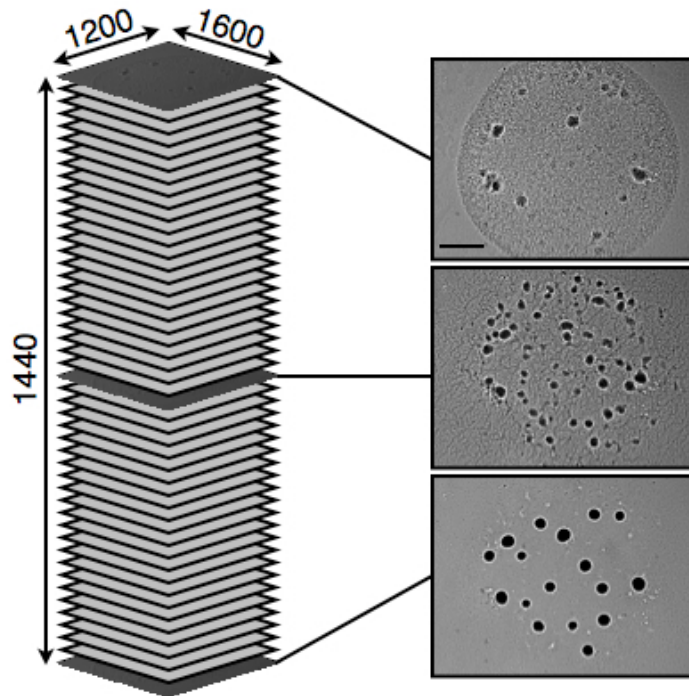
Figure 3.6: Sequential image matrix. This cartoon represents a stack of sequential images compiled into a video. If shown at a high enough rate, the images will appear as a smooth video.

Variations on Assay. The TM chamber is highly adaptable and can be used to visualize many different microorganisms under a variety of conditions. It has been used to successfully generate time-lapse videos of several prokaryotic behaviors including *M. xanthus* gliding motility, *Pseudomonas aeruginosa* twitching motility, *Seratia marscences* swarming motility, and the novel *Mycobacterium smegmata* sliding motility (Figure 3.7).
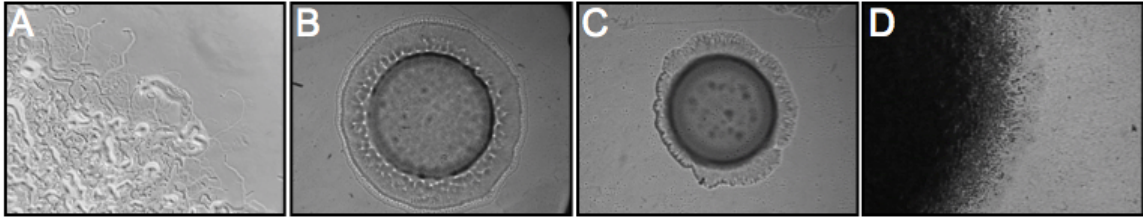
Figure 3.7: Adaptability of the TM chamber. (A) an image of *M. xanthus* gliding motility on CTTYE in 1.0% agar. (B) and (C) are images of *P. aeruginosa* twitching motility and *S. marscences* swarming motility, respectively. Both (B) and (C) were assayed on LB in 1.0% agar. (D) *M. smegmata* sliding motility on LB in 0.5% agar.

Variables in this assay can be environmental or genetic in nature. Because the most thoroughly studied *M. xanthus* behavior is development, we have developed a series of assays that manipulate nutrient levels, limiting them either in part or entirely. By these methods, we are able to observe and record swarm behavior under nutrient-permissive (swarm expansion) or nutrient-limiting (development and chemotaxis) conditions. Mutant cells can be incorporated into expanding or developing swarms, and they can represent the entire swarm or a fraction of it, thereby effectively creating a chimeric swarm. Mutant swarms can be used singularly as a means of testing phenotypic predictions that are based on analysis of the mutated gene. Chimeric swarms can be used to test the intercellular interactions of genes within a swarm.

Swarm visualization can be performed using either phase-contrast microscopy, which records the behavior of the swarm as a single entity, or fluorescence microscopy, which records the behavior of individual fluorescent cells that have been diluted in a non-fluorescent population (an example of a chimera).

The adaptability of the assay was extremely useful when examining *M. smegmata* sliding motility. This type of motility only manifests on soft agar (< 0.7% agar), which is extremely fragile and breaks easily. When soft agar is called for, larger gaskets can be used help to stabilize the media (Figure 3.5, B). The larger gaskets can also be useful when observing the interactions of multiple groups of cells (i.e. an *M. xanthus* swarm consuming prey bacteria).

The TM chamber has proven useful to several members of the *M. xanthus* community. John Merlie (Zusman Laboratory, University of California, Berkeley) used it to characterize the role of FrzS in *M. xanthus* social motility (Merlie *et al.*). Patrick Curtis (Shimkets Laboratory, University of Georgia) used it to discover that fruiting bodies are established vertically in a series of tiers, each involving the addition of a cell monolayer on top of the uppermost layer (Curtis *et al.*, 2007).

3.4 Summary

Traditional methods of searching for single gene function are often difficult and time consuming. Combining genome-scale data into a single, user-friendly map that groups ORFs together based on implied functionality, whether it be phylogenomics or coexpression, has provided easy access to the seemingly overwhelming amount of data in a raw genome sequence. While implied function does not necessarily equate to exact gene function, it is an important first step toward characterizing groups of genes into genetic networks. Utilizing the high-throughput mutagenesis protocol described here, we have the ability to

successfully generate large numbers of mutant strains in a short amount of time

and at a significant reduction in cost. Additionally, the construction of the

microscope cluster and the development of the TM chamber have provided the

ability to characterize those mutant strains efficiently and cheaply.

3.5 References

Alter, O., Brown, P. O., & Botstein, D. (2000). Singular value decomposition for genome-wide expression data processing and modeling. *Proc Natl Acad Sci U S A, 97*, 10101-6.

Barabási, A. L., & Oltvai, Z. N. (2004). Network biology: understanding the cell's functional organization. *Nat Rev Genet, 5*, 101-13.

Bustamante, V. H., Martínez-Flores, I., Vlamakis, H. C., & Zusman, D. R. (2004). Analysis of the Frz signal transduction system of *Myxococcus xanthus* shows the importance of the conserved C-terminal region of the cytoplasmic chemoreceptor FrzCD in sensing signals. *Mol Microbiol, 53*, 1501-13.

Caberoy, N. B., Welch, R. D., Jakobsen, J. S., Slater, S. C., & Garza, A. G. (2003). Global mutational analysis of NtrC-like activators in *Myxococcus xanthus*: identifying activator mutants defective for motility and fruiting body development. *J Bacteriol, 185*, 6083-94.

Curtis, P. D., Taylor, R. G., Welch, R. D., & Shimkets, L. J. (2007). Spatial Organization of *Myxococcus xanthus* During Fruiting Body Formation. *J Bacteriol, 189*, 9126-30.

Dalton, H. M., Poulsen, L. K., Halasz, P., Angles, M. L., Goodman, A. E., & Marshall, K. C. (1994). Substratum-induced morphological changes in a marine bacterium and their relevance to biofilm structure. *J Bacteriol, 176*, 6900-6.

Dworkin, M. (1983). Tactic behavior of *Myxococcus xanthus*. *J Bacteriol, 154*, 452-9.

Dworkin, M., & Eide, D. (1983). *Myxococcus xanthus* does not respond chemotactically to moderate concentration gradients. *J Bacteriol, 154*, 437-42.

Eisen, M. B., Spellman, P. T., Brown, P. O., & Botstein, D. (1998). Cluster analysis and display of genome-wide expression patterns. *Proc Natl Acad Sci U S A, 95*, 14863-8.

Ge, H., Liu, Z., Church, G. M., & Vidal, M. (2001). Correlation between transcriptome and interactome mapping data from Saccharomyces cerevisiae. *Nat Genet, 29*, 482-6.

Gertz, J., Elfond, G., Shustrova, A., Weisinger, M., Pellegrini, M., Cokus, S., *et al.* (2003). Inferring protein interactions from phylogenetic distance matrices. *Bioinformatics, 19*, 2039-45.

Hughes, T. R., Marton, M. J., Jones, A. R., Roberts, C. J., Stoughton, R., Armour, C. D., *et al.* (2000). Functional discovery via a compendium of expression profiles. *Cell, 102*, 109-26.

Jakobsen, J. S., Jelsbak, L., Jelsbak, L., Welch, R. D., Cummings, C., Goldman, B., *et al.* (2004). Sigma54 enhancer binding proteins and *Myxococcus xanthus* fruiting body development. *J Bacteriol, 186*, 4361-8.

Kaiser, D. (2004). Signaling in myxobacteria. *Annu Rev Microbiol, 58*, 75-98.

Kim, S. K., Lund, J., Kiraly, M., Duke, K., Jiang, M., Stuart, J. M., *et al.* (2001). A gene expression map for Caenorhabditis elegans. *Science, 293*, 2087-92.

Kroos, L., Kuspa, A., & Kaiser, D. (1990). Defects in fruiting body development caused by Tn5 lac insertions in *Myxococcus xanthus. J Bacteriol, 172*, 484-7.

Marcotte, E. M., Pellegrini, M., Ng, H. L., Rice, D. W., Yeates, T. O., & Eisenberg, D. (1999). Detecting protein function and protein-protein interactions from genome sequences. *Science, 285*, 751-3.

Merlie, J., Mignot, T., Taylor, R. G., Sliusarenko, O., Oster, G., Welch, R. D., *et al.* The novel response regulator Fr+S plays a role in the efficiency of type IV pili-dependent motility in *Myxococcus xanthus. In Preparation,*

Mignot, T., Merlie, J. P., & Zusman, D. R. (2005). Regulated pole-to-pole oscillations of a bacterial gliding motility protein. *Science, 310*, 855-7.

O'Toole, G. A., & Kolter, R. (1998). Flagellar and twitching motility are necessary for Pseudomonas aeruginosa biofilm development. *Mol Microbiol, 30*, 295-304.

O'Toole, G., Kaplan, H. B., & Kolter, R. (2000). Biofilm formation as microbial development. *Annu Rev Microbiol, 54*, 49-79.

Overbeek, R., Fonstein, M., D'Souza, M., Pusch, G. D., & Maltsev, N. (1999). The use of gene clusters to infer functional coupling. *Proc Natl Acad Sci U S A, 96*, 2896-901.

Pazos, F., & Valencia, A. (2002). In silico two-hybrid system for the selection of physically interacting protein pairs. *Proteins, 47*, 219-27.

Pellegrini, M., Marcotte, E. M., Thompson, M. J., Eisenberg, D., & Yeates, T. O. (1999). Assigning protein functions by comparative genome analysis: protein phylogenetic profiles. *Proc Natl Acad Sci U S A, 96*, 4285-8.

Plamann, L., Davis, J. M., Cantwell, B., & Mayor, J. (1994). Evidence that asgB encodes a DNA-binding protein essential for growth and development of *Myxococcus xanthus. J Bacteriol, 176*, 2013-20.

Srinivasan, B. S., Caberoy, N. B., Suen, G., Taylor, R. G., Shah, R., Tengra, F., *et al.* (2005). Functional genome annotation through phylogenomic mapping. *Nat Biotechnol, 23*, 691-8.

Stoodley, P., Hall-Stoodley, L., & Lappin-Scott, H. M. (2001). Detachment, surface migration, and other dynamic behavior in bacterial biofilms revealed by digital time-lapse imaging. *Methods Enzymol, 337*, 306-19.

Suen, Jakobsen, Goldman, Singer, Garza, & Welch (2006). Bacterial Post-Genomics: The Promise and Peril of Systems Biology. *J Bacteriol, 188*, 7999-8004.

Taylor, R. G., & Welch, R. D. (2008). Chemotaxis as an emergent property of a swarm. *Submitted.*

Viswanathan, P., Ueki, T., Inouye, S., & Kroos, L. (2007). Combinatorial regulation of genes essential for *Myxococcus xanthus* development involves a response regulator and a LysR-type regulator. *Proc Natl Acad Sci U S A, 104*, 7969-74.

Werner-Washburne, M., Wylie, B., Boyack, K., Fuge, E., Galbraith, J., Weber, J., *et al.* (2002). Comparative analysis of multiple genome-scale data sets. *Genome Res, 12*, 1564-73.

Whitworth, D. E. (2008). *Myxobacteria : multicellularity and differentiation* . Washington, DC : ASM Press,.

Wu, S. S., & Kaiser, D. (1997). Regulation of expression of the pilA gene in *Myxococcus xanthus*. *J Bacteriol, 179*, 7748-58.

Youderian, P., Burke, N., White, D. J., & Hartzell, P. L. (2003). Identification of genes required for adventurous gliding motility in *Myxococcus xanthus* with the transposable element mariner. *Mol Microbiol, 49*, 555-70.

Chapter 4: *M. xanthus* Development as a Dynamic Process

4.1 Introduction

Development represents a swarm level emergent response to nutrient limitation. It has been described as an ordered, temporal sequence of gene expression events, accomplished through a cascade of TRs, and coordinated by signaling between cells resulting in fruiting body formation and sporulation (Kaiser & Welch, 2004; Kroos & Kaiser, 1987; Kuspa & Kaiser, 1989; Jelsbak *et al.*, 2005). The formation of fruiting bodies is complicated from an engineering standpoint, and even more complex when considering the requisite behavioral genetics. A swarm represents a distributed system; a geographically dispersed collection of genetically identical cells that must function together and coordinate their behavior through a communication network (Crespi, 2001). As a swarm develops to form fruiting bodies, self-organization occurs in stages: rippling, streaming, and then aggregation (Kiskowski *et al.*, 2004; Welch & Kaiser, 2001; Igoshin *et al.*, 2004; Kroos & Maddock, 2003). Complexity is added sequentially so that the order imposed by each pattern can add to the final structure. Rippling occurs after development is initiated, and may be a way to orient cells over long distances (Figure 4.1, A). Streaming moves cells toward aggregation centers after the cells have been aligned (Figure 4.1, B), and fruiting represents the final structure with all of its spatial and temporal complexity completed (Figure 4.1, C).
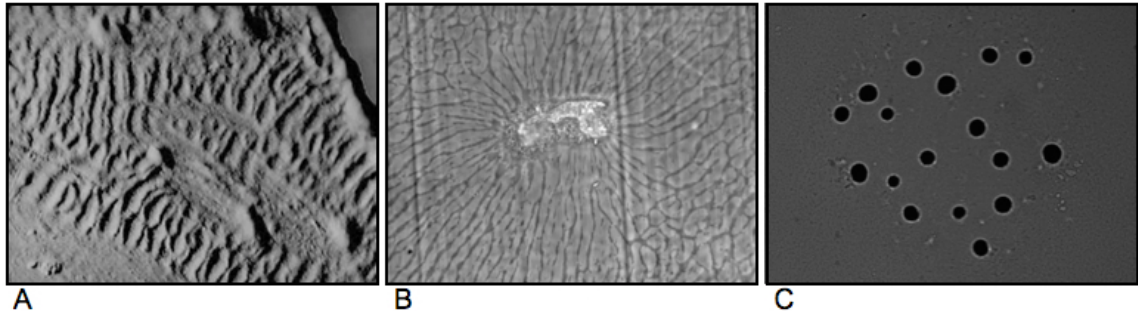
Figure 4.1: Developmental patterns of *M. xanthus* swarms. (A) Rippling. Cells form traveling waves that move across the surface of a swarm (Courtesy of H. Reichenbach). (B) Streaming. Once cells have picked an aggregation point, the surrounding cells change their behavior and appear to move toward the aggregation point. In this picture, the aggregation point is in the direct center. (C) Fruiting. Fruiting bodies are three-dimensional structures that have a species-specific shape.

When considering an *M. xanthus* swarm as a single entity, swarm patterns represent a discernable phenotype, such that the effects of mutation can be characterized by quantifying aberrant behaviors in a mutant swarm. Continuous observation of the emergence, propagation, and transition of these dynamic patterns within the developing mutant swarm could provide information concerning the function of the mutated ORF and the point in development at which the ORF is required. Although fruiting bodies are three-dimensional structures, their formation can be observed in two dimensions using brightfield time-lapse microscopy. The swarm begins as a circular, relatively evenly distributed population of cells. Over a period of 72 hours the cells within a swarm aggregate, and the increased cell density appears as darkened spots within the image (Figure 2.3).

This chapter will demonstrate that development is a dynamic process involving complex patterns that usually go undetected using standard assays. Although, due to the robustness of *M. xanthus'* regulatory networks, many mutant

strains ultimately complete the development process (spore-filled fruiting bodies), our understanding will not be complete until it is viewed as a dynamic process.

4.2 Treatment of Development as a Binary Process

The standard assays for the analysis of development focus on the endpoint of fruiting body formation (Appendix II). A starving population of *M. xanthus* is considered to have normal development if it forms discernable fruiting bodies that contain resistant spores within a set time. A qualitative assessment of this assay shows that different strains of *M. xanthus* can produce strikingly different fruiting bodies. Even though mutants are occasionally characterized as having a developmental delay, these tests do not account for fruiting bodies of abnormal size or shape. Nor do they account for differences in the number of fruiting bodies produced by the swarm.

Consider the images depicted in Figure 4.2. All three images show *M. xanthus* swarms that were assayed under standard development conditions. All three swarms successfully developed fruiting bodies in approximately the same amount of time that it would take for a wild type swarm to do the same. Using the standard definition for development, all three swarms test positive (or normal), although there are clear differences in fruiting body formation among the three when viewed qualitatively. Although these swarms represent developmental extremes, some mutant strains present less obvious differences that do not become apparent until development is observed as a dynamic process.
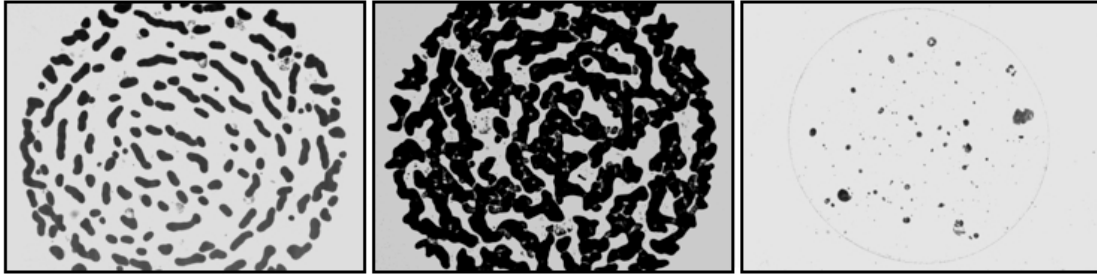
Figure 4.2: Extremes found in 'normal' development. The three images depict swarms that have successfully completed the development process. The swarm in the first image has a large number elongated fruiting. The swarm in the second image has a few very large fruiting bodies. The swarm in the last image has very few small fruiting bodies. All swarms developed myxospores-filled fruiting bodies. For normal wild type development, see figure 4.1, C.

4.3 Treatment of Development as a Dynamic Process

The developmental process has both a spatial and a temporal component; in order to observe this process dynamically, any assay would have to incorporate both aspects. We designed and tested an assay that would, in addition to detecting the presence or absence of fruiting bodies, produce a rich data set that incorporated both spatial and temporal elements of *M. xanthus* development. To examine development, we recorded this process from start to finish using the procedures described in Chapter 3.

In collaboration with the laboratory of Professor Lee Kroos (Michigan State University), we performed an analysis of time-lapse videos for patterns that are inherent in *M. xanthus* development. Specifically, we analyzed fruiting body size, number, placement and time of appearance as variables to distinguish one mutant from another in 33 of the 38 mutant ECF sigma factors. These were chosen from the BLAST annotation of the partial genome sequence and generated via homologous recombination in the laboratory of Professor Anthony Garza (Syracuse University). As mentioned in Chapter 2, the ECF Sigma factors

are important regulators of transcription and are known to respond to external stimuli and regulate the transcription of genes directly involved in functions such as transport, secretion, and homeostasis (Helmann, 2002). Standard analysis of these mutants (i.e. testing for the formation of fruiting bodies) showed an abnormal phenotype in only two of these mutant strains. We hypothesized that an examination of the time-lapse images would reveal more deviations in phenotype than would be revealed using standard development assays.

Using the TM chamber described in Chapter 3, we recorded time-lapse images over a period of hours until development was completed (defined as the point at which the final number of fruiting bodies has completely formed). The only limitation to this assay was the time that wild type *M. xanthus* swarms require to form complete fruiting bodies (up to 72 hours). In order to more efficiently video the mutant strains, we modified the assay to accelerate the process.

We exploited a signal in *M. xanthus* to accelerate development. Onset of the *M. xanthus* starvation-induced developmental program involves a response to the metabolic by-product guanosine 3'-di-5'-(tri)di-phosphate nucleotides [(p)ppGpp] (Singer & Kaiser, 1995; Harris *et al.*, 1998). Under starvation conditions, (p)ppGpp is produced when the cells ribosomes arrest due to a lack of usable amino acids. Because the trigger is chemokinetic in nature, once a threshold is reached the developmental program is activated. To accelerate this effect, we supplemented TPM agar with sodium citrate and sodium pyruvate. These supplements facilitate the synthesis of ATP by feeding directly into the

Krebs Cycle, but they do not allow the synthesis of essential amino acids. Therefore, rather than slowing down its metabolism in response to low nutrient levels, the adequate ATP levels cause *M. xanthus* to maintain high metabolic activity, including the initiation of protein synthesis, however, ribosomal activity will still be arrested for lack of amino acids. Hypothetically, this results in a sharp increase in (p)ppGpp and causes the swarm to undergo a more rapid and synchronous shift toward development.

When tested, we found that this rapid development media (RDM) shortened the minimal developmental timeline by 75%, from 72 to 16 hours (Figure 4.3). Development, although accelerated, is not negatively affected; fruiting bodies formed on RDM contain similar numbers of resistant spores when compared to fruiting bodies formed on TPM.
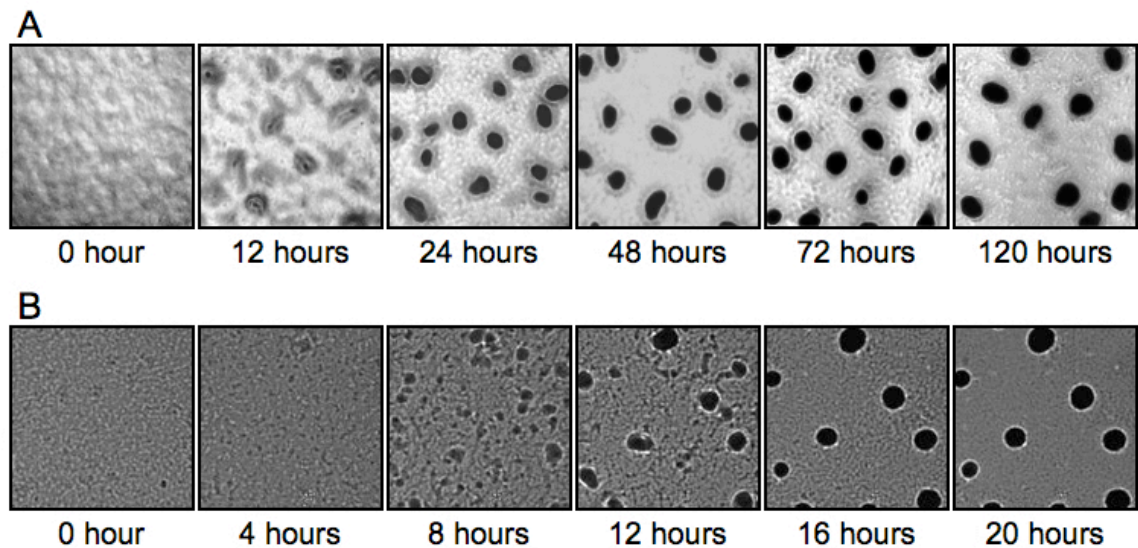
Figure 4.3: Comparison of time-lapse images of wild-type *M. xanthus* swarm development on non-supplemented starvation media (TPM) and supplemented media (RDM). (A) Fruiting bodies fully form on TPM between 48 and 72 hours verses (B) between 12 and 16 hours on RDM. Images in A are re-printed from Caberoy *et al*., 2003.

We used the computer program Lispix (Gillen & Bright, 2003), to extract the data of interest. Lispix is able to capture each fruiting body as a "blob" and determine the number, position, size and circularity for each mutant. Analysis of the 33 ECF sigma factor mutant strains when assayed and observed under dynamic development conditions showed distinct variation with respect to the emergence, propagation, and transition of patterns (Table 4.1).

Table 4.1: ECF sigma factor development phenotype. The number of fruiting bodies, average area of fruiting bodies, and average circularity of fruiting bodies represent metrics that could be easily included with the presence/absence (+/−) descriptive presented in the standard development assay. The start of aggregation and end of aggregation describe dynamic swarm patterns.

Mutant Strain	Number of FB	Average Area of FB (% of wild type)[a]	Average Circularity of FB (% of wild type)[b]	Start of Aggregation (min)[c]	End of Aggregation (min)[d]
wild type	25	100%	100%	450	1020
MXAN0203	8	116%	95%	300	900
MXAN0233	5	128%	76%	465	1185
MXAN0681	4	174%	93%	585	1200
MXAN0947	5	129%	83%	390	1005
MXAN1510	5	126%	96%	360	1215
MXAN1661	20	11%	35%	1050	--
MXAN2184	12	23%	92%	945	--
MXAN2204	14	112%	88%	360	870
MXAN2395	4	174%	81%	480	1095
MXAN2436	3	137%	87%	855	1185
MXAN2500	2	183%	92%	615	--
MXAN2929	7	89%	57%	645	--
MXAN3426	12	60%	85%	750	--
MXAN3959	3	180%	81%	660	1440
MXAN4309	4	89%	90%	570	1170
MXAN4315	3	210%	72%	615	--
MXAN4733	59	52%	45%	570	1125
MXAN4949	27	31%	74%	960	--
MXAN4987	1	151%	83%	885	--
MXAN5101	3	145%	97%	420	945
MXAN5245	3	136%	37%	525	--
MXAN5506	12	120%	84%	435	1140
MXAN5731	14	44%	92%	420	--
MXAN6058	16	93%	91%	300	1260
MXAN6173	2	302%	57%	540	--
MXAN6461	3	135%	91%	300	750
MXAN6681	15	50%	79%	735	--

MXAN6759	83	24%	40%	585	--
MXAN7214	3	204%	83%	375	1095
MXAN7289	15	66%	92%	435	915
MXAN7454	20	81%	90%	435	1005

[a] The area of each fruiting body within a swarm is calculated and reported as an average.
[b] Circularity is measured as a number between 0 and 1. A circularity value of 1.0 indicates a perfect circle. As the value approaches 0.0, it indicates an increasingly elongated polygon. A wild type fruiting body has an average circularity of 0.92 ± 0.01 SD.
[c] The start of aggregation is recorded when the first fruiting bodies appear. This is usually indicated by darkening areas within the swarm.
[d] The end of aggregation is recorded when the final number of fruiting bodies have stabilized and the individual fruiting bodies are no longer moving. -- indicates aggregation continued past the 24-hour assay time.

Of the 33 mutant swarms assayed, 2 failed to form fruiting bodies –

confirming the results of the standard assay. Of the remaining 31 swarms,

however, all presented unique phenotypes: 12 started aggregating earlier than

wild type (3 of which started more than 2 hours earlier) and 19 started

aggregating later than wild type (13 of which started more than 2 hours later), 7

ended aggregating earlier than wild type (2 of which ended more than 2 hours

earlier) and 24 ended aggregating later than wild type (20 of which ended more

than 2 hours later). In addition, 18 of the mutant swarms have larger and 13

swarms have smaller fruiting bodies than wild type, and 10 swarms have fruiting

bodies that are less than 80% as round as those of wild type. Representative

mutant strains that show the differences in 1) size, 2) shape, 3) number of fruiting

bodies, and 4) variations in development time of three of the ECF mutant strains

are illustrated in Figure 4.4.
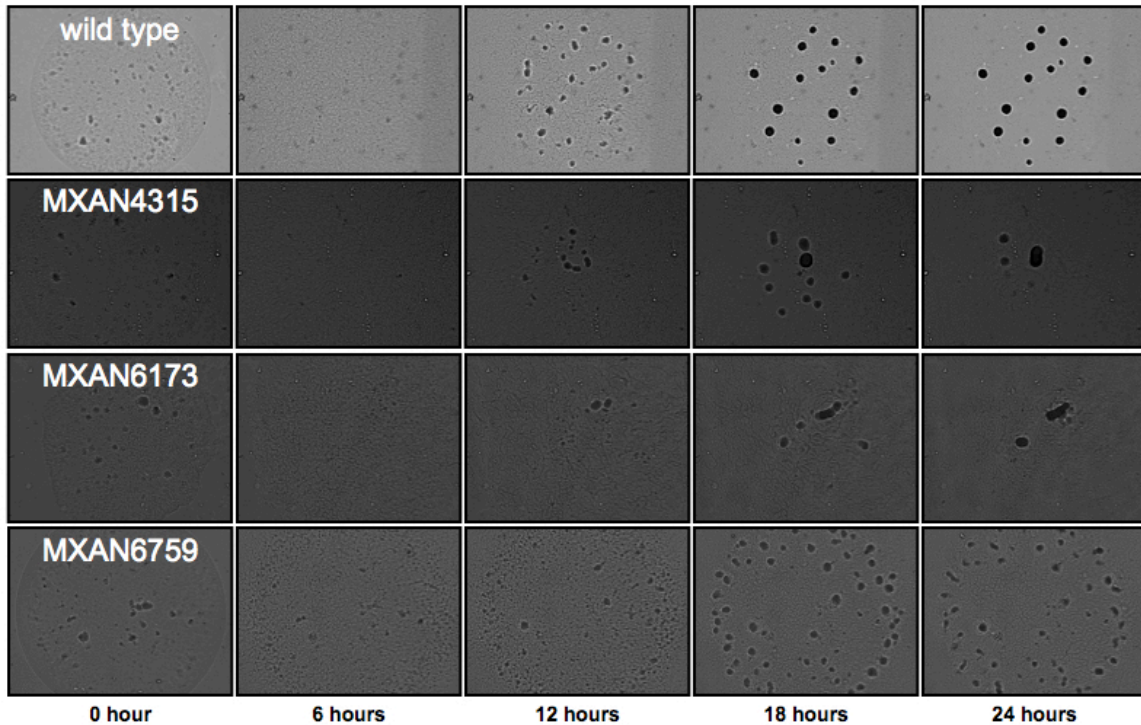
Figure 4.4: RDM development of a wild type swarm and 3 ECF sigma factor mutants. Even though most end with the formation of fruiting bodies, each mutant swarm has a phenotype that is reproducible and unique. Nearly all of the other 32 ECF sigma factors mutants examined also developed a unique phenotype.

In addition to revealing distinct differences among the ECF sigma factor mutant strains that presented no phenotype using standard assays, additional notably unique patterns were revealed by observing development dynamically. One mutant strain, MXAN5731, was of particular interest. The strain begins development by forming multiple fruiting bodies very early. These fruiting bodies are highly mobile and seem to merge freely with each other or disappear entirely (Figure 4.5, A). Interestingly, near the end of the development process, the fruiting bodies stop moving. They appear to settle into one position, only to start a highly coordinated pulsing pattern where all of the fruiting bodies rapidly dissolve and reform several times (Figure 4.5, B). This pattern can be seen in

several of the other mutant strains and could represent some sort of late-onset rippling.
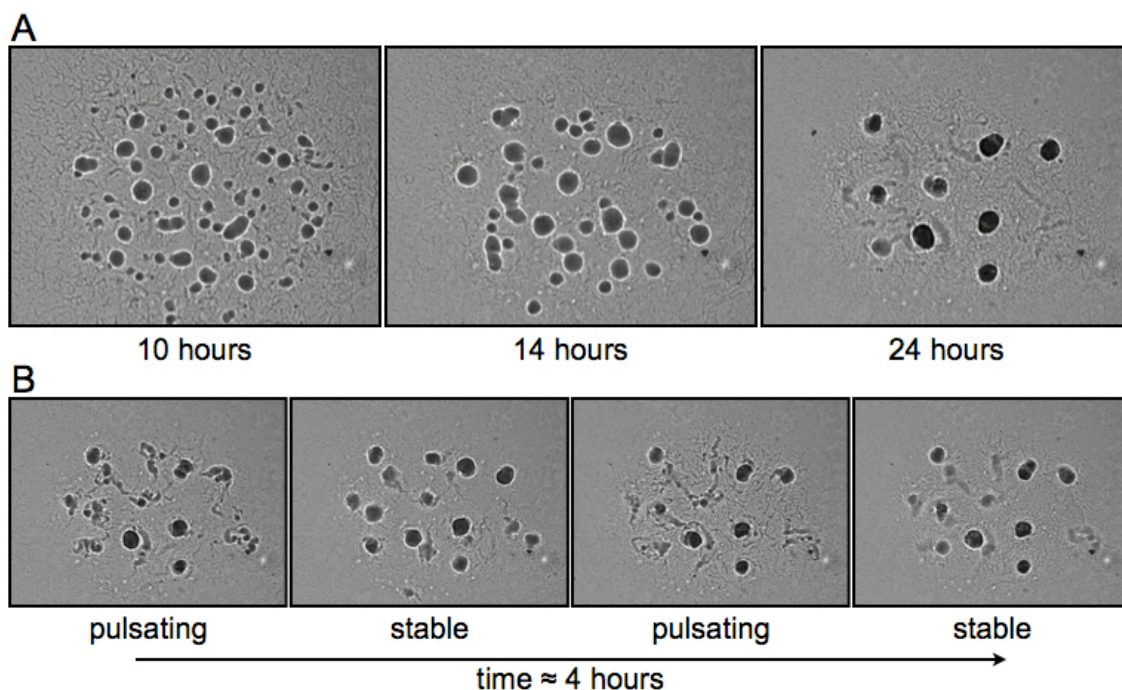
Figure 4.5: ECF sigma factor mutant strain MXAN5731. This strain presents two unique phenotype. (A) Early forming fruiting bodies are highly mobile. This can be seen by comparing the fruiting body placement among the images. (B) Near the end of the developmental process, and once definite aggregation points are established, the fruiting bodies start to pulsate in a coordinated fassion.

Clearly, the observation of development as a dynamic process provides additional data that has help further classify mutant strains into more descriptive phenotypic categories.

4.4 Data Storage and Analysis for Future Iterations

One benefit of collecting time-lapse images in this manner is that the raw data can be stored for future analysis if improved analysis methods are developed. There are a number of additional variables available in the Lispix software package, which can be utilized to quantify differences in mutant

development. Stuart Angus (Welch Laboratory, Syracuse University) is currently

analyzing the position of fruiting bodies in relation to their nearest neighbor within

the swarm to determine if aggregation points are randomly distributed (Figure

4.6). His results are promising, further proving the usefulness of the Lispix

software package. In addition to nearest neighbor analysis, future phenotypic

classifications could include: measuring the percent of the population that is

rippling, determining the timing and velocity of streaming, characterizing the rate

of swarm expansion prior to and during development, and quantifying the range

of pixel contrast over the surface of the swarm.

Fruiting Body	x-coord	y-coord
0	124.7	259
1	131	309.1
2	171.4	322.2
3	177.4	125.7
4	200.2	218.1
5	203.3	451.3

Fruiting Body	# Neighbors	Avg. Dist.	Distances					
0	6	91.5	50.5	143.3	85.9	97.3	93.2	78.6
1	4	86.8	50.5	42.5	94.6	159.5		
2	4	55.3	42.5	78.6	44.1	56.1		
3	6	112.7	95.2	143.3	198	68.4	99.9	71.4
4	5	62.8	95.2	34.2	54.3	44.5	85.9	
5	6	87.2	85.7	57.5	44.4	30.9	145.3	159.5
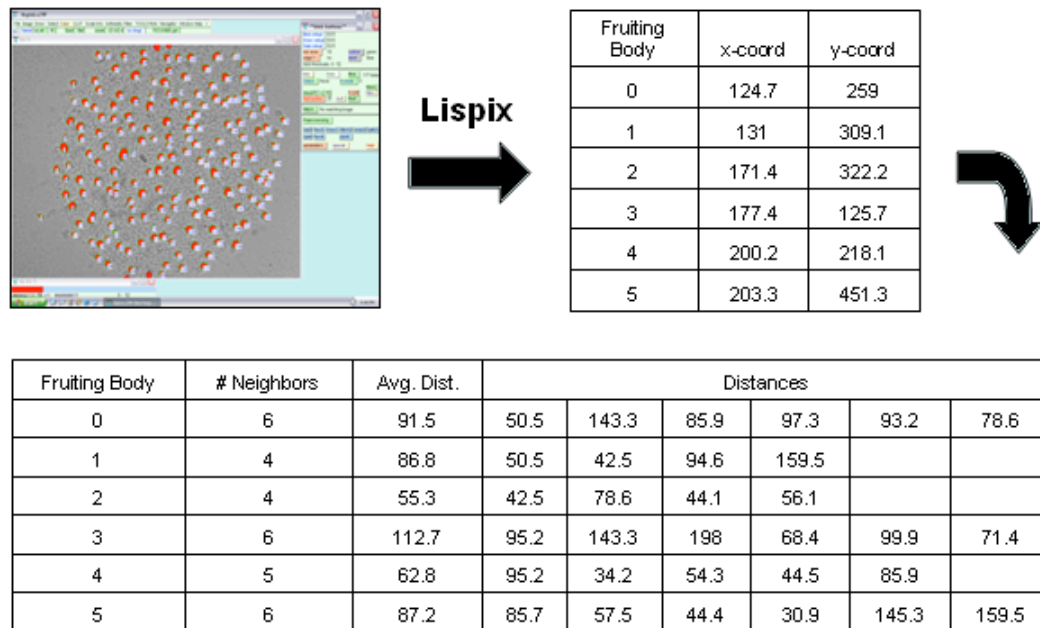
Figure 4.6: Flow chart of Lispix analysis of fruiting bodies. This example demonstrates the ability to determine each fruiting body's nearest neighbor within the swarm. Fruiting bodies are automatically identified within images, the perimeter of each fruiting body is measured, the area is quantified, the centroid is located, and nearest neighbor distances are calculated.

4.5 Summary

Development is a robust process: most of the reaction variables can be altered without catastrophic effect. In many cases, changes can be made in swarm size or cell density, growth conditions can be modified with respect to media or substrate, and mutations can be introduced into the population without preventing the end product of development. In order to better understand development, we observed it as a process.

Due to the methods developed here, subtle variations in developmental phenotypes can now be compared, characterized, and clustered, so that meaningful differences can be identified. When measured over time, the size and shape of fruiting bodies, in addition to their relative position within the swarm, can be used to differentiate mutant phenotypes that were previously characterized as wild type. In collaboration with Professor Kroos, we analyzed a total of 35 ECF sigma factors. Standard development assays revealed no discernable phenotype for all but two of these mutants. Time-lapse viewing of development as a dynamic process, however, revealed aberrant phenotypes for all ECF sigma factor mutant strains. Detailed descriptions of each strain were generated and essential phenotypic features that differentiate the strain were characterized and quantified. Currently, the Kroos Laboratory is conducting sporulation assays for the ECF sigma factor mutant strains.

Our ultimate goal is to create an evolving analysis pipeline that will quantify different aspects of the developmental process. From this, meaningful

associations can be made between genes based on the quantifiable clustering of

phenotype.

4.6 References

Crespi (2001). The evolution of social behavior in microorganisms. *Trends Ecol Evol, 16*, 178-83.

Gillen, G., & Bright, D. (2003). Tools and procedures for quantitative microbeam isotope ratio imaging by secondary ion mass spectrometry. *Scanning, 25*, 165-74.

Harris, B. Z., Kaiser, D., & Singer, M. (1998). The guanosine nucleotide (p)ppGpp initiates development and A-factor production in *Myxococcus xanthus*. *Genes Dev, 12*, 1022-35.

Helmann, J. D. (2002). The extracytoplasmic function (ECF) sigma factors. *Adv Microb Physiol, 46*, 47-110.

Igoshin, O. A., Welch, R., Kaiser, D., & Oster, G. (2004). Waves and aggregation patterns in myxobacteria. *Proc Natl Acad Sci U S A, 101*, 4256-61.

Jelsbak, L., Givskov, M., & Kaiser, D. (2005). Enhancer-binding proteins with a forkhead-associated domain and the sigma54 regulon in *Myxococcus xanthus* fruiting body development. *Proc Natl Acad Sci U S A, 102*, 3010-5.

Kaiser, D., & Welch, R. (2004). Dynamics of fruiting body morphogenesis. *J Bacteriol, 186*, 919-27.

Kiskowski, M. A., Jiang, Y., & Alber, M. S. (2004). Role of streams in myxobacteria aggregate formation. *Phys Biol, 1*, 173-83.

Kroos, L., & Kaiser, D. (1987). Expression of many developmentally regulated genes in Myxococcus depends on a sequence of cell interactions. *Genes Dev, 1*, 840-54.

Kroos, L., & Maddock, J. R. (2003). Prokaryotic development: emerging insights. *J Bacteriol, 185*, 1128-46.

Kuspa, A., & Kaiser, D. (1989). Genes required for developmental signalling in *Myxococcus xanthus*: three asg loci. *J Bacteriol, 171*, 2762-72.

Singer, M., & Kaiser, D. (1995). Ectopic production of guanosine penta- and tetraphosphate can initiate early developmental gene expression in *Myxococcus xanthus*. *Genes Dev, 9*, 1633-44.

Welch, R., & Kaiser, D. (2001). Cell behavior in traveling wave patterns of myxobacteria. *Proc Natl Acad Sci U S A, 98*, 14907-12.

Chapter 5: *Myxococcus xanthus* Chemotaxis as a Dynamic Process

5.1 Introduction

Development represents only one swarm-level emergent response to nutrient limitation. Some researchers have reported a second: *M. xanthus* exhibits a positive chemotactic response to a gradient of nutrients (Shi *et al.*, 1993; Kearns & Shimkets, 1998). These findings are controversial, however, since other reports claim there is no response (Dworkin & Eide, 1983; Tieman *et al.*, 1996). This chapter will address these discrepancies found in the literature and quantitatively show that swarm level chemotaxis does, in fact, occur in *M. xanthus*. It is important to note that in this chapter an *M. xanthus* behavior is described, not a molecular mechanism, nor will comparisons to the canonical, rule-based form of chemotaxis found in flagellated bacteria be made. This chapter will show, however, that *M. xanthus* chemotaxis manifests as a multicellular behavior that involves cell motility in response to nutrient limitation in much the same way as development does.

5.2 Chemotaxis in Flagellated Bacteria

Bacteria are often considered too small to detect a concentration gradient. To account for this, the cells move via a 'biased random-walk' by alternating between runs and tumbles (Figure 5.1, A) and using the methylation state of receptors as a memory of past concentrations of attractants or repellents (Sourjik, 2004). Bacteria that are propelled by flagella modulate their directional bias by controlling the rotation of their flagella. The enteric bacteria do this by

coordinating peritrichous flagella (even distribution of flagella over the entire surface of the cell). To produce a run, the flagella rotate counter-clockwise and work together by forming a bundle; to produce a tumble, the flagella rotate clockwise, unbundle, and work against each other (Baker *et al.*, 2006). Tumbles result in random reorientation of the cell. When moving up a gradient of attractant, the tumble frequency is suppressed, which increases the length of the run resulting in the biased random-walk (Figure 5.1, B).
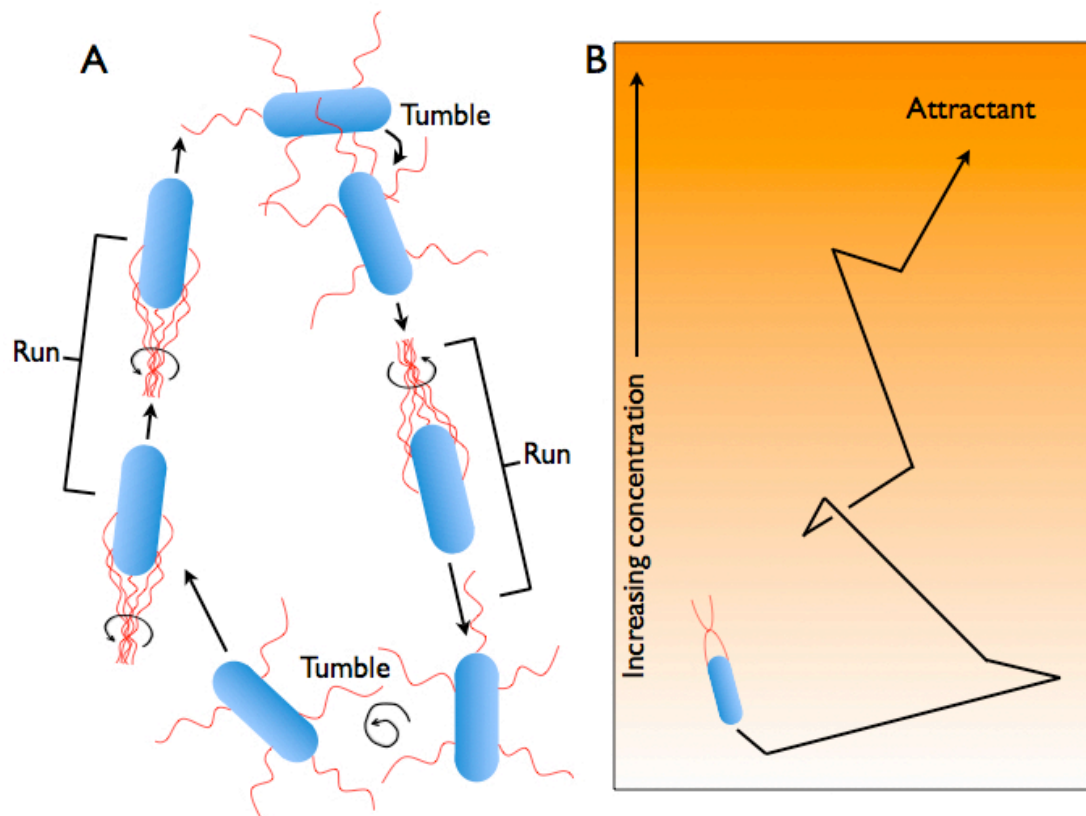
Figure 5.1: Biased random-walk. (A) The enteric bacteria chemotax via runs and tumbles: during runs, the flagella rotate counter-clockwise and form a bundle; during tumbles, the bundles fall apart as the flagella rotate clockwise. (B) While moving up the concentration gradient toward the attractant, tumbles are suppressed, resulting in longer runs.

The best-studied bacterial example is the chemotaxis pathway in *E. coli* (Figure 5.2) (Baker *et al.*, 2006; Parkinson *et al.*, 2005; Sourjik, 2004). Signals

are sensed by membrane-bound methyl-accepting chemotaxis proteins (MCPs), which regulate the activity of the histidine protein kinase CheA through the linker protein CheW. In the absence of an attractant, or in the presence of a repellent, there is an increase in the rate at which CheA is autophosphorylated, increasing the rate of phosphoryl group transfer to the response regulator, CheY. The relatively high levels of phosphorylated CheY increases the probability that cells will tumble, resulting in a change in direction (Welch *et al.*, 1993). In the presence of an attractant, or the absence of a repellent, autophosphorylation of CheA is suppressed resulting in decreased cell tumbles. Phosphorylated CheY is dephosphorylated by the phosphatase CheZ. Adaptation to a stimulus is controlled by the CheR methyltransferase and the CheA-activated CheB methylesterase, which modulate the methylation state of a complex of MCPs (Szurmant & Ordal, 2004; Sourjik, 2004). Methylation and demethylation of the MCP occurs to compensate for changes in CheA kinase activity caused by attractant binding.
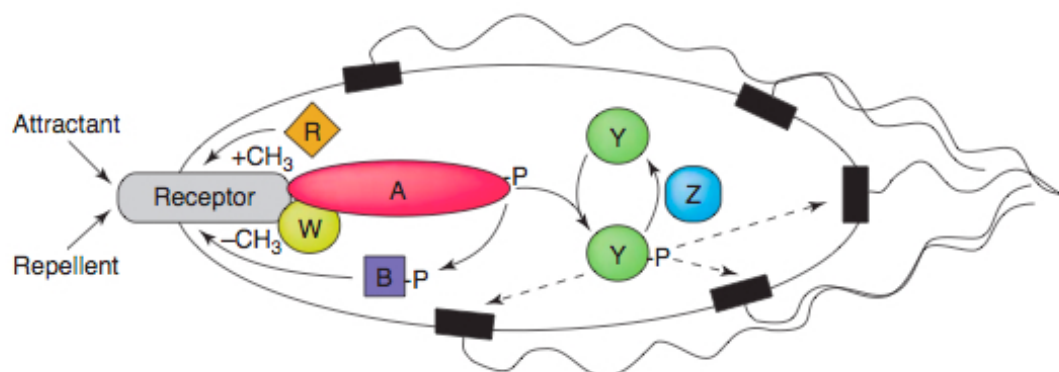
Figure 5.2: Chemotaxis pathway (*E. coli*). Changes in attractant or repellent concentrations are sensed by a protein assembly consisting of transmembrane receptors, an adaptor protein CheW, and a histidine kinase CheA. Autophosphorylation activity of CheA is inhibited by attractant binding and enhanced by repellent binding to receptors. The phosphoryl group is rapidly transferred from CheA to the response regulator

CheY. Phosphorylated CheY (CheY-P) diffuses to the flagellar motors and changes the direction of motor rotation from counterclockwise to clockwise to promote tumbles. CheZ phosphatase ensures a rapid turnover of CheY-P, which is essential to quickly re-adjust bacterial behavior. Adaptation in chemotaxis is mediated by two enzymes, methyltransferase CheR and methylesterase CheB, which add or remove methyl groups at four specific glutamyl residues on each receptor monomer. Receptor modification increases CheA activity and decreases sensitivity to attractants. Feedback is provided by CheB phosphorylation through CheA that increases CheB activity. (Reprinted from Sourjik, 2004)

5.3 Chemotaxis in *M. xanthus*

The question as to whether *M. xanthus* utilizes chemotaxis as a mechanism to find nutrients is controversial. It is complex in that if chemotaxis manifests as an emergent behavior, then groups of cells would appear to behave differently than individual cells, making quantification difficult. Some reports use increases and decreases in the reversal frequencies of individual cells as a metric to quantify chemotaxis; others examine the methylation state of Che homologs (Ward & Zusman, 1997). Neither approaches give a complete picture of emergence, however, because they examine either cells outside the context of the swarm or protein interactions, rather than swarm behavior. The genetics of and the controversy behind *M. xanthus* chemotaxis are discussed below.

5.3.1 Genetics of Chemotaxis in *M. xanthus*

A total of eight chemosensory-like systems have been identified in the *M. xanthus* genome: *frz*, *dif*, *che3*, *che4*, *che5*, *che6*, *che7*, and *che8* (Figure 5.3) (for in depth review, see Zusman *et al.*, 2007). Briefly, the Frz system regulates cellular reversals in which the leading cell pole becomes the new lagging cell pole. It has been shown that in the presence of a gradient of nutrients, *M.*

xanthus cellular reversal frequency is suppressed (Shi *et al.*, 1993; Kearns & Shimkets, 1998); this behavior that has been equated to the run-and-tumble motility found in *E. coli*. The Dif system regulates pilus-mediated motility and extracellular polysaccharide (EPS) biosynthesis (Yang *et al.*, 1998; Li *et al.*, 2003). In addition, pili may function as part of a sensory apparatus for the perception of signals for the Dif pathway, because the presence of pili is required for EPS production (Black & Yang, 2006). The Che3 system controls developmental genes and seems to play a role in sensing levels of nutrients – *che3* operon is controlled by the NtrC-like EBP CrdA (for an explanation of the role of NtrC-like EBPs in chemotaxis, see Section 5.5.2) (Kirby & Zusman, 2003). Not much is known about the remaining 5 systems: the Che6 system controls type IV pilus assembly and the Che7 system plays a role in temperature stress resistance (Zusman *et al.*, 2007).
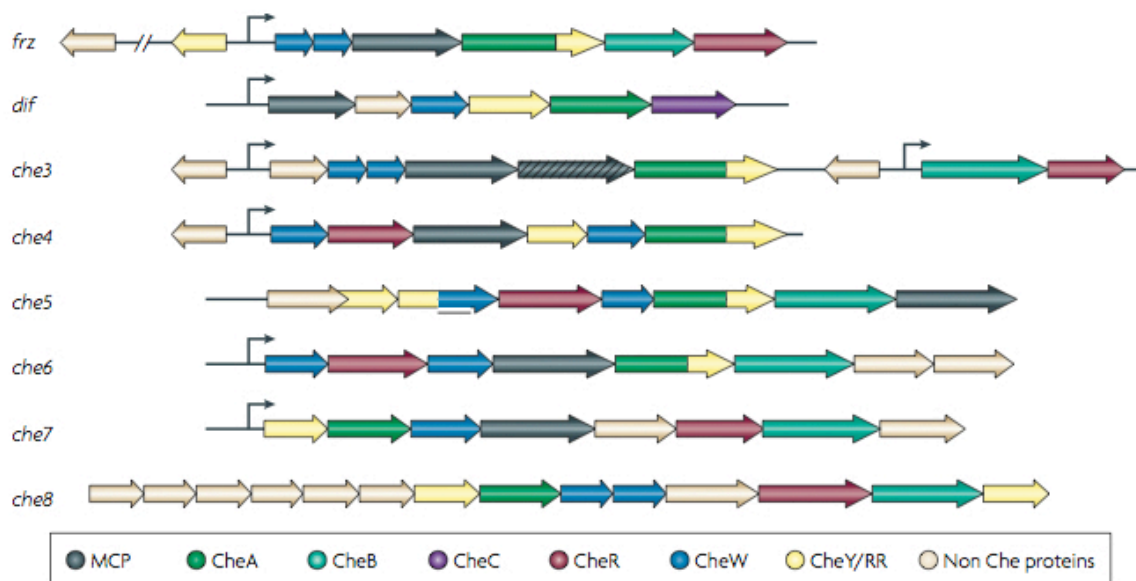
Figure 5.3: Multiple chemosensory gene clusters in *M. xanthus*. Chemotaxis pathways in *M. xanthus* were identified by computer searches for ORFs that encode chemotaxis homologues. Arrows represent directionality of transcription for that gene. (Reprinted from Zusman *et al.*, 2007)

5.3.2 History of Chemotaxis in *M. xanthus*

It is important to note that, by referring to the behavior outlined in this chapter as chemotaxis, we are not implying a mechanistic connection between chemotaxis in *M. xanthus* and chemotaxis in flagellated bacteria (Alexandre & Zhulin, 2001). Chemotaxis is strictly defined as directed movement toward attractants or away from repellents (Adler, 1975); it describes a dynamic pattern without behavioral or mechanistic qualification, and it therefore has more than one mechanism of action (Armitage & Lackie, 1990). In fact, were it not for this broad definition of chemotaxis, we would likely refer to this behavior in some other way, given the long and controversial history of chemotaxis in *M. xanthus* that complicates every study. Because of this, we will provide a summary of that controversy.

It was first hypothesized that chemotaxis directed cells toward aggregation points during development; in 1954, Lev reported that fruiting bodies produced diffusible substances that stimulated fruiting body formation (Lev, 1954). McVittie and Zahler claimed to confirm the existence of a chemotactic substance in 1962 (McVittie & Zahler, 1962), but no substance was ever isolated. In 1981, Shimkets and Dworkin reported that development requires cells to be touching one another (Shimkets & Dworkin, 1981), and this finding meant that models for development no longer required cells to communicate with each other over long distances via a diffusible chemoattractant. An unintended effect of the Shimkets and Dworkin study was to shift the focus of research away from fruiting bodies as

the source of a chemoattractant, and toward external chemical signals from nutrients and prey.

In 1983, Dworkin concluded that directed motility in *M. xanthus* does occur, but not as a response to chemical gradients (Dworkin, 1983). He concluded that what seemed to be chemotaxis was, in fact, elasticotaxis, the directed movement of cells perpendicular to stress lines in agar. In an accompanying report, Dworkin and Eide reported no swarm chemotaxis toward gradients of a variety of defined and complex materials, including the nutrients casitone and yeast extract (Dworkin & Eide, 1983). Furthermore, they speculated that chemotaxis is neither "mechanistically appropriate nor developmentally or ecologically useful" for *M. xanthus*, due to the fact that the cells exist in a swarm and move too slowly to detect diffusing nutrients. This speculation assumed only the biased-random-walk model of individual cell chemotaxis, and it effectively ended the study of swarm chemotaxis in *M. xanthus* for almost a decade.

In 1993, Shi *et al*. devised a chemotaxis assay that was based on a one-dimensional steep and stable chemical gradient (Shi *et al*., 1993), and reported that *M. xanthus* swarms do show directed movement toward nutrients, including casitone and yeast extract. In 1996, Tieman *et al*. claimed to improve the assay, but reported no directed movement toward the same nutrients (Tieman *et al*., 1996). Both sets of contradictory findings were based on qualitative assessments of swarm expansion; we were able to quantify the figure in the Tiemen *et al*. manuscript that showed swarm expansion in the presence of a

nutrient gradient using the methods described in Section 5.5.1, and found that, although it was not clear to the authors, *M. xanthus* did exhibit directed movement, and therefore the Tieman *et al*. results actually corroborated the results of Shi *et al*.

There are two mechanistically different types of chemotaxis experiments in *M. xanthus*, swarm experiments and cell experiments. All of the research discussed thus far involves swarm experiments, which examine the directed movement of a swarm toward an attractant or away from a repellent. In contrast, cell experiments examine changes in the reversal frequency of isolated cells, not directed movement, and there is evidence that individual cells are not capable of directed movement (McBride & Zusman, 1996). In 1996, McBride and Zusman reported that individual *M. xanthus* cells could not detect microcolonies of *E. coli*; once contact was established through random movement, however, cells remained in the microcolony while feeding. Measuring changes in reversal frequency is not the equivalent of directed movement; at best it is a measure of chemokinesis (non-directed motility) and an indirect measure of chemotaxis, although there are some important similarities to the standard chemotaxis model. In 1998, Kearns and Shimkets demonstrated that individual *M. xanthus* cells reported chemokinetic behavior in response to the slow diffusing lipid phosphatidylethanolamine (PE) gradients (Kearns & Shimkets, 1998). When the *M. xanthus* cells were placed on a PE gradient, they suppressed cell reversals. After an hour, the cells showed adaptation by returning to the pre-stimulus cell-reversal frequency.

Other than the 1983 report by Dworkin and Eide and the 1996 report by Tieman *et al.*, all studies on *M. xanthus* swarms have reported directed movement up a gradient of nutrients. More than anything else, these data clearly demonstrate the importance of a quantifiable metric when performing a comparative analysis of behavior. By providing such a metric, we will be able to measure asymmetric expansion and begin to characterize its behavioral genetics.

5.4 Chemotaxis as an Emergent Property of a Swarm

Unlike development, where sporulation efficiency functions as a quantifiable metric, all previous analyses of *M. xanthus* swarm chemotaxis have been qualitative in nature. Thus, genetic effects could not be ranked or clustered according to phenotype, and this has made a rigorous comparative analysis nearly impossible. An *M. xanthus* chemotactic response is an example of swarm symmetry breaking, and a rigorous quantitative assay is required for comparative analysis and characterization. To this end, we have developed a variation of the TM chamber discussed in Chapter 3 to quantify the *M. xanthus* chemotactic response. We call this the tracking assay.

5.4.1 Methods for Examining *M. xanthus* Swarm Chemotaxis

Mutant strains were constructed and cultures were prepared as outlined in Chapter 3.

Nutritive disk construction. A sterile 0.5-mm-thick silicone rubber gasket was placed on top of a flame-sterilized glass microscope slide, forming a small well. Molten 1% agar in CTTYE broth was poured into this well and covered by a second flame-sterilized microscope slide, and the slides were clamped together to flatten the CTTYE agar. When the CTTYE agar had cooled and hardened, the clamps and one of the slides were removed. A 1 mm diameter 'nutritive disk' was extracted from the well using a micro-sampling pipette with a 100 µl glass disposable tip (Fisher).

Tracking assay apparatus construction. The nutritive disk was deposited into the well created by a gasket on a slide and the TM chamber was filled with TPM buffer and completed as outlined in Chapter 3. A 0.5 µl aliquot of re-suspended (5×10^9 cells/ml) *M. xanthus* liquid culture spotted on the assay surface so the swarm edge was 1.14 ± 0.04 mm away from the CTTYE disk (now embedded within the TPM/agar) (Figure 5.4, A and B). The time interval between spotting and the initiation of image acquisition is no more than 5 minuets, and this time is taken into account when calculating T_0 and T_n.

Swarm image acquisition. Completed tracking assay slides were placed on the heated microscope stage and maintained at 32°C. Images were acquired every 60 seconds for a period of 24 hours and compiled into time-lapse videos as outlined in Chapter 3.

Initiation and quantification of the tracking assay. The tracking assay is initiated when the 0.5 µl of 3×10^6 *M. xanthus* cells dries (Figure 5.4, B). Reaching the nutritive disk or an elapsed time of 24 hours represented a

verifiable endpoint (T_n).   We marked the swarm and nutritive disk circumferences at T_0 and used them to determine both the swarm and nutritive disk centroids. We then used these two points to draw a straight line that transected both the T_0 center (called the original centroid) of the T_n swarm and the center of the nutritive disk (called the center line). Next, we drew two straight lines tangential to the nutritive disk that transected the T_n swarm's original centroid (Figure 5.4, C). This defined two equal areas of the swarm that were geometrically opposite, one being closest to the nutritive disk (leading edge), and the other being furthest from the nutritive disk (lagging edge). The swarm expands during the assay through a series of group translocations called flares (Fontes & Kaiser, 1999), and symmetry breaking is detected by measuring the ratio of the furthest distance traveled by a flare on the leading edge to the furthest distance traveled by a flare on the lagging edge from T_0 to T_n, where n is the number of hours required for the first flare of the leading edge to reach the nutritive disk (Figure 5.4, C). Perpendicular lines from the end of both of the flare length lines to the centerline were added to create normalized points on the centerline. The distances from the original swarm edge along the centerline to these normalized points were then used to generate tracking ratios (for a detailed explanation, see section 5.4.2). Tracking ratios were ranked and compared using the Duncan's Multiple-Range Test procedure within the statistical analysis software package SAS (SAS Institute Inc.). Images were processed using the ImageJ (http://rsb.info.nih.gov/ij) and Photoshop (Adobe Systems Inc.) software packages.
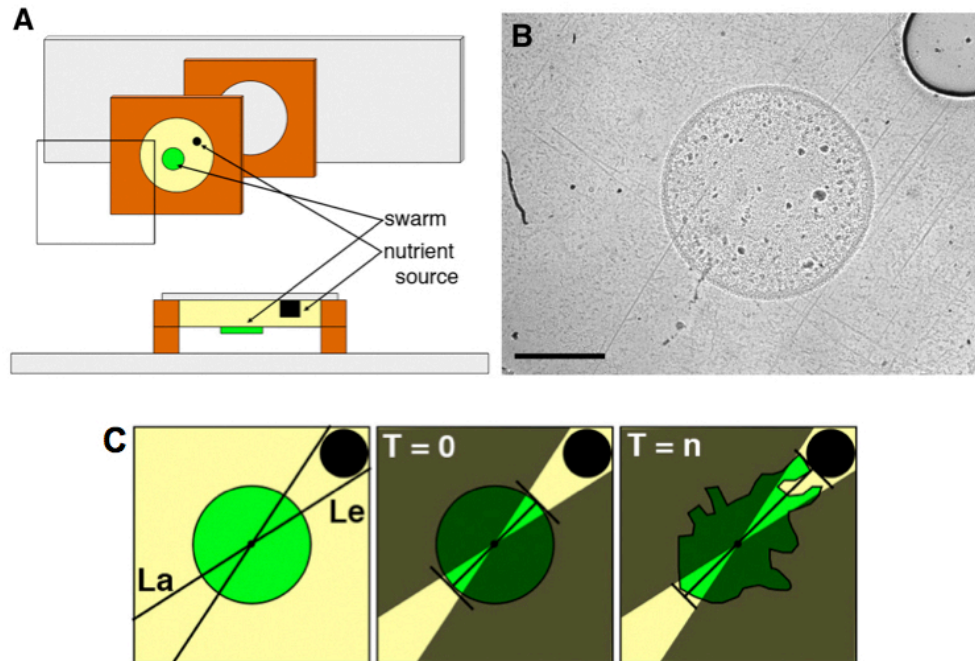
Figure 5.4: Tracking assay and quantification. A glass cover slip behind a silicon gasket creates a well that contains an agar substrate with embedded nutritive disk. This is aligned with a second gasket that has been placed on a microscope slide. (A) Exploded view and cross section of the apparatus. (B) 20X brightfield image of tracking assay apparatus at T_0. (C) Diagram of quantification protocol used to define and measure the leading (Le) and lagging (La) edges to determine TR. See text for explanation of T_0 and T_n. Scale bar in (B), 1 mm.

Confirmation of nutritive gradient. To measure the lower limit of diffusion in 1% agar, the CTTYE in the nutritive disk was replaced with Quantum dots (Q-dots) (Quantum Dot Corp.), inert fluorescent semiconductors that approximate the size of a large protein (~10 nm diameter) and fluorescent images were acquired as described above. Q-dots produced a visible fluorescent gradient that diffused 1 mm within the first three hours, and more than 2 mm within the first 6 hours (Figure 5.5). These results confirm that, even if the *M. xanthus* chemoattractant(s) are as large as a 10 nm diameter protein, the diffusion front will cross the expanding swarm before the first 2 hours of the assay.
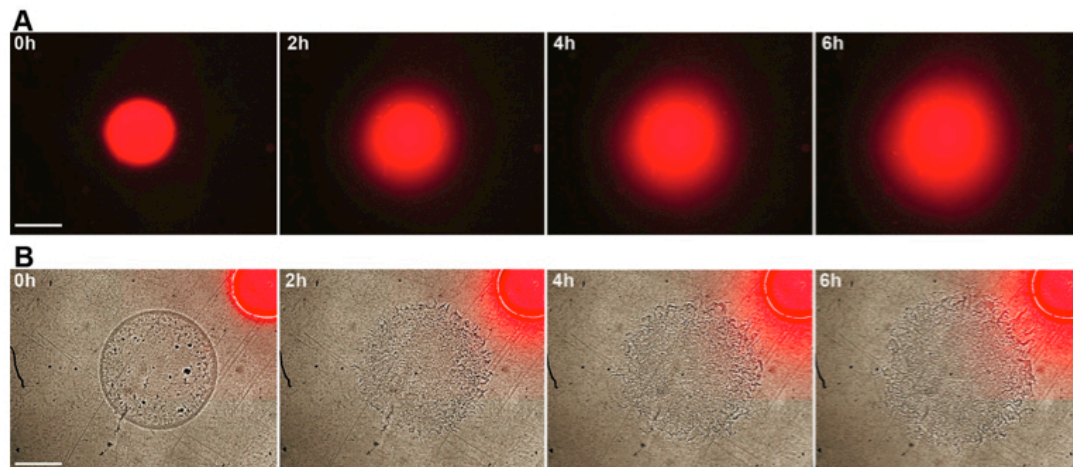
Figure 5.5: Nutrient diffusion. Panel (A) shows the diffusion of fluorescent Q-dots over a period of 6 hours. Panel (B) is a merge of the diffusion images with images of wild type exhibiting chemotaxis. This illustrates the position of the diffusion front in relation to the swarm. Scale bars in (A) and (B), 1 mm.

Elimination of elasticotaxis as a variable. To determine if the asymmetry of swarm expansion during a tracking assay was due to stress forces caused by the placement of the nutritive disk, we replaced the it with a non-nutritive disk containing 1% agar in TPM. The tracking assay was performed under these conditions, and results were quantified as described above.

5.4.2 Results of the Tracking Assay Experiments

The tracking assay surface is non-nutritive agar in which a smaller nutritive agar disk is completely embedded. The nutritive agar and non-nutritive agar disk are identical in composition, except for the presence of 1% casitone and 0.5% yeast extract in the nutritive agar disk; over several hours a gradient extends out from the nutritive disk into the non-nutritive agar. Because the nutritive disk is completely covered by non-nutritive agar, the assay surface is smooth,

eliminating any possible swarm response to surface irregularities, such as elasticotaxis (Dworkin, 1983; Fontes & Kaiser, 1999).

Swarm asymmetry is reported as a tracking ratio, which is a measure of the directionality of expansion. A tracking ratio > 1.0 indicates expansion toward the nutrient source, a tracking ratio < 1.0 indicates expansion away from the nutrient source, and a tracking ratio = 1.0 indicates symmetry in expansion. Wild type cells have a tracking ratio of 1.94 ± 0.20 SE (Figure 5.6, A); in contrast, a non-nutrient control disk results in a tracking ratio of 1.01 ± 0.03. The asymmetry in swarm expansion indicates that cells are moving up the gradient and toward the nutritive disk; however, we must eliminate the possibility that this asymmetry is a growth response to differing nutrient levels across the swarm. Higher nutrient levels further up the gradient could accelerate growth and division rates of cells at the leading edge, which is always closer to the nutritive disk, thus increasing the rate of expansion and resulting in a tracking ratio > 1.0. We used a genetic approach to explore this hypothesis, by performing a series of experiments with motility mutant strains DK1218 and DK1253 (Hodgkin *et al.*, 1979; Hodgkin & Kaiser, 1979). As mentioned earlier, *M. xanthus* moves across agar via gliding motility, which can be genetically dissected into two distinct subdivisions called adventurous (A) and social (S) motility; DK1218 (genotype *cglB2*) is defective in A motility, while DK1253 (genotype *tgl-1*) is defective in S motility. Either A or S motility alone are sufficient to produce swarm expansion. If the asymmetric expansion observed in wild type swarms is caused by increased growth and division rates as a function of proximity to the nutritive disk,

then the genetics of cell motility would be of no consequence, and both DK1218 and DK1253 swarms should produce tracking ratios greater than 1.0. This is not observed: DK1253 swarms exhibit asymmetric expansion (tracking ratio = 1.23 ± 0.06) (Figure 5.6, B), but DK1218 swarms expand symmetrically (tracking ratio = 0.90 ± 0.15) (Figure 5.6, C). Therefore, the asymmetry of wild type swarm expansion requires motility. In fact, it specifically requires A motility.

An *M. xanthus* cell reverses direction by switching its leading pole (Spormann & Kaiser, 1995), and isolated cells on an agar substrate have been shown to respond to a nutrient gradient by changing the frequency of their reversals (Shi *et al.*, 1993; Kearns & Shimkets, 1998). This change lacks any observable polarity however, so that it produces no net cell translocation that could cause it to move up a gradient. Therefore, the response of isolated cells to a gradient of nutrients has been more accurately described as a form of non-vectoral chemokinesis (Ward *et al.*, 1998), rather than chemotaxis. Although these isolated cell data may seem to contradict the results of the tracking assay, they are at least partially consistent: if chemotaxis in *M. xanthus* is the result of all the cells in a swarm sensing and responding to a gradient autonomously by changing their reversal frequencies to move up the gradient in 'run-and-tumble' fashion, then all cells and every flare within the gradient would move toward the nutritive disk. No swarm exhibits this phenotype. Instead, a swarm expands away from the center at all points during a tracking assay, and these observations are consistent with individual cell data that report a chemokinetic response. An observation that is not consistent with chemokinesis is that the

flares on the leading edge of a wild type swarm can be easily distinguished from

flares on the lagging edge: leading edge flares appear larger, thicker, and

straighter (Figure 5.6, D) than lagging edge flares, which appear more 'spidery'

(Figure 5.6, E). Perhaps a cell exhibits chemokinesis when isolated and

chemotaxis when in a swarm, because a swarm provides the 'context'; within

which *M. xanthus* cells interact with their environment?
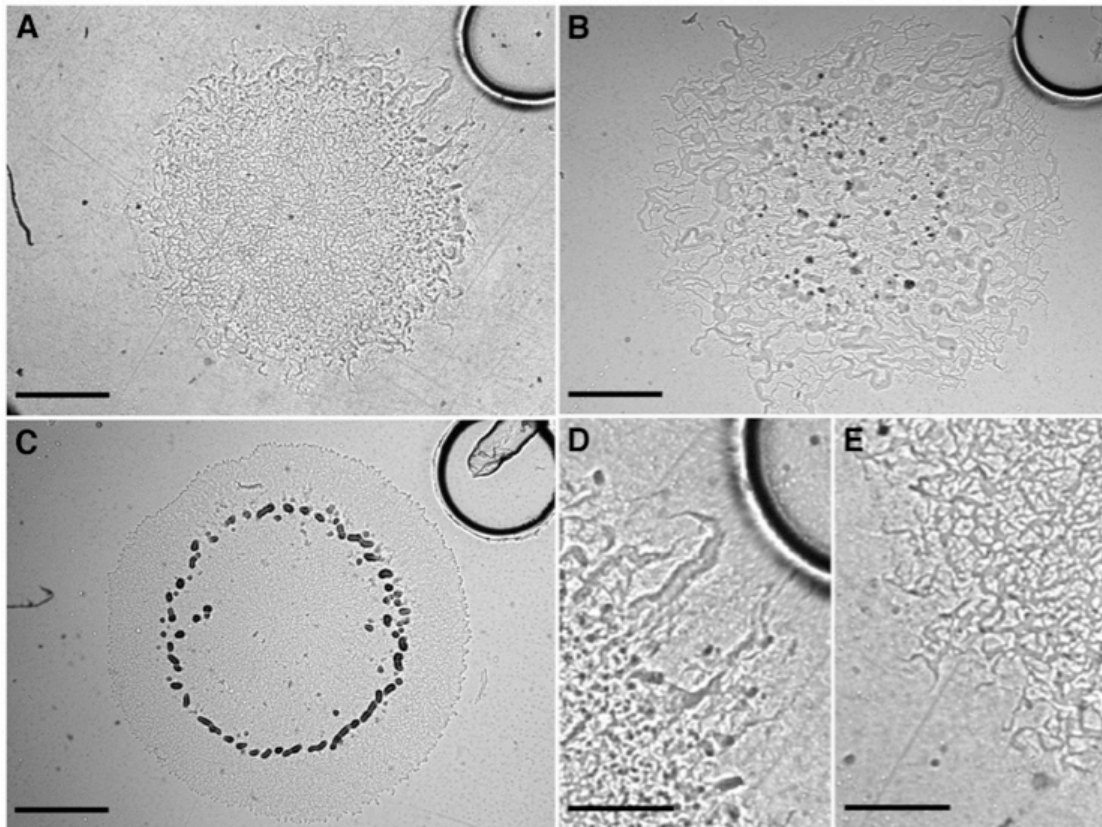
Figure 5.6: Symmetry breaking during a tracking assay in *M. xanthus*. (A) A swarm of DK1622 (wild type); T_n = 6 hours, TR = 1.94 ± 0.20. (B) A swarm of DK1253 (A+S-); T_n = 18 hours, TR = 1.23 ± 0.06. (C) A swarm of DK1218 (A-S+); T_n = 23 hours, TR = 0.90 ± 0.15. (D) and (E) Higher magnification view of DK1622 leading and lagging edges, respectively. Scale bars in (A) to (C), 1 mm; scale bar in (D) and (E), 0.5 mm.

Several physical properties are known to contribute to a swarm's context:

the mass of a swarm that exerts stress on the agar substrate, which individual

cells can sense and respond to through elasticotaxis (Dworkin, 1983; Fontes &

Kaiser, 1999); the exopolysaccharide (EPS) matrix generated by the swarm,

which individual cells require for normal motility (Shimkets, 1990; Kaiser, 2004);

the quorum sensing and cell-cell signals that require groups of cells in close

proximity, and that can alter individual cell behavior (Kaiser, 2004). Perhaps

there is some subset of these properties that enables a single *M. xanthus* cell to

direct its reversal frequency so that it moves up a gradient of nutrients. To

investigate this hypothesis, we performed the tracking assay using a swarm in

which a small number (1%) of motile wild type cells were distributed throughout a

swarm (99%) of DK11316 non-motile mutant cells (Yu & Kaiser, 2007) (genotype

pilA::Tc^R, Δ*cglB*) (Figure 5.7, A). This swarm chimera provides a significant

subset of swarm context, such as the elasticotactic force, the EPS matrix, and 3

x 10^6 living cells in close proximity for quorum sensing and cell-cell contact

signaling. Although the cells in this swarm can communicate with each other,

they cannot move together as a group because only 1% of cells capable of

movement, and they are distributed throughout the swarm. Under these

conditions, if the 1% wild type cells exhibit chemotaxis, by moving up the nutrient

gradient from within the chimeric swarm, then more would emerge from the

leading edge than from the lagging edge. This is not observed. Instead, equal

numbers of cells emerge from both edges (Figure 5.7, B) and travel the same

maximum distance away from the swarm center (Figure 5.7, C). These data

confirm that individual *M. xanthus* cells do not exhibit chemotaxis, even within the

context of a non-motile living swarm. *M. xanthus* chemotaxis is a multicellular

behavior that requires the movement of a swarm and, in this way, it is like

development.
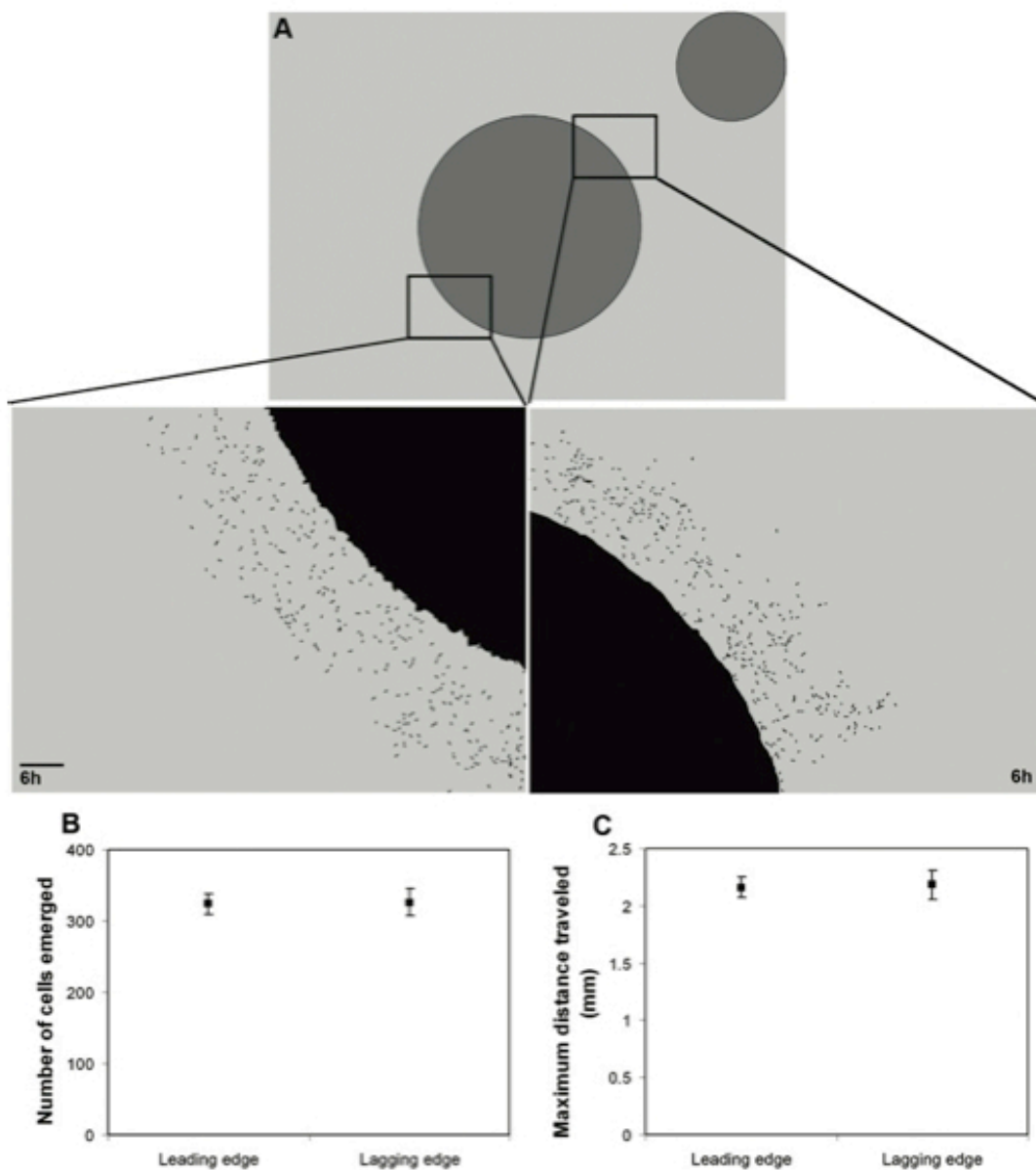
Figure 5.7: Chimeric swarm behavior. DK1622 (wild type) cells diluted 1:100 into a DK11316 (A-S-) mutant background were subjected to the tracking assay for 6 hours, and images were captured of the leading and the lagging edges. Thresholded images (A) diagram leading and lagging edge reference points at T_0, and show individual cells that have moved outside the non-motile swarm at $T_n = 6$. The number (B), and maximum distance traveled (C) by individual cells that emerged from both leading and lagging edges are shown. Scale bar in (A), 0.1 mm. Images of leading and lagging edges in (A) were processed to help clarify individual cells using Photoshop filters in the following order: auto levels, find edges, then threshold.

From a genomic perspective, development is a spatiotemporal cascade of transcription events controlled, at least in part, by σ^{54} EBPs that exhibit significant homology to the NtrC-like class of activators (Morett & Segovia, 1993; Keseler & Kaiser, 1997; Diodati *et al.*, 2006). The *M. xanthus* genome contains 53 NtrC-like EBPs, an inordinate number compared to other prokaryotes, and approximately one third of NtrC-like EBPs are involved in the control of development (Goldman *et al.*, 2006; Caberoy *et al.*, 2003). These EBPs might also function in chemotaxis. Further evidence that the NtrC-like EBPs control chemotaxis lies in the fact that: (1) CrdA (an NtrC-like EBP) interacts with the CheA homolog Che3A (Kirby & Zusman, 2003), (2) the NtrC-like EBP *nla19* interacts with the CheA homolog DifE (Lancero *et al.*, 2005), and (3) the NtrC-like EBP FrgC has been identified as a putative response regulator in the Frz system (Cho *et al.*, 2000). Therefore, we examined the distribution of defective chemotaxis phenotypes among *M. xanthus* mutant strains containing one NtrC-like EBP disrupted through homologous recombination. Mutant strains with no observable deviation from wild type phenotype were of particular interest because aberrant chemotaxis phenotypes would not be obscured by a more general motility defect. Using a set of standard assays (cell growth, swarm motility, and development) (Caberoy *et al.*, 2003), 26 out of 53 mutant strains appeared to have an overall wild type phenotype. We then performed tracking assays on these 26 strains and ranked them by mean tracking ratio (Figure 5.8). The overall distribution of tracking ratios is continuous, with significantly different mutant classes ($F_{27,72}$ = 2.04, P = 0.0088). Using Duncan's Multiple-Range Test,

we identified 10 strains displaying tracking ratios significantly different from wild type (Figure 5.8, inset).
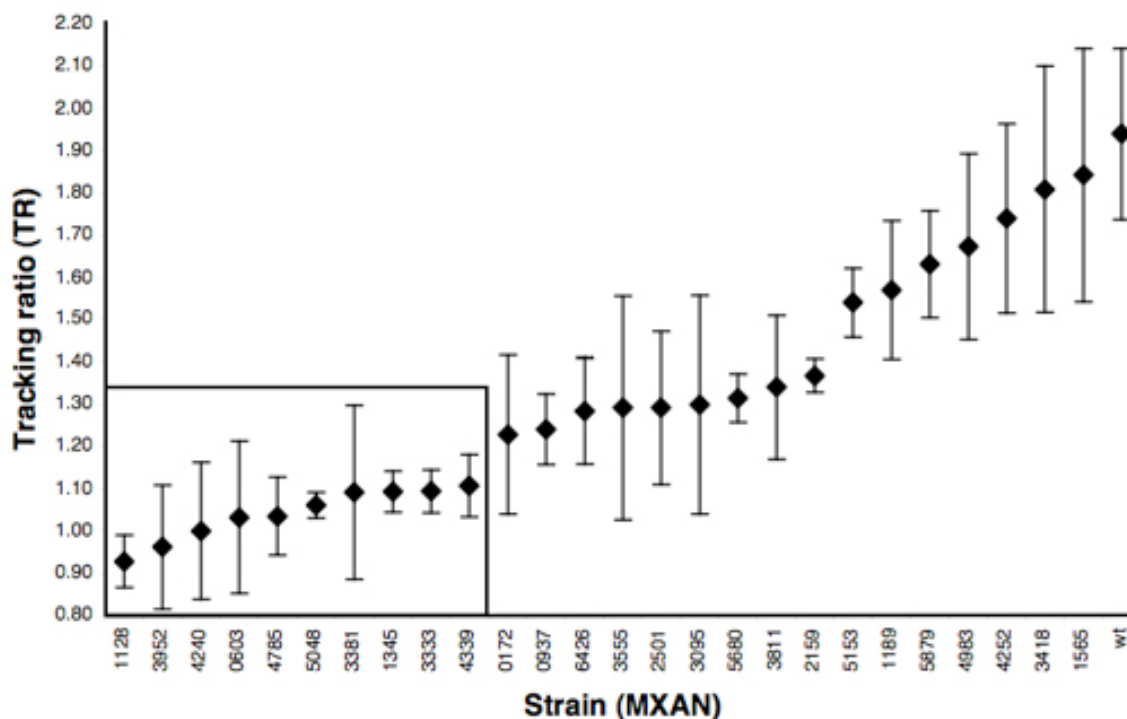
Figure 5.8: Ranking NtrC-like EBPs by TR. Tracking assays were performed on each of the 26 NtrC-like EBP single gene disruption mutant strains that displayed no defect in growth rate, swarm expansion, or development. TR results are displayed in the order of increasing mean; TR ± SE (n = 3). NtrC-like EBPs found to be 'chemotaxis-specific' are inset.

5.5 Summary

M. xanthus chemotaxis satisfies all six requirements for emergence, as defined by Goldstein *et al*. (Goldstein, 1999): A swarm is an entity, rather than a population, in that it represents a global, or macro 'level' (*i*) that exhibits coherence or correlation (*ii*). Chemotaxis is dynamical processes (*iii*) that are ostensive (*iv*), and that exhibit both radical novelty (*v*) and supervenience (*vi*). Given the wide variety of other molecular mechanisms that control behavior in *M. xanthus*, including quorum sensing (Bassler *et al*., 1994), localized cell-cell

contact-mediated communication (Shimkets, 1990; Kaiser, 2004), and stigmergy (Dworkin, 1983; Fontes & Kaiser, 1999), we postulate that the most plausible model for *M. xanthus* chemotaxis resembles a form of swarm intelligence, rather than the canonical biased random walk of microbial chemotaxis.

In this chapter, we have quantified *M. xanthus* swarm chemotaxis in response to a two-dimensional gradient of nutrients, and demonstrated that the response is the result of neither asymmetric growth nor elasticotaxis. Swarm motility is required for *M. xanthus* chemotaxis, as opposed to cell motility, and this distinction means that, like development, it is a multicellular response to an external stimulus. Also, like development, *M. xanthus* chemotaxis is affected by the disruption of genes that regulate transcription, specifically the NtrC-like EBPs, and a quantitative analysis reveals a continuous distribution of swarm phenotypes for both responses (A.G. Garza, personal communication). These data indicate that *M. xanthus* chemotaxis may have a complex and branching signal transduction schema, similar to the one proposed for the control of development (Kroos, 2007).

As mentioned in Chapter 2, an examination of the *M. xanthus* 9 Mb genome reveals some striking features. For example, in addition to its 53 NtrC-like activators, it encodes for 99 serine/threonine kinases and 137 sensor and hybrid histidine kinases (Goldman *et al.*, 2006). This is a significant overrepresentation of two component parts, and the complex set of parallel, branched, and overlapping connections that can be assembled from this signal transduction 'parts list' has the characteristics of a neural network. Its potential

for adaptation has been likened to a form of cellular intelligence (Hellingwerf, 2005). A swarm-intelligent model for *M. xanthus* chemotaxis resolves apparent inconsistencies in the data presented in this study. For example, it can explain why a swarm can exhibit chemotaxis, while individual cells exhibit only chemokinesis; if the chemotaxis signal transduction network crosses between cells, then it is not enough for all cells to sense the gradient - they must all also respond to it. It also explains the wide range of tracking ratios observed for the NtrC-like EBP mutant strains, because a continuous distribution is the expected result for a network that is complex and highly redundant. Given the size and structure of its genome, we propose that other *M. xanthus* swarm behaviors are likely controlled in a similar fashion.

5.6 References

Adler, J. (1975). Chemotaxis in bacteria. *Annu Rev Biochem, 44*, 341-56.

Alexandre, G., & Zhulin, I. B. (2001). More than one way to sense chemicals. *J Bacteriol, 183*, 4681-6.

Armitage, J. P., & Lackie, J. M. (1990). *Biology of the chemotactic response*. New York: Cambridge University Press.

Baker, M. D., Wolanin, P. M., & Stock, J. B. (2006). Signal transduction in bacterial chemotaxis. *Bioessays, 28*, 9-22.

Bassler, B. L., Wright, M., & Silverman, M. R. (1994). Multiple signalling systems controlling expression of luminescence in Vibrio harveyi: sequence and function of genes encoding a second sensory pathway. *Mol Microbiol, 13*, 273-86.

Black, W. P. P., & Yang, Z. (2006). Type IV pili function upstream of the Dif chemotaxis pathway in *Myxococcus xanthus* EPS regulation. *Mol Microbiol, 62*, 447-56.

Caberoy, N. B., Welch, R. D., Jakobsen, J. S., Slater, S. C., & Garza, A. G. (2003). Global mutational analysis of NtrC-like activators in *Myxococcus xanthus*: identifying activator mutants defective for motility and fruiting body development. *J Bacteriol, 185*, 6083-94.

Cho, K., Treuner-Lange, A., O'Connor, K. A., & Zusman, D. R. (2000). Developmental aggregation of *Myxococcus xanthus* requires frgA, an frz-related gene. *J Bacteriol, 182*, 6614-21.

Diodati, M. E., Ossa, F., Caberoy, N. B., Jose, I. R., Hiraiwa, W., Igo, M. M., *et al.* (2006). Nla18, a key regulatory protein required for normal growth and development of *Myxococcus xanthus*. *J Bacteriol, 188*, 1733-43.

Dworkin, M. (1983). Tactic behavior of *Myxococcus xanthus*. *J Bacteriol, 154*, 452-9.

Dworkin, M., & Eide, D. (1983). *Myxococcus xanthus* does not respond chemotactically to moderate concentration gradients. *J Bacteriol, 154*, 437-42.

Fontes, M., & Kaiser, D. (1999). Myxococcus cells respond to elastic forces in their substrate. *Proc Natl Acad Sci U S A, 96*, 8052-7.

Goldman, B. S., Nierman, W. C., Kaiser, D., Slater, S. C., Durkin, A. S., Eisen, J., *et al.* (2006). Evolution of sensory complexity recorded in a myxobacterial genome. *Proc Natl Acad Sci U S A, 103*, 15200-5.

Goldstein, J. (1999). Emergence as a Construct: History and Issues. *Emergence, 1*, 49-72.

Hellingwerf, K. J. (2005). Bacterial observations: a rudimentary form of intelligence? *Trends Microbiol, 13*, 152-8.

Hodgkin, J., & Kaiser, D. (1979). Genetics of gliding motility in *Myxococcus xanthus* (Myxobacterales): genes controlling movement of single cells. . *Mol Gen Genet, 171*, 167-76.

Hodgkin, J., & Kaiser, D. (1979). Genetics of gliding motility in *Myxococcus xanthus* (Myxobacterales): two gene systems control movement. *Mol Gen Genet, 171*, 177-91.

Kaiser, D. (2004). Signaling in myxobacteria. *Annu Rev Microbiol, 58*, 75-98.

Kearns, & Shimkets (1998). Chemotaxis in a gliding bacterium. *Proc Natl Acad Sci U S A, 95*, 11957-62.

Keseler, I. M., & Kaiser, D. (1997). sigma54, a vital protein for *Myxococcus xanthus*. *Proc Natl Acad Sci U S A, 94*, 1979-84.

Kirby, J. R., & Zusman, D. R. (2003). Chemosensory regulation of developmental gene expression in *Myxococcus xanthus*. *Proc Natl Acad Sci U S A, 100*, 2008-13.

Kroos, L. (2007). The Bacillus and Myxococcus developmental networks and their transcriptional regulators. *Annu Rev Genet, 41*, 13-39.

Lancero, H. L., Castaneda, S., Caberoy, N. B., Ma, X., Garza, A. G., & Shi, W. (2005). Analysing protein-protein interactions of the *Myxococcus xanthus* Dif signalling pathway using the yeast two-hybrid system. *Microbiology, 151*, 1535-41.

Lev (1954). Demonstration of a Diffusible Fruiting Factor in Myxobacteria. *Nature, 173*, 501.

Li, Y., Sun, H., Ma, X., Lu, A., Lux, R., Zusman, D. R., *et al.* (2003). Extracellular polysaccharides mediate pilus retraction during social motility of *Myxococcus xanthus*. *Proc Natl Acad Sci U S A, 100*, 5443-8.

McBride, M. J., & Zusman, D. R. (1996). Behavioral analysis of single cells of *Myxococcus xanthus* in response to prey cells of Escherichia coli. *FEMS Microbiol Lett, 137*, 227-31.

McVittie, A., & Zahler, S. A. (1962). Chemotaxis in Myxococcus. *Nature, 194*, 1299-300.

Morett, E., & Segovia, L. (1993). The sigma 54 bacterial enhancer-binding protein family: mechanism of action and phylogenetic relationship of their functional domains. *J Bacteriol, 175*, 6067-74.

Parkinson, J. S., Ames, P., & Studdert, C. A. (2005). Collaborative signaling by bacterial chemoreceptors. *Curr Opin Microbiol, 8*, 116-21.

Shi, W., Köhler, T., & Zusman, D. R. (1993). Chemotaxis plays a role in the social behaviour of *Myxococcus xanthus*. *Mol Microbiol, 9*, 601-11.

Shimkets, L. J. (1990). Social and developmental biology of the myxobacteria. *Microbiol Rev, 54*, 473-501.

Shimkets, L. J., & Dworkin, M. (1981). Excreted adenosine is a cell density signal for the initiation of fruiting body formation in *Myxococcus xanthus*. *Dev Biol, 84*, 51-60.

Sourjik, V. (2004). Receptor clustering and signal processing in *E. coli* chemotaxis. *Trends Microbiol, 12*, 569-76.

Spormann, A. M., & Kaiser, A. D. (1995). Gliding movements in *Myxococcus xanthus*. *J Bacteriol, 177*, 5846-52.

Szurmant, H., & Ordal, G. W. (2004). Diversity in chemotaxis mechanisms among the bacteria and archaea. *Microbiol Mol Biol Rev, 68*, 301-19.

Tieman, S., Koch, A., & White, D. (1996). Gliding motility in slide cultures of *Myxococcus xanthus* in stable and steep chemical gradients. *J Bacteriol, 178*, 3480-5.

Ward, M. J., & Zusman, D. R. (1997). Regulation of directed motility in *Myxococcus xanthus*. *Mol Microbiol, 24*, 885-93.

Ward, M. J., Mok, K. C., & Zusman, D. R. (1998). *Myxococcus xanthus* displays Frz-dependent chemokinetic behavior during vegetative swarming. *J Bacteriol, 180*, 440-3.

Welch, M., Oosawa, K., Aizawa, S., & Eisenbach, M. (1993). Phosphorylation-dependent binding of a signal molecule to the flagellar switch of bacteria. *Proc Natl Acad Sci U S A, 90*, 8787-91.

Yang, Z., Geng, Y., Xu, D., Kaplan, H. B., & Shi, W. (1998). A new set of chemotaxis homologues is essential for *Myxococcus xanthus* social motility. *Mol Microbiol, 30*, 1123-30.

Yu, R., & Kaiser, D. (2007). Gliding motility and polarized slime secretion. *Mol Microbiol, 63*, 454-67.

Zusman, D. R., Scott, A. E., Yang, Z., & Kirby, J. R. (2007). Chemosensory pathways, motility and development in *Myxococcus xanthus*. *Nat Rev Microbiol, 5*, 862-72.

Chapter 6: Conclusions and Future Directions

6.1 Introduction

M. xanthus is a soil bacteria that exists as a multicellular swarm. Each individual cell is dependent on the swarm to complete its life cycle: a complex, iterative process that involves communication via a variety of signals resulting in coordinated swarm behaviors. Development and chemotaxis are two examples. Both of these behaviors manifest as dynamic, emergent patterns that are controlled through transcription. The sequencing of the *M. xanthus* genome revealed a striking number of TRs suggesting a complex regulation network has evolved to control pattern formation.

6.2 Contributions to the Field of *M. xanthus* Research

The work described in this dissertation has been conducted from a genome first perspective. In other words, the TRs that were found to control emergent behaviors were of interest because of their lack of discernible phenotypes using standard assays. Based on their homology, and previous research, these ORFs should produce dramatic, swarm-level phenotypes. We hypothesized that since no differences in phenotype were observed, we weren't looking at the behaviors correctly or even the correct behaviors, and perhaps, the current assays needed to be refined as well as new assays created. As a means of annotating *M. xanthus* ORFs that otherwise have no annotation, we developed a TM chamber that consists of two silicone gaskets and an agar slab sandwiched between a microscope slide and a glass cover slip. *M. xanthus* swarms assayed in this TM chamber remain wet and aerobic for more that a week. This allows for long-term

observation of dynamic swarm patterns. To analyze these features, we constructed a cluster of eight microscopes, each with independent data acquisition computers for time-lapse image acquisition. Data from the assay is stored as image stacks in a terabyte RAID system, which is directly networked to each of the microscope computers.

By observing and analyzing *M. xanthus* mutant strains in this way, we were able to make interesting and novel discoveries, and further characterize two large classes of TRs: the ECF sigma factors and the NtrC-like EBPs. We demonstrated that by observing and analyzing the ECF sigma factor mutant strains dynamically, patterns that could not otherwise be discerned using standard assays became apparent. In this way, we were able to reveal unique developmental phenotypes for all 33 mutant strains assayed. Using standard methods, only two mutant strains displayed unique phenotypes. In addition to the developmental phenotypes, we were able to characterize swarm-level chemotaxis and demonstrate that even though individual cells are only capable of changing the frequency at which they reverse, a swarm is capable of sensing and responding to a nutrient gradient by following it to its source in two-dimensional space. Furthermore, by examining NtrC-like EBP mutant strains that presented normal phenotypes using standard assays, we were able to determine that this behavior is under transcriptional control. Previous to this work, only approximately 30% of the NtrC-like EBPs were found to have a discernable phenotype. Using the novel methods described above, we were able to further characterize an additional 20% of these mutant strains.

6.3 Development of Genomic and High-Throughput Methods

In order to further examine mutant phenotypes responsible for *M. xanthus* emergent behaviors, we require the ability to create sets of mutant strains. It would be extremely inefficient to select ORFs to disrupt randomly, because a large percentage of the ORFs in the genome would have to be disrupted before discernable clusters could be achieved. Using the standard annotation of the genome is also not efficient, because that selects for similarity between ORFs, not which function together. Instead, by using the phylogenomic map to choose sets of ORFs that are likely to function together, we can select for ORFs with similar phenotypes. We tested this hypothesis on a small number of ORFs that we predicted to be motility mutants based on their phylogenomic analysis. All turned out to be motility mutants, indicating that the phylogenomic map could effectively enrich sets of gene disruptions for specific phenotypes. The phylogenomic map gives us the ability to selectively disrupt ORFs that are likely to have similar phenotypes, thereby creating useful sets of known and unknown mutants for functional analysis.

To aid in the characterization of these predictions, we developed a high-throughput mutagenesis protocol based on homologous recombination to systematically generate *M. xanthus* mutant strains. This method has given us the ability to generate 96 mutant strains at a time with a success rate of 76%. This method has also proven to be both time and cost effective.

6.4 Future Directions

Integral to this dissertation is the hypothesis that many emergent *M. xanthus* behaviors are controlled by TRs. Therefore, a future goal of this research is to determine which sets of ORFs in the *M. xanthus* genome are under direct transcriptional control by the TRs that regulate these behaviors. In the following section, a research outline for the integration of microarray data into an experimental pipeline for the identification of functional interaction in *M. xanthus* is presented. The main challenge in integrating genomics datasets into an experimental setting is sorting through the large amount of data that must be processed. The typical use of genomics datasets within an experimental context is to obtain an extensive list of predictions and then test these predictions one at a time. While this approach proves effective with a manageably small test set, it is not uncommon for the test set to grow extensively large, numbering in the many hundreds. The testing of these predictions by standard experimental assays such as genetic analysis thus becomes both time and cost prohibitive. We have developed an experimental pipeline that incorporates large-scale microarray datasets for the identification of the downstream targets of transcriptional regulators (Figure 6.1).
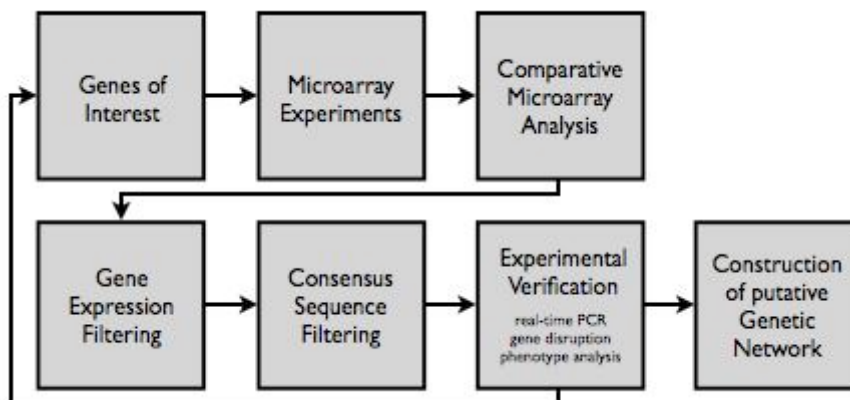
Figure 6.1: The integration of experiment-based functional genomics datasets to an experimental pipeline. In this example, a strain of the target organism inactivated for a specific TR is subjected to comparative microarray analysis over a time course. Sets of up- and down-regulated ORFs are retained and filtered through a coexpression map. This reduced set is further filtered by searching the upstream intergenic regions of each predicted ORF for the presence of a putative binding site. Experimental verification of these predictions are then used to construct a putative genetic network, and specific ORFs of interest characterized in this manner can be used as the specific ORF of interest for the next cycle of the pipeline.

To identify ORFs that are potentially controlled by TRs, gene expression studies using the cDNA microarray for *M. xanthus* will be conducted. Experiments will focus on the TRs that have been shown to control emergent behaviors in *M. xanthus*. In order to identify ORFs that are differentially expressed, RNA isolated from these mutant strains will be collected and compared to wild type cells under both development and chemotaxis conditions. To identify the putative downstream target ORFs, this list will then be filtered using the coexpression map introduced in Chapter 3. The upstream intergenic regions of the ORFs retained from coexpression filtering will be characterized for the presence of TR binding sites. DNA binding assays and real-time PCR will be conducted to confirm these results. This method, in conjunction with the ability to characterize TRs using two independent self-organizing behaviors, such as

development and chemotaxis, will further help to identify the ORFs responsible for emergent *M. xanthus* behaviors.

Case Study: The laboratory of Professor Anthony Garza (Syracuse University), in collaboration with Garret Suen (Welch Laboratory, Syracuse University), has already demonstrated the effectiveness of this approach. Developmental time-course microarray experiments for the NtrC-like EBP mutant MXAN4042 have been completed and the expression profiles at time 0h, 2h, 4h, and 6h analyzed. For each microarray experiment, only those ORFs that showed at least a four-fold change in steady-state RNA levels (i.e. -0.5 < log2(Cy3/Cy5) > 2) were extracted. Each time point was compared to its corresponding wild type time-point and only those ORFs that were differentially expressed were retained. This produced a list of 846 ORFs, which represents approximately 10% of the total genome.

To identify the direct downstream targets of MXAN4042 from this extensive list of predictions, a coexpression map for *M. xanthus* based on 212 different microarray experiments was constructed. As mentioned in Chapter 3, the coexpression map clusters ORFs that share similar gene expression patterns across a wide variety of experimental conditions. Using the coexpression map, a list of 100 of the most tightly correlated ORFs for MXAN4042 was generated. When comparing the set of 846 ORFs from the time-course experiment against the top 100 predictions retained for MXAN4042, a total of 50 ORFs were found to overlap.

To further characterize the putative downstream targets selected by microarray analysis and coexpression filtering, the 50 ORFs selected from the developmental time course experiments and coexpression filtering were characterized for the presence of putative NtrC-like binding sites using the computer program PromScan (available at: http://www.promscan.uklinux.net/) seeded with known NtrC-like TR binding sites from *M. xanthus* and other prokaryotes. A total of 9 targets were isolated in this manner. DNA binding assays were employed to confirm that MXAN4042 is capable of binding to the upstream regions of these targets. Further characterization through gene disruption and phenotypic analysis also confirm these results. The current success rate is greater than 50%.

These results demonstrate the utility of this approach to identify the primary downstream targets of TRs. Thus far, prudent attention to fiscal discipline has forced us to postpone microarray experiments. However, once funds become available, we plan on applying these same techniques to identify the downstream targets of the TRs that were found to be defective in both development and chemotaxis. We will also perform real-time PCR on the list of ORFs generated by PromScan to confirm that expression patterns are consistent with the microarray data.

In addition to identifying the primary targets of specific TRs, we hope to identify those ORFs that are part of the overall pathway controlled by each specific TR. Using the primary targets of each TR, we can utilize the phylogenomic map and generate a list of ORFs that are tightly correlated to each

primary target. Characterization of these selected ORFs through gene disruption and phenotypic assays will allow us to reconstruct the pathways that are under the transcription control of each specific TR.

6.5 Final Conclusions

Both *M. xanthus* development and chemotaxis represent swarm-level, dynamic, emergent patterns. We developed novel tools to examine these patterns and found there to be a close correlation between them and TRs. We have exploited this correlation to learn more about functional genetic networks responsible for self-organization in *M. xanthus*. As our understanding of development and chemotaxis increases, additional patterns will be selected, and phenotype assessment will therefore become increasingly quantitative.

An *M. xanthus* swarm represents a manifestation of prokaryotic multicellularity. Component cells are superposable subunits with a genetic instruction set optimized for existence within the swarm. This instruction set specifies both individual and group behavior through interdependent signal transduction networks, which link inputs from neighboring cells and the environment to outputs that control each response. Autonomy diminishes and evolution is driven toward complexity, so that swarms evolve new ways to interact with the environment that are beyond the capability of individual cells. Understanding how the instructions of an individual can specify self-organized behavior will give us a better understanding of how organisms shifted from single cell existence to multicellularity.

Appendix I: Microcinematography Protocol

This protocol is to be used as a tool for learning how to make reproducible *M. xanthus* swarm time-lapse videos. This protocol can be applied to both development and vegetative growth/swarm expansion assays.

Cell Prep
Start by creating a sterile environment.
- Clean workspace, don gloves, and light burner (Fig. 1).

1.   Measure cell density - should be around Klett 100 (Fig. 2).
2.   Pipette 1 ml cells into a 2.5 ml microcentrifuge tube.
3.   Pellet cells by centrifugation for 2 min at 16,000 x g (or max speed).
4.   Decant and discard supernatant.
5.   Wash cell pellet with 1 ml TPM (salt-balanced, nutrient-free media).
           - resuspend and vortex
6.   Re-pellet cells by spinning for 2 min at 16,000 x g (or max speed).
7.   Decant and discard supernatant (Fig. 3).
CRITICAL STEP
8.   Resuspend pellet with media of choice (see next page) using a combination
       of pipetting and vortexing.
       IMPORTANT: This step ensures that there are no chunks of cells left in the
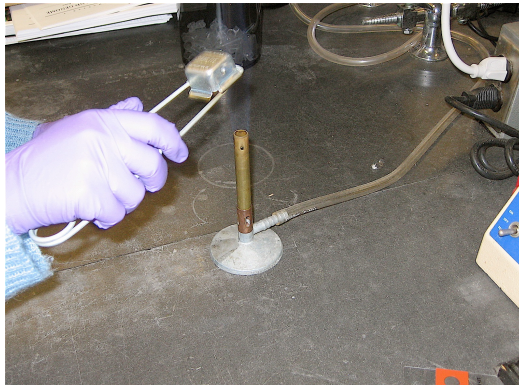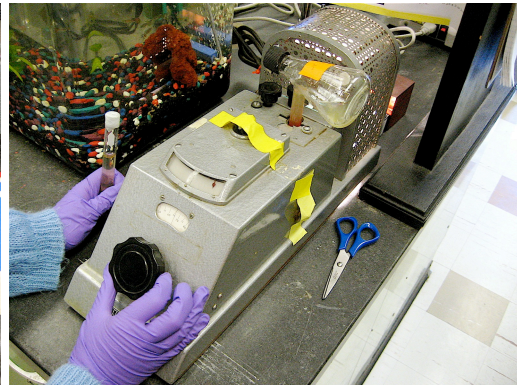   tube. This may take a while.

Figure 1   Figure 2

Agar Prep
The type of media/agar used depends on the kind of time-lapse movie needed.

CTTYE: nutrient rich media used to make vegetative swarming (motility)
                movies.

TPM: salt-balanced, nutrient-free media used to make development movies
                (formation of fruiting bodies).

RDM: salt-balanced, nutrient-free media with the addition of Sodium Citrate
                & Sodium Pyruvate to reduce fruiting time (from 24 to ~8 hours).

1.   Pipette 10 ml of desired media into a 15 ml conical tube.
2.   Add 0.1 g agarose (less diffractive than agar).
3.   Boil until agarose melts (Fig. 4).
4.   Remove from heat and allow to cool to 65°C (if using RDM, let cool to
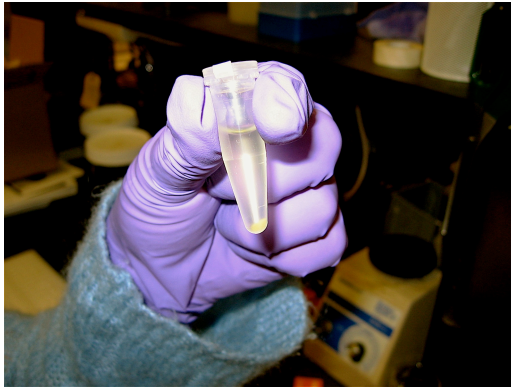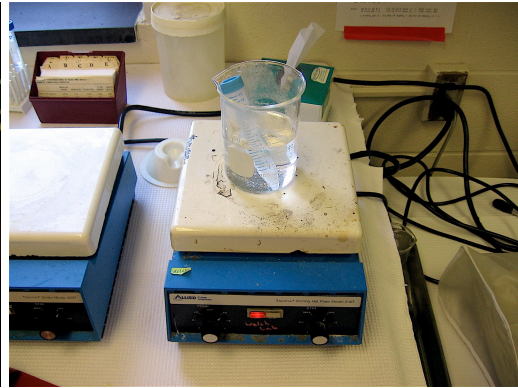   65°C before adding Sodium Citrate & Sodium Pyruvate.

Figure 3   Figure 4

Assay Prep 1 - set up plate complexes
For steps 1 through 3, refer to Fig. 5

NOTE: Figure 5 consists of all the parts needed to make 4 complete slide complexes.

1.   Flame sterilized slide (sterilized side up) with an autoclaved gasket placed on top (Fig. 5 - top). This will form the bottom of the assay.
2.   Parafilm (or labeling tape) covered support slide topped with a flame sterilized   cover slip (sterilized side up) topped with an autoclaved gasket (Fig. 5 - center). This will form the top of the assay.
3.   Flame sterilized slide (sterilized side up) used to flatten the agarose (Fig. 5 - bottom).

IMPORTANT: Make sure the gaskets form a seal with the glass by pressing it down with forceps, otherwise the media/agarose may dry out.
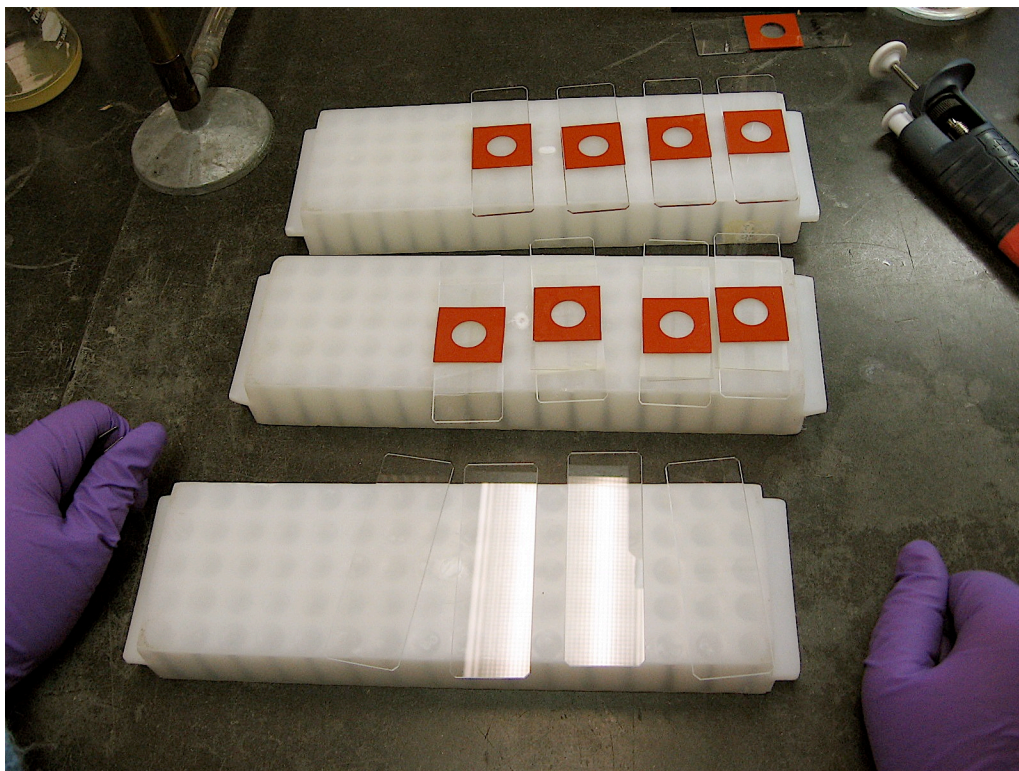

 Figure 5

Assay Prep 2 - pour plate
Once the various slide complexes are assembled, pour the media/agarose.

IMPORTANT: Steps 4 through 6 must be done to one slide complex at a time; otherwise the media/agarose could start to solidify resulting in poor movie quality.

CRITICAL STEP
4.   Pipette ~300 μl of media/agarose into the well created by the gasket on the cover slip (Fig. 6). The media/agarose should mound up (Fig. 7).
CRITICAL STEP
5.   Place the flame sterilized slide with no gasket (from step 3) on top of the media/agarose (Fig. 8).
                    IMPORTANT: This slide must be set down at an angle to prevent bubbles from forming.
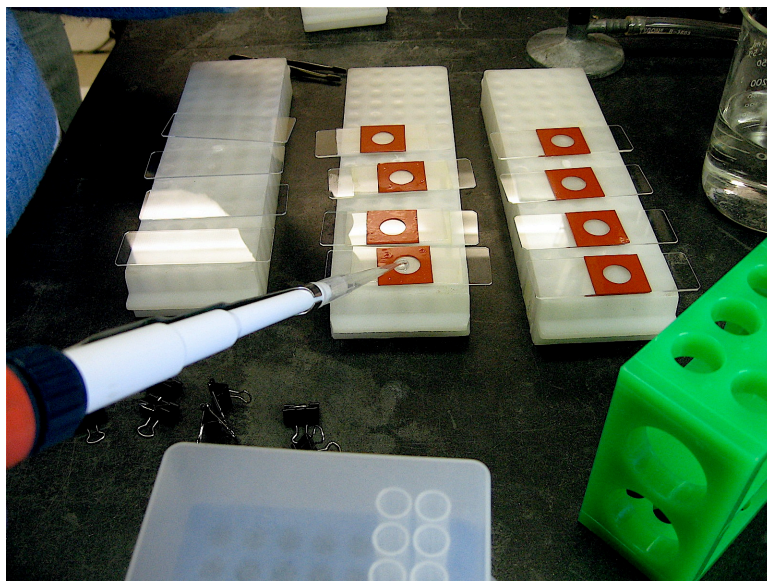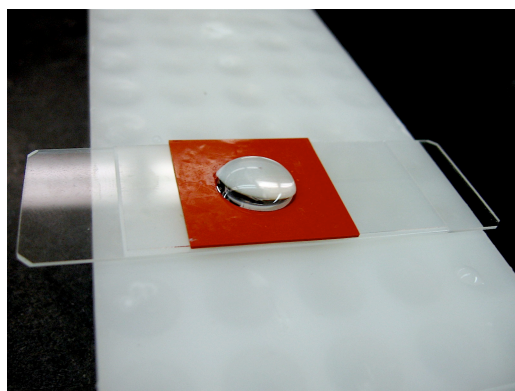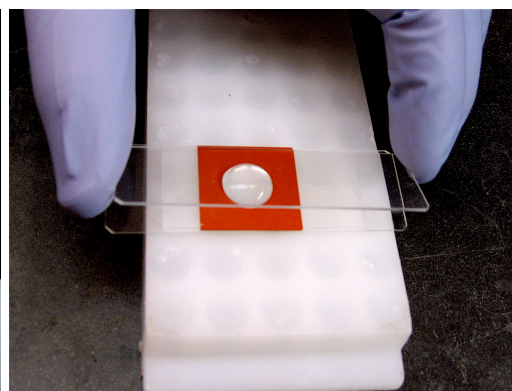

 Figure 6

Figure 7

Figure 8

Assay Prep 3 - separate plate

6. Once the slide (from step 5) is in place, clamp the complex together with mini binder clips - one on each side (Fig. 9).
7. Place the clipped complex at 4C and allow the media/agarose to set. This usually takes about 5 min.

IMPORTANT: For best results, steps 8 through 10 should be performed at 4°C.

IMPORTANT: To prevent the media/agarose from drying out, steps 8 through 22 should only be performed on one slide complex at a time.

8. Once the media/agarose has set, remove the binder clips and squeeze the end of the complex to loosen the parafilm wrapped slide. (Fig. 10)
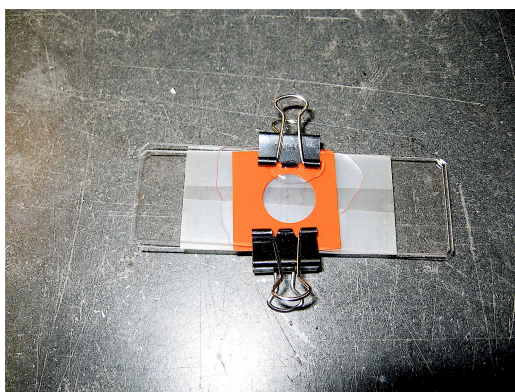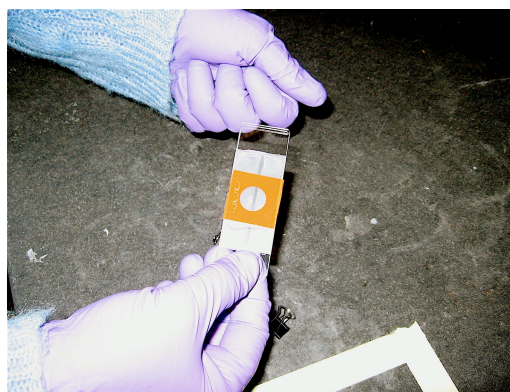9. Remove the parafilm wrapped slide and place it on the bench for further use.

Figure 9

Figure 10

Assay Prep 4 - separate and dry plate
CRITICAL STEP

10. Using forceps as a wedge, separate the cover slip/gasket/media/agarose complex from the support slide (with no gasket) and discard support slide (Fig. 11).

    IMPORTANT: Do not use a prying motion to separate the cover slip/ gasket complex. This could result in the cover slip breaking and/or the media/agarose sticking to the support slide.

11. Place the cover slip/gasket/media/agarose complex on the parafilm covered slide (gasket side up) and remove from 4°C. Place this complex next to the burner to allow all visible moisture evaporate from the newly exposed media/agarose - no more than 1 min (Fig. 12).

    IMPORTANT: Do not let the media/agarose dry for too long as this could change the *M. xanthus* swarm behavior.
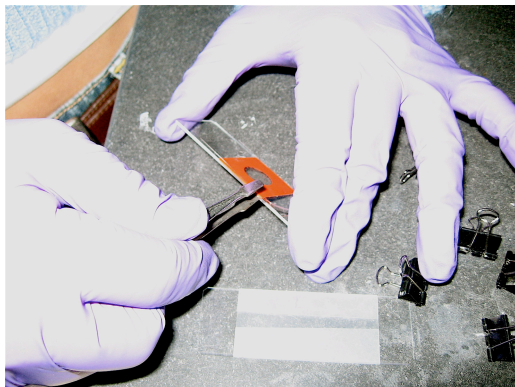

Figure 11   Figure 12

Assay Prep 5 - spot cells
CRITICAL STEP
12. Once the excess moisture has evaporated, pipette 0.5 μl of the concentrated cells (step 8 of cell prep section) onto the media/agarose (Fig, 13).

> IMPORTANT: It is extremely important to make sure that the cells are deposited by moving the pipette straight down and then straight up. This ensures that the swarm will be circular.

> IMPORTANT: It is extremely important not to touch the pipette tip to the media/agarose. This will make a depression on the surface and change the behavior of the *M. xanthus* swarm.

> TIP: Depress the pipette tip before approaching the media/agarose. This will   allow a drop of cells to appear on the bottom of the pipette tip and make it easier to deposit the cells.

13. Once the cells are deposited, place the complex next to the burner to allow the cell spot to dry - no more than 20 sec.

Figure 13

Assay Prep 6 - assemble assay

14. Once the cell spot has dried, align the slide/gasket complex (from step 1) with the gasket on the cover slip/gasket/media/agarose/cell complex (from step 13) and gently press together to form a seal (Fig. 14).

CRITICAL STEP
15. Clean the surfaces of the slide and cover slip with a kimwipe to remove the residue left by the parafilm (Fig. 15).
16. Place the completed slide complex on the heated stage (slide down, cover slip up) as soon as possible after wipe down (step 15) to prevent condensation form forming. If condensation has formed, let slide complex sit on the heated stage for several minutes before starting the Spot software macro (Fig. 16).
17. Depending on the type of behavior being observed, choose the appropriate objective (2X for swarm expansion, 4X for development, 10X for either).
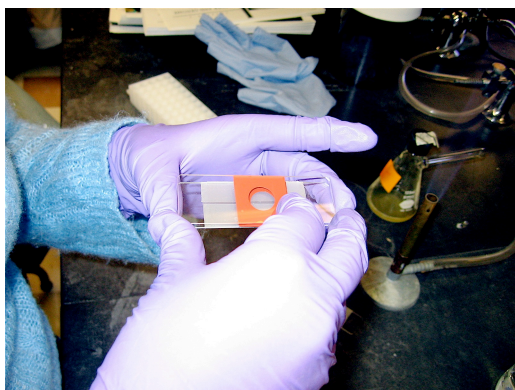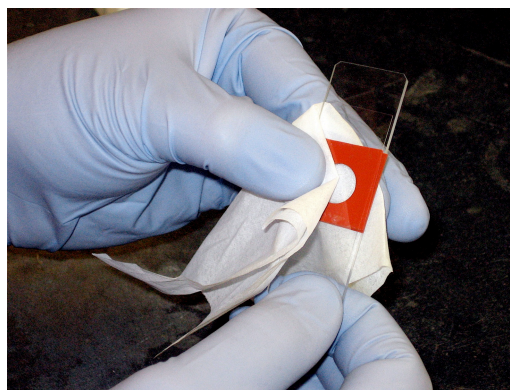
Figure 14   Figure 15

Movie Prep
CRITICAL STEP
18. Turn on the camera and microscope, and check the light levels (make sure the light is not turned all the way down). Start up the computer. Once running, check to make sure "Current Image Folder" is empty. Double click the Spot Advanced icon to start the image acquisition program (Fig. 17).
19. Click the live image window and focus the microscope. The image should appear similar to the one seen in Fig. 18. Notice the uniform agar surface.
20. To start acquiring images, click the macro menu and choose "play."
21. Select the appropriate macro and click run. The computer should start acquiring images immediately.
CRITICAL STEP
22. Check the focus regularly during the first hour, as the media/agar tends to settle causing the focus to drift.
23. Clean work area.
24. Once image acquisition is complete, transfer acquired images for storage and break down the slide complex with 90% ethanol.
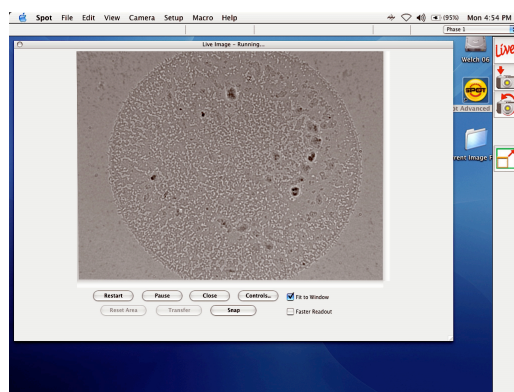

Figure 16

Figure 17

Figure 18

Appendix II: Standard Development Protocols

The following protocols are used to quantify the *M. xanthus* developmental

process:

Aggregation Assay. *M. xanthus* strains are grown in CTTYE+Kan at 32°C with

vigorous swirling. When cell reach mid-exponential growth phase, cultures are

washed, pelleted, and re-suspended in TPM buffer (10.0mM Tris-HCl, 1.0mM

KH_2PO_4, and 8.0mM $MgSO_4$) to a density of 5×10^9 cells/ml. Aliquots (20 µl) of

cell suspension are then spotted onto plates containing TPM media and 1.5%

agar.   Cell suspensions are allowed to dry and are then incubated at 32°C.

Images of aggregating *M. xanthus* cells are obtained at the following intervals

after inoculation: 0 hr, 12 hr, 24 hr, 48 hr, 96 hr, and 120 hr. These images are

compared to those of a wild-type swarm taken at the same intervals.

Sporulation Assay. *M. xanthus* strains are grown in CTTYE+Kan media at

32°C with swirling. When cell reached mid-exponential growth phase, cultures

are washed, pelleted, and re-suspended in TPM buffer to a density of 5×10^9

cells/ml. Three sets of 5 aliquots (20 µl) of cell suspension are then spotted onto

plates containing TPM media and 1.5% agar. Cell suspensions are allowed to

dry and are incubated at 32°C for 5 days to allow the swarm to develop. On day

5, each set of 5 spots is scraped off of the plates and suspended in 500 µl of

TPM buffer. Each scraped cell suspensions is then subjected to three 10-second

bursts with a model 100 Sonic Dismembrator (Fisher) using an intensity setting of

1.5. After sonication, the suspension is incubated at 50°C for 2 hours. Serial

dilutions of the sonicated and heat treated cell suspensions are added to 3 ml of

CTTSA, poured onto CTTYE+Kan plates and incubated for 5 days at 32°C. After

this incubation, visible colonies are counted, recorded, and compared to wild-

type to determine sporulation efficiency. This sporulation test represents the only

standard assay for development that is quantifiable.

Acknowledgments

I would like to acknowledge many people for helping me during my time at Syracuse University. I would especially like to thank my advisor, Dr. Roy Welch, for his generosity and commitment. Throughout my doctoral work his encouragement and advise on both a professional and personal level helped me to succeed. I know that my friendship with Roy is one that will stand the test of time. I couldn't have done it without you, man!

I am extremely grateful for having an exceptional doctoral committee and wish to thank Dr. Anthony Garza, Dr. Tom Starmer, Dr. Larry Shimkets, Dr. Melissa Pepling, and Dr. Dacheng Ren for their support and encouragement. In addition, I wish to thank Dr. Michael Consgrove for his assistance in my time of need – and finding Elvis in a world that thought he was gone.

I extend my thanks to colleagues and friends, especially Garret Suen and Kim Murphy. Without you, I would have lost my mind many years earlier. I'd like to thank my mother for her continued encouragement and constant prayers. You were right, I could accomplish anything I set my mind to. I'd also like to thank God for providing me with the tools necessary for earning a Ph.D.

Last, but most importantly, I'd like to thank my wife for helping me rise to every challenge. Her continual support, positive attitude, and sense of humor made enduring the hardships of graduate school (and northern living) not only bearable, but fun too. I love you Heather.

VITA

NAME OF AUTHOR: Rion G. Taylor

PLACE OF BIRTH: Augusta, GA, U.S.A.

DATE OF BIRTH: 9 March 1976

UNDERGRADUATE SCHOOLS ATTENDED:
Augusta State University, Augusta, GA, U.S.A.

DEGREES AWARDED:

Bachelors of Science in Biology, 2000, Augusta State University

AWARDS AND HONORS:

Syracuse University Research Grant, 2007

President, Biology Graduate Student Organization, 2007 – 2008

Syracuse University Graduate Student Travel Grant, 2005

American Society for Microbiology Travel Grant, 2005

PUBLICATIONS:

1. **Taylor RG**, Welch RD. Chemotaxis as an emergent property of a swarm. *J. Bactol*. In Press.

2. Curtis, P. D., **Taylor, R. G.**, Welch, R. D. and Shimkets, L. J. (2007). Spatial Organization of *Myxococcus xanthus* During Fruiting Body Formation. *J Bacteriol,* 189, 9126-30.

3. Suen, G., Arshinoff, B.I., **Taylor, R.G.** & R.D. Welch. (2007). Practical Applications of Bacterial Functional Genomics. *Biotechnology & Genetic Engineering Reviews* 24: 213-242.

4. Srinivasan, B.S., Caberoy, N.B., Suen, G., **Taylor, R.G**., Shah, R., Tengra, F., Goldman, B.S., Garza, A.G., and Welch, R.D. (2005). Functional genome annotation through phylogenomic mapping. *Nat Biotechnol,* 23, 691-8.